scientific reports

Check for updates

OPEN

Continuous short-term acclimation to moderate cold elicits cardioprotection in rats, and alters β-adrenergic signaling and immune status

Aneta Marvanova[1], Petr Kasik[1], Barbara Elsnicova[1], Veronika Tibenska[1], František Galatik[1], Daniela Hornikova[1], Veronika Zvolska[1], Pavel Vebr[1], Petr Vodicka[2], Lucie Hejnova[1], Petr Matous[3], Barbara Szeiff Bacova[4], Matus Sykora[4], Jiri Novotny[1], Jiri Neuzil[1,5,6], Frantisek Kolar[7], Olga Novakova[1,7] & Jitka M. Zurmanova[1]✉

Moderate cold acclimation (MCA) is a non-invasive intervention mitigating effects of various pathological conditions including myocardial infarction. We aim to determine the shortest cardioprotective regimen of MCA and the response of β1/2/3-adrenoceptors (β-AR), its downstream signaling, and inflammatory status, which play a role in cell-survival during myocardial infarction. Adult male Wistar rats were acclimated (9 °C, 1–3-10 days). Infarct size, echocardiography, western blotting, ELISA, mitochondrial respirometry, receptor binding assay, and quantitative immunofluorescence microscopy were carried out on left ventricular myocardium and brown adipose tissue (BAT). MultiPlex analysis of cytokines and chemokines in serum was accomplished. We found that short-term MCA reduced myocardial infarction, improved resistance of mitochondria to Ca^{2+}-overload, and downregulated β1-ARs. The β2-ARs/protein kinase B/Akt were attenuated while β3-ARs translocated on the T-tubular system suggesting its activation. Protein kinase G (PKG) translocated to sarcoplasmic reticulum and phosphorylation of $AMPK^{Thr172}$ increased after 10 days. Principal component analysis revealed a significant shift in cytokine/chemokine serum levels on day 10 of acclimation, which corresponds to maturation of BAT. In conclusion, short-term MCA increases heart resilience to ischemia without any negative side effects such as hypertension or hypertrophy. Cold-elicited cardioprotection is accompanied by β1/2-AR desensitization, activation of the β3-AR/PKG/AMPK pathways, and an immunomodulatory effect.

Despite recent progress in biomedicine, ischemic heart disease remains the most common cause of death and comorbidity worldwide. This grim picture stems from the fact that many promising therapeutic approaches demonstrated in animal models have failed in clinical trials[1,2]. Cold acclimation (CA) has so far been successfully studied also in the context of improving health complications in the metabolic syndrome[3,4], which includes chronic inflammation and oxidative stress. In humans, chronic CA significantly increases antioxidant capacity in blood serum and decreases homocysteine levels, suggesting a beneficial effect on the cardiovascular system[5]. Nevertheless, hypertension and left ventricle hypertrophy and other detrimental effects were repeatedly documented in animals exposed to severe cold[6]. Clinical trials using moderate cold in treatment of obesity and diabetes have been reported[7–9]. Since the beneficial effect of CA depends on the intensity of the cold and the mode

[1]Faculty of Science, Department of Physiology, Charles University, Vinicna 7, 128 00 Prague 2, Czech Republic. [2]Institute of Animal Physiology and Genetics, Czech Academy of Sciences, Libechov, Czech Republic. [3]First Faculty of Medicine, Center for Advanced Preclinical Imaging (CAPI), Charles University, Prague, Czech Republic. [4]Centre of Experimental Medicine, Institute for Heart Research, Slovak Academy of Sciences, Bratislava, Slovak Republic. [5]Institute of Biotechnology, Czech Academy of Sciences, Prague-West, Czech Republic. [6]School of Pharmacy and Medical Science, Griffith University, Southport, QLD, Australia. [7]Institute of Physiology, Czech Academy of Sciences, Prague, Czech Republic. ✉email: jitka.zurmanova@natur.cuni.cz

of adaptation regarding the given organism, it is necessary to understand when and under which conditions the protective effect of CA occurs and what is its molecular basis.

We have recently shown that an appropriate moderate cold acclimation (MCA) regimen presents a promising cardioprotective intervention. Chronic gradual MCA (8–6°C, 5 weeks) reduced the extent of myocardial infarction without negative side effects such as hypertension and hypertrophy. This model also improved mitochondrial resistance to Ca^{2+}-overload, and preserved the β1-adrenergic receptor (β-AR) function[10,11].

A β-AR signaling in the heart controls cardiac function under both physiological and pathophysiological conditions[12] and, importantly, it is a powerful regulator of immune response in context of ischemic injury[13–15]. The β1-ARs are coupled to G-stimulatory (Gs) proteins, which in turn stimulate protein kinase A (PKA) via hormone-stimulated cAMP formation by adenylyl cyclase[16]. Sustained activation of β1-AR signaling is deleterious and can promote apoptosis of cardiomyocytes, which occurs during hypertension or chronic heart pathologies, leading to progressive hypertrophy and culminating in heart failure[17,18]. It is generally accepted that minor β2/3-AR subtypes in the heart also stimulate adenylyl cyclase activity. However, both β2/3-ARs can also couple to G-inhibitory (Gi) proteins to attenuate β1-AR hyperactivation[19]. In this framework, activation of Gi-coupled signaling pathways, β2-ARs/protein kinase B (Akt) and β3-ARs/protein kinase G (PKG) have been confirmed as cardioprotective under certain stress conditions such as chronic hypoxia[20], exercise training[21], and the recently demonstrated recovery phase of chronic CA[10]. Stimulation of β2/3-ARs mediates protection against hypertrophic or fibrotic remodeling[19,22]. Recently, β3-AR coupling to AMPK, a key metabolic sensor, has been identified as a cardioprotective mechanism that preserves the downstream autophagy process[23].

CA is a highly complex adaptive process mediated via whole body neuroendocrine stimuli of the adrenergic system, reinforcing the thyroidal hormones action and leading to formation of brown adipose tissue (BAT)[24]. The β1/3-AR receptor/cAMP/PKA and AMP-activated protein kinase (AMPK) pathways play a crucial role in BAT formation. Both pathways control non-shivering thermogenesis of BAT via increased glucose uptake, mitochondrial biogenesis, fatty acid metabolism, and upregulation of uncoupling protein-1 (UCP1)[25]. Besides heat production, mature brown adipocytes are characterized by secretory function, releasing several protective bioactive molecules (batokines) into the bloodstream. The batokine fibroblast growth factor 21 (FGF21) serves as a marker of BAT maturation, and its plasma levels in humans are associated with cold-induced BAT activity[26]. It was proposed that UCP1 and BAT-released FGF21 target the heart to exert cardioprotective effects[27]. High metabolic activity and dissipation of energy is a promising intervention for diabetic patients even during short-term MCA[3].

The major goal of the present study is to find out the minimum duration of MCA that improves cardiac tolerance to acute ischemia/reperfusion (I/R) injury. And subsequently, to explore a series of plausibly connected events that may explain MCA-induced cardioprotection as a basis for future mechanistic studies using reductionist approaches. Thus, we asked the following questions. (1) What is the role of β1/2/3-AR downstream signaling and mitochondria in the MCA-elicited cardioprotection? (2) Is there a role for circulating batokines (FGF21, IL-6) in the cardioprotection? (3) How does the novel cardioprotective regimen of MCA affect the inflammatory status of the heart and the whole organism? Answers to these questions should provide a new insight into the complexity of cardioprotective mechanisms induced by short-term MCA.

Results

Optimization of cold acclimation protocol and its safety profile

In the present study, we tested whether short-term exposure to cold results in an improvement of cardiac ischemic tolerance. Based on our preliminary data, we chose 1, 3 and 10 days of cold exposure at a temperature below the threshold of shivering thermogenesis and (9 ± 1°C)[11,28] and characterized the time course of BAT activation (mitochondrial biogenesis, AMPK activation, UCP1, and FGF21 levels), a possible release of batokines into the circulation and the cytokine profile in the blood serum, as well as myocardial responses, in order to reveal potential players in cold-elicited cardioprotection.

The effect of short-term MCA on basic parameters is documented in Table 1. Data show that the weight of BAT and the BAT/body weight ratio, a marker of the cold-acclimated phenotype, increased by 54% and 60%, respectively, after 10 days. The weight of adrenal glands, a marker of cold stress, did not change significantly during the 10 days of acclimation. The lack of a change in adrenal gland/body weight supports the notion of well tolerable (moderate) cold stress stimuli. Concerning the cardiac and body parameters, the MCA did not affect the body weight, body temperature, heart weight or the heart/body weight ratio, ruling out hypothermia, hypertension, and myocardial hypertrophy. Also, it did not affect the heart rate and the mean arterial blood pressure during the I/R (Table 2). The data above indicate that short-term moderate cold acclimation causes a cold-adaptive phenotype on day 10 without any negative side effects within the tested parameters.

Characterization of BAT maturation during moderate cold acclimation

To determine the activation and maturation of BAT in the early stages of MCA, we analyzed the morphological changes, and expression and distribution of specific markers of BAT maturation. We found a 30% increase in the BAT mitochondrial mass, expressed as fractional area of cryosections, already after 1 day of MCA, and an increase of 40% on days 3 and 10 (Fig. 1a, c). Co-localization of UCP1 with mitochondria increased slightly after 1 day and elevated by 10% on days 3 and 10 (Fig. 1a, b), while mitochondrial UCP1-dependent respiration was markedly elevated after 10 days (by 20%) (Fig. 1d). Immunofluorescence analysis of BAT cryosections revealed that the level of FGF21, the main batokine produced during BAT maturation, increased after 10 days (Fig. 1e, h). Similarly, FGF21 colocalization with the mitochondrial compartment increased after 10 days (Fig. 1e, f), while it decreased after 1 and 3 days of MCA. Nuclear localization of FGF21 gradually decreased with its increasing

	Control	1 day	3 days	10 days
N	8	8	8	8
BW (g)	385 ± 16	363 ± 13	356 ± 21	370 ± 30
BAT (mg)	257 ± 47	270 ± 57	266 ± 86	396 ± 71**
BAT/BW	0.67 ± 0.12	0.74 ± 0.16	0.74 ± 0.23	1.07 ± 0.11***
RT (°C)	37.0 ± 0.23	36.9 ± 0.54	36.7 ± 0.27	36.9 ± 0.31
HW (mg)	1016 ± 83	1059 ± 79	1018 ± 58	1030 ± 86
LV + S/BW	2.07 ± 0.23	2.21 ± 0.26	2.24 ± 0.08	2.16 ± 0.13
RV/BW	0.57 ± 0.05	0.57 ± 0.06	0.61 ± 0.07	0.62 ± 0.07
HW/BW	2.64 ± 0.22	2.78 ± 0.26	2.86 ± 0.11	2.79 ± 0.12
ADG/BW	0.15 ± 0.03	0.16 ± 0.04	0.18 ± 0.02	0.18 ± 0.03

Table 1. Body weight (BW); brown adipose tissue (BAT); rectal temperature (RT); heart weight (HW); left ventricle (LV); ventricular septum (S); right ventricle (RV); adrenal glands (ADG); (n = 8); values are means ± S.D.; **p < 0.01, ***p < 0.001 vs. control. One-way ANOVA with Dunnett's multiple comparison test.

Heart rate, beats/min				
	Control	1 day	3 days	10 days
N	8	12	12	12
Baseline	390 ± 17	403 ± 20	398 ± 22	382 ± 30
Ischemia	384 ± 33	395 ± 23	382 ± 31	380 ± 33
Reperfusion	375 ± 29	395 ± 30	385 ± 36	382 ± 35
Blood pressure, mmHg				
Baseline	91 ± 24	83 ± 18	92 ± 16	70 ± 18*
Ischemia	77 ± 19	73 ± 11	88 ± 18	74 ± 23
Reperfusion	76 ± 16	70 ± 12	84 ± 17	70 ± 17

Table 2. Heart rate and mean arterial blood pressure (n = 8–12); values are means ± S.D.; *p < 0.05, vs. Control; two-way ANOVA with Dunnett's multiple comparison test (the effect of cold acclimation) and two-way ANOVA with Šidák's multiple comparison test (the effect of I/R).

localization in mitochondria (Fig. 1e, f, g). The pAMPK$^{\alpha\ r172}$/AMPK ratio, reflecting the metabolic activity of BAT, was elevated by 108% after 3 days and was elevated by 72% on day 10 of MCA (Fig. 1i).

Myocardial ischemic tolerance during moderate cold acclimation

Analysis of the extent of I/R injury revealed that 3- and 10-day moderate cold exposure reduced myocardial infarction to 34% and 37% of the area at risk (AR), respectively, compared with 50% in the control group, while 1 day of cold exposure had no effect (Fig. 2a, left). The average ratio of normalized AR to the left ventricle (AR/LV) reached 45—49% and did not differ between the groups (Fig. 2a, right). Increased resilience of isolated cardiomyocytes to hypoxia/reoxygenation elicited by 10 day of MCA was also observed (data not shown). Echocardiography did not reveal any differences between the groups, and the unchanged diameters of the anterior and posterior LV walls excluded cold-elicited hypertrophy after 10 days of cold exposure (Fig. 2b).

Mitochondria and AMPK in cold-elicited cardioprotection

To uncover a possible role of MPT pore in the cardioprotective mechanism, we tested the maximal mitochondrial swelling rate using 200 μM Ca^{2+} and found that it was reduced in both 'protected' groups: on day 3 by 19% and day 10 by 21% compared to the control group (Fig. 3a). The concentration of malondialdehyde in the LV heart homogenate did not show significant changes during the MCA, which excludes oxidative stress development during its acute phase (Fig. 3b). Using quantitative immunofluorescence microscopy and western blotting of mitochondrial fractions, we examined translocation of the HK2 isoform to the outer mitochondrial membrane, which is known to prevent MPT pore opening. Co-localization of HK2 increased after 3 days of MCA (Fig. 3c, d), which was confirmed by elevated level of HK2 protein in the mitochondrial fraction (Fig. 3e). Both values returned to the control level after 10 days of MCA (Fig. 3c–e). Importantly, phosphorylation of p-AMPK$^{\alpha\ r172}$ increased after 10 days of MCA as well as the p-AMPK$^{\alpha\ r172}$/AMPK ratio (Fig. 3f), suggesting stimulation of the pleiotropic role of AMPK in the cardioprotection of cold-acclimated rats.

Myocardial β-adrenergic signaling during moderate cold acclimation

The balance in the isoforms of β1/2/3-ARs and their downstream pathways play an important role in the cardioprotective phenotype. Therefore, we analyzed the total number and affinity of β-ARs using a specific binding assay, as well as the expression and localization of β2- and β3-ARs in the crude membrane fraction. After 3 and

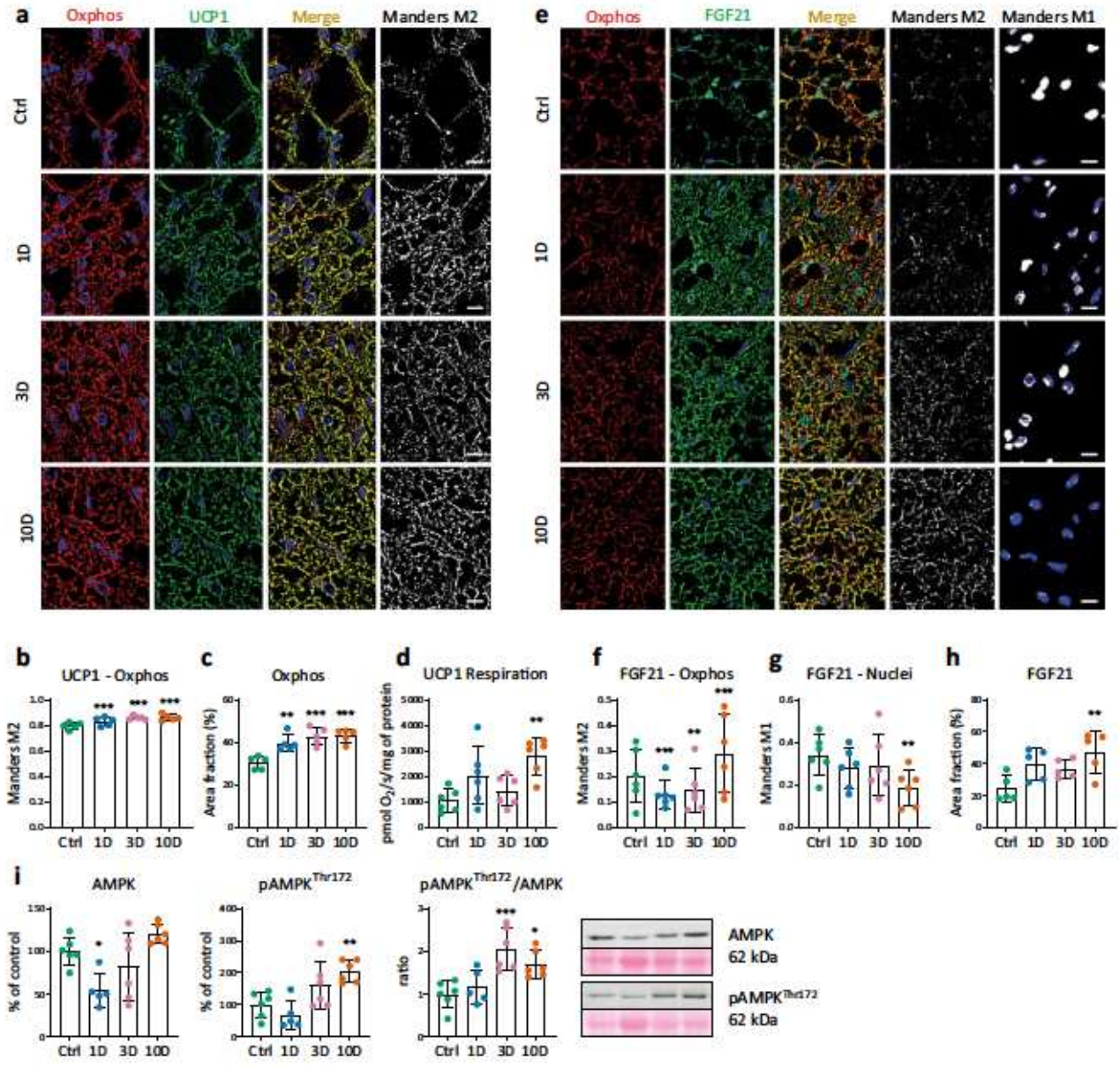

Figure 1. Characterization of brown adipose tissue (BAT) maturation during cold exposure (9 ± 1 °C) for 1–3–10 days (1D, 3D, 10D) and in control rats (Ctrl). (**a**) Representative images of BAT mitochondria (red color; anti-OXPHOS Abs) and the uncoupling protein UCP1 (green color), blue color indicates nuclear DAPI staining. Merged column shows colocalization of UCP1 with OXPHOS (yellow-orange color), black and white images show corresponding colocalized pixels (Mander's M2 correlation coefficient), quantified in the graph (**b**) (n = 5). (**c**) Mitochondrial density represented by the area fraction shown as red signal. (**d**) UCP-dependent respiration of isolated mitochondria (n = 5–6). (**e**) Representative image of FGF21 (green color) and mitochondria (red color). Merged column shows colocalization of FGF21 with mitochondria (yellow-orange, Mander's M2) and with nuclei (blue-green, Mander's M1), respectively. Black and white images show corresponding colocalized pixels quantified in graphs (**f,g**). (**h**) FGF21 density represented by area fraction (%) of green positive signal. **i.** Relative protein level of total AMPK and p-AMPK^{Thr172} obtained by western blots, and the p-AMPK^{Thr172}/AMPK ratio (n = 5–6). Data presented in graphs were analyzed by One-way ANOVA with Dunnett's multiple comparison test. Values are means ± SD; *p < 0.05, **p < 0.01, ***p < 0.001 vs. control. Scale bar 10 µm.

10 days of MCA, the total number of myocardial β-ARs was 16% and 18% lower, respectively, compared to controls (Fig. 4a), reflecting a decline in major β1-ARs. Immunofluorescence analysis revealed changes in the localization of both β2- and β3-AR proteins after MCA (Fig. 4b, e). Despite the very low T-tubular occupancy by β2-ARs in the controls, β2-ARs decreased even more on days 3 and 10 (Fig. 4b, c). Conversely, the association of β2-ARs with the surface sarcolemma increased after 3 days (not shown). The occupancy of T-tubules by β3-ARs increased after 3 and 10 days, and their localization within the sarcolemmal compartment showed no

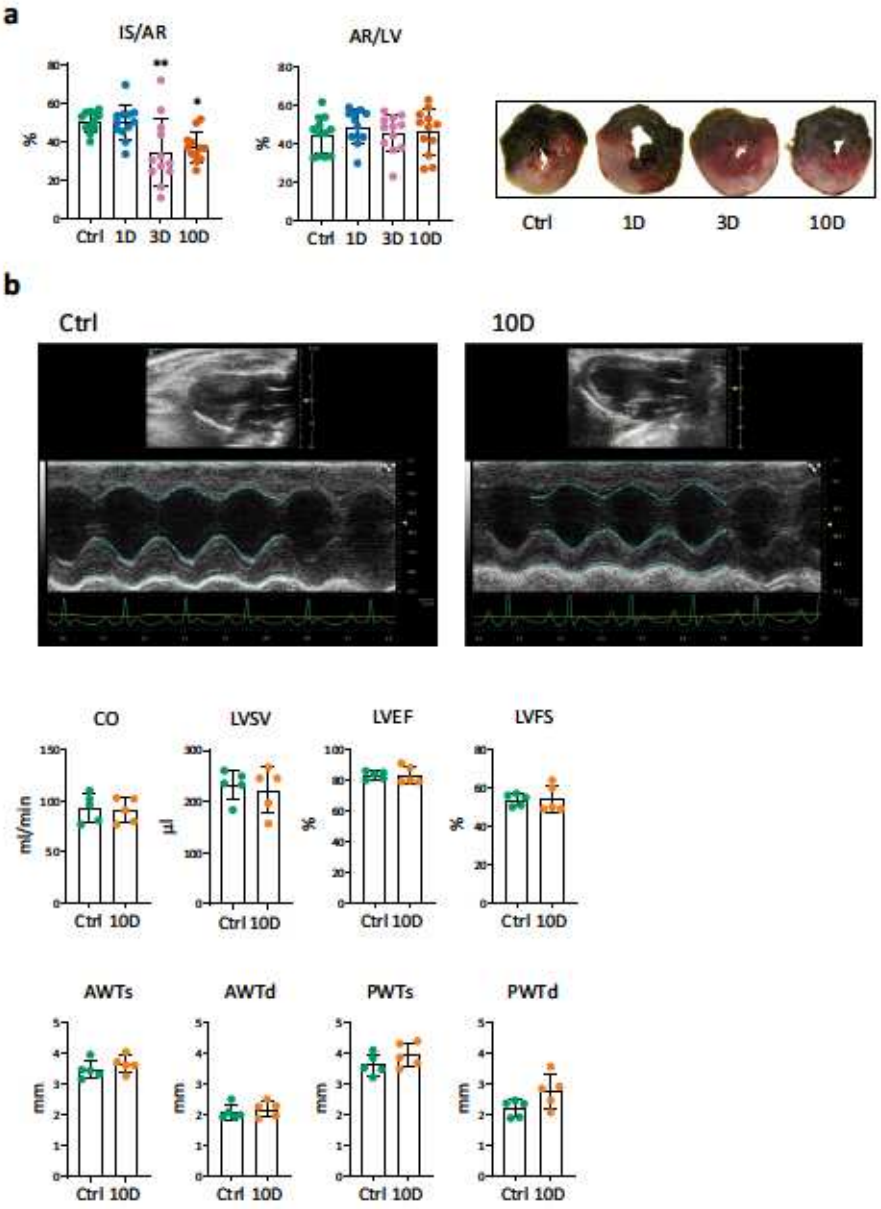

Figure 2. The effect of short-term cold acclimation on myocardial sensitivity to ischemia/reperfusion injury and cardiac function. (**a**) The extent of myocardial infarction in vivo in control rats (Ctrl) and those exposed to 9 ± 1 °C for 1–3-10 days (1D, 3D, 10D) and respective representative images. Infarct size (IS) was expressed as a percentage of area at risk (AR); AR was normalized to the cross-section area of left ventricle (LV) (n = 12). (**b**) Echocardiographic data of rats prior and after 10D of the exposure. Representative M-mode tracing of the left ventricle and following echocardiographic measurements; the cardiac output (CO), left ventricular stroke volume (LVSV), ejection fraction (LVEF), fractional shortening (LVFS) and systolic/diastolic anterior (AWTs/d) and posterior (PWTs/d) left ventricular wall thickness were evaluated by the Vevo LAB software. Data presented in graphs were analyzed by One-way ANOVA with Dunnett's multiple comparison test. Values are means ± SD; *p < 0.05; **p < 0.01 vs. Ctrl.

significant changes during MCA (Fig. 4e, f). On the other hand, levels of β2- and β3-AR proteins, assessed by western blotting, were unchanged in the crude membrane fraction (Fig. 4d, g).

Expression of $G_{\alpha s}$ and $G_{\alpha i1/2}$ in crude membrane fractions increased significantly only after 1 day, while $G_{\alpha i3}$ was not affected (Fig. 5a). Expression and phosphorylation of PKA, a component of the downstream β1/β2-ARs/$G_{\alpha s}$ pathway, were not significantly altered by MCA (Fig. 5b). Expression of total PKB/Akt, a downstream kinase of β2/β3-ARs/G_i pathways was not significantly altered. However, the phosphorylation of Akt at Ser473 residue declined after 10 days (p = 0.05) (Fig. 5c) suggesting suppression of its activity. Regarding PKG, a downstream kinase of β3-ARs/$G_{\alpha i1/2}$, we detected a translocation of PKG1 to the membrane of the sarcoplasmic reticulum

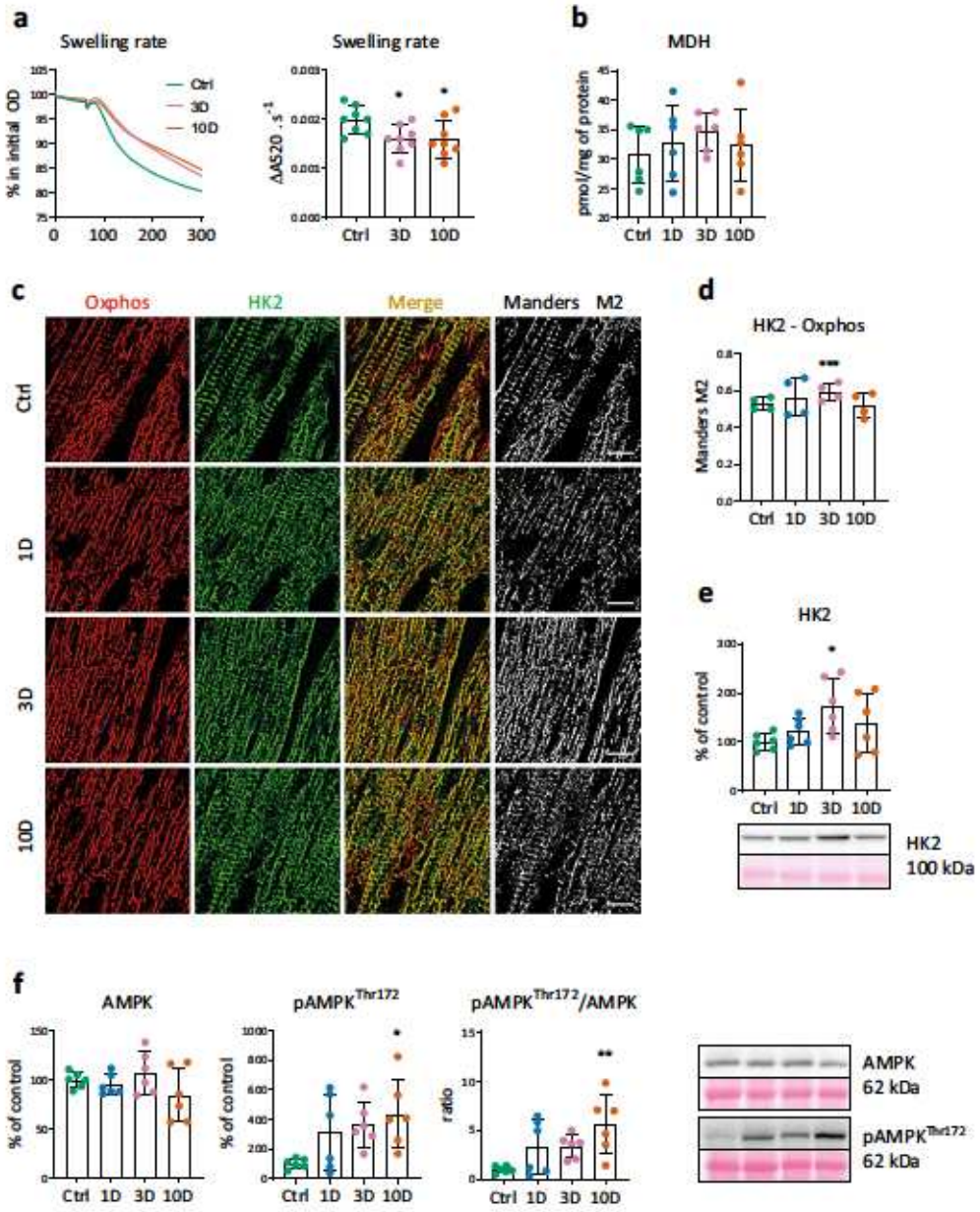

Figure 3. Effect of short-term cold acclimation on mitochondrial resilience to Ca^{2+} overload, oxidative stress marker (malondialdehyde, MDH), hexokinase 2 (HK2) translocation to mitochondria and AMPK in the left ventricle (LV) of control rats (Ctrl) and those exposed to 9 ± 1 °C for 1–3-10 days (1D, 3D, 10D). (**a**) Representative recordings of induced mitochondrial maximal swelling rate at 200 µM Ca^{2+} (left) expressed as the change of absorbance (DA) per 1 s (right) (n = 6). (**b**) Concentration of malondialdehyde (MDH) in LV homogenates (n = 6). (**c**) Representative images documenting mitochondrial compartment (red color; anti-OXPHOS Abs) and HK2 isoform (green color). Merged column represents respective co-localization (yellow-orange color), black and white images show corresponding co-localized pixels. (**d**) Quantification of the colocalizations Mander's M2 coefficients. Scale bars, 10 µm, (n = 4–5; five ROIs for each). (**e**) Level of HK2 protein in mitochondrial fraction expressed as the percentage of Ctrl (n = 6). (**f**) Relative levels of AMPK and p-AMPK^{Thr172} proteins in homogenate, and the p-AMPK^{Thr172}/AMPK ratio (n = 6). Data presented in graphs were analyzed by One-way ANOVA with Dunnett's multiple comparison test. Values are means ± SD; *p < 0.05,**p < 0.01, ***p < 0.001 vs. Ctrl.

identified by staining with anti-phospholamban antibody after 3 days of MCA (Fig. 5d, e), while its expression was not altered (Fig. 5f).

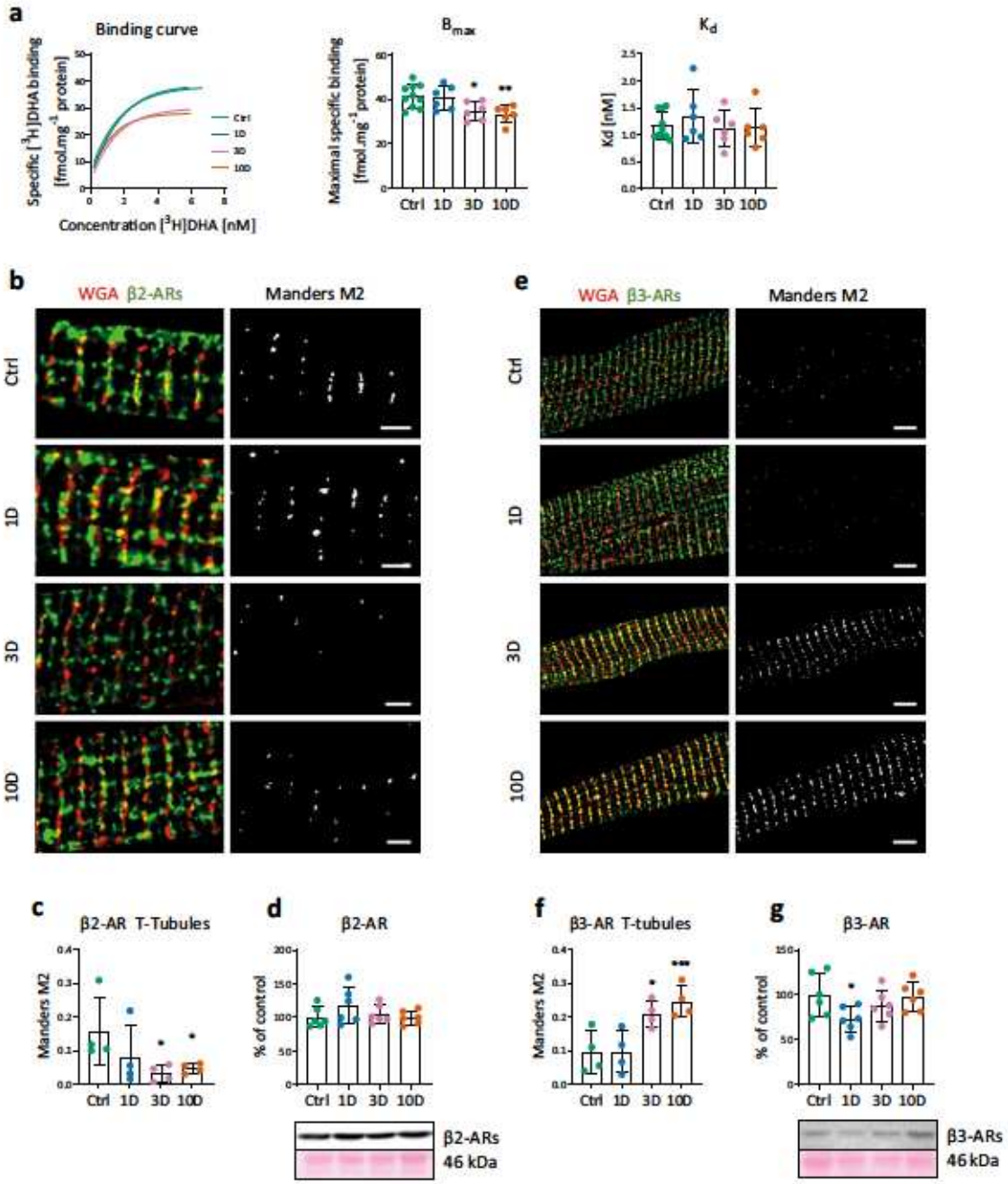

Figure 4. Effect of short-term cold acclimation (MCA) on the total number of β-adrenergic receptors (β-ARs) and their subcellular distribution on day 1–3–10 days of MCA (1D, 3D, 10D) and in control rats (Ctrl). (**a**) Representative saturation binding curves constructed by assessing binding of [3H]-dihydroalprenolol ([3H]-DHA) to myocardial crude membranes using increasing concentration of the radioligand (three saturation binding experiments were performed in triplicate, and the graph shows typical saturation binding curves), β-AR maximal binding capacity (Bmax), and receptor affinity (Kd) (n = 6). (**b,e**) Representative images documenting colocalization of β2- and β3-ARs, respectively (green color) with the T-tubular system stained by WGA (red color). Black and white images represent colocalized pixels. Scale bars, 2 µm (**b**) and 5 µm (**e**). (**c,f**) Quantification of the colocalization with the T-tubular compartment was calculated as Mander's M2 coefficient (n = 4). (**d,g**) Relative protein levels of β2- and β3-ARs in the crude membrane fraction (n = 6). Data shown in the graphs were analyzed by One-way ANOVA with Dunnett's multiple comparison test. Values are means ± SD; *p < 0.05, **p < 0.01, ***p < 0.001 vs. Ctrl.

FGF21 and inflammatory markers during moderate cold acclimation

Regarding the heart, the spatial expression and distribution of the batokine FGF21, one of the cytokine candidates

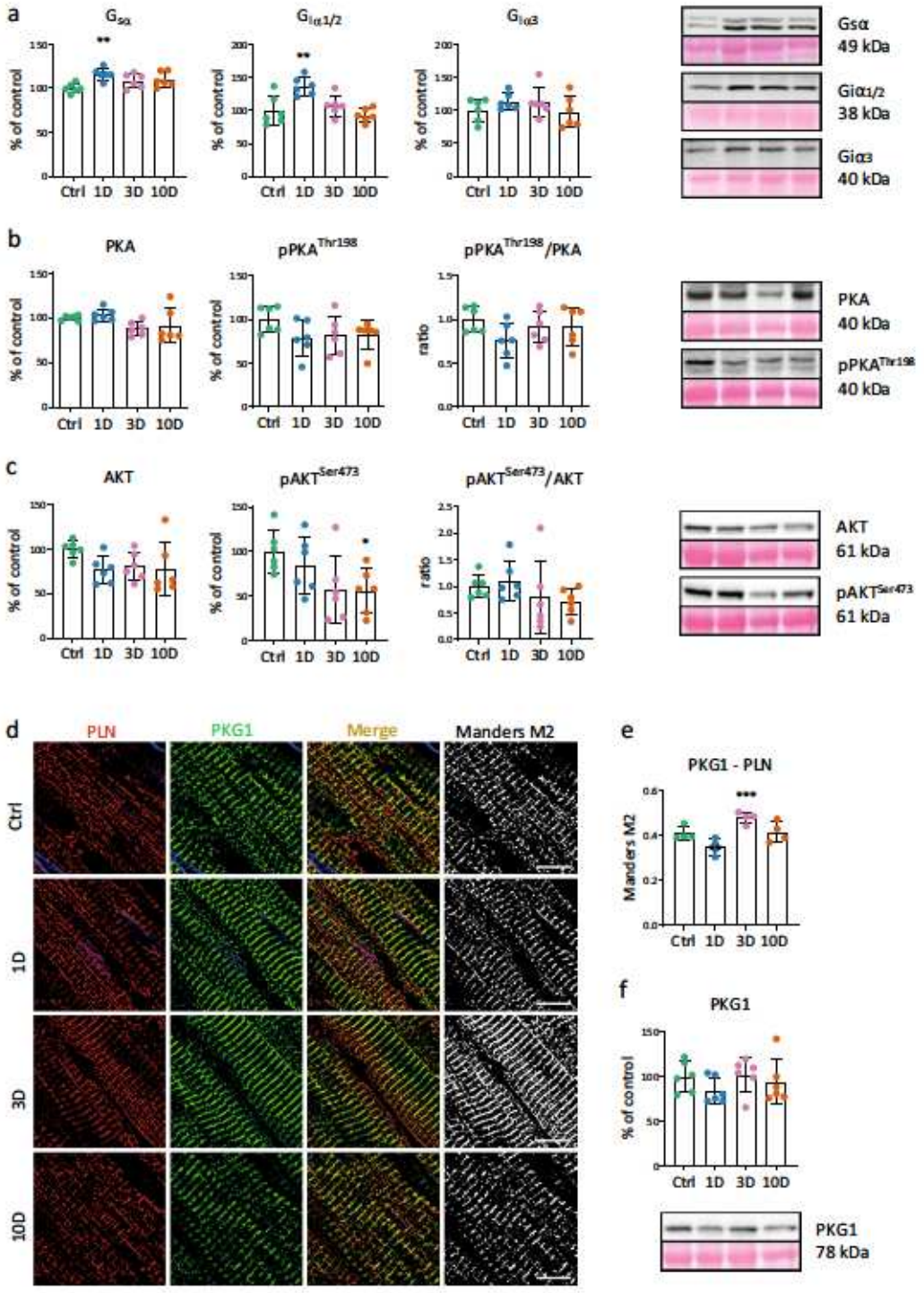

Figure 5. Effect of short-term cold acclimation (CA) on the β1/2/3-ARs-signalling pathways. (**a**) Relative G-protein (Gsα, Giα1/2, and Giα3) levels in a crude membrane fraction expressed as percentage on day 1–3-10 days (1D, 3D, 10D) of CA, and in control rats (Ctrl) (n = 6). (**b**) Relative protein levels of protein kinase A (PKA), p-PKAThr198, and p-PKA^{Thr198}/PKA ratio (n = 6). (**c**) Relative protein levels of protein kinase B/Akt (Akt), p-Akt^{Ser473}, and p-Akt^{Ser473}/Akt ratio (n = 6). (**d**) Representative images documenting localization of phospholamban (PLN, red color) and protein kinase G (PKG1, green color). Merged column represents co-localization (yellow-orange color), black and white images show corresponding co-localized pixels. Scale bar 10 µm. (**e**) Quantification of colocalization with the T-tubular compartment were calculated as a Mander's M2 coefficient (n = 4). (**f**) Relative protein level of PKG1 in the crude membrane fraction (n = 6). Data shown in the graphs were analyzed by One-way ANOVA with Dunnett's multiple comparison test. Values are means ± SD; *p = 0.05, **p < 0.01, ***p < 0.001 vs. Ctrl.

for cardioprotection, were quantified in longitudinal LV sections by immunofluorescence (Fig. 6a) similarly as shown for BAT in Fig. 1. The area fraction of FGF21 reflecting its spatial expression did not differ between the groups (Fig. 6a, b). However, we observed differences in the subcellular distribution FGF21 in the heart and in BAT. In BAT, Mander's correlation coefficients M1 and M2 documented altered colocalization of FGF21 with mitochondria and nuclei during MCA, while in the heart FGF21 colocalized with mitochondria (Fig. 6a, c) but not with nuclei (Fig. 6a, d). Colocalization with mitochondria did not differ between the groups (Fig. 6c).

ELISA analysis revealed that the concentration of the pro-inflammatory cytokine IL-6 significantly decreased on day 3 and remained decreased on day 10 of MCA in LV homogenates. The anti-inflammatory cytokine IL-10 did not change significantly and only tended to decrease resulting in the IL-6/IL-10 ratio remaining unaltered (Fig. 6e). This suggests a moderate anti-inflammatory effect of MCA in the LV myocardium.

Serum concentration of cytokines

Next, we evaluated number of cytokines level in the serum. The heatmap in Fig. 7a shows changes in concentrations of 14 cytokines (G-CSF, GM-CSF, IFNγ, IL-1α, IL-1β, IL-2, IL-4, IL-5, IL-6, IL-10, IL-12p70, IL-13, IL-17A, TNFα) and 8 chemokines (Eotaxin, GROα, IP-10, MCP-1, MCP-3, MIP-1α, MIP-2, RANTES) expressed as scaled log10 (MFI). MCA elicited gradual changes in concentration of most tested cytokines that can be divided into 3 main clusters. The first cluster (I) on the heatmap includes 1 chemokine (GROα) and most of the cytokines that declined during MCA (GROα, G-CSF, GM-CSF, IFNγ, IL-1α, IL-4, IL-5, IL-6, IL-10, IL-12p70, IL-17A). The significant differences are shown in Fig. 7b. The middle cluster (II) on the heatmap includes 2 chemokines (MIP1a, MIP2) and 4 cytokines (IL-1β, IL-2, IL-13, TNFα), showing a moderate trend to decrease during the

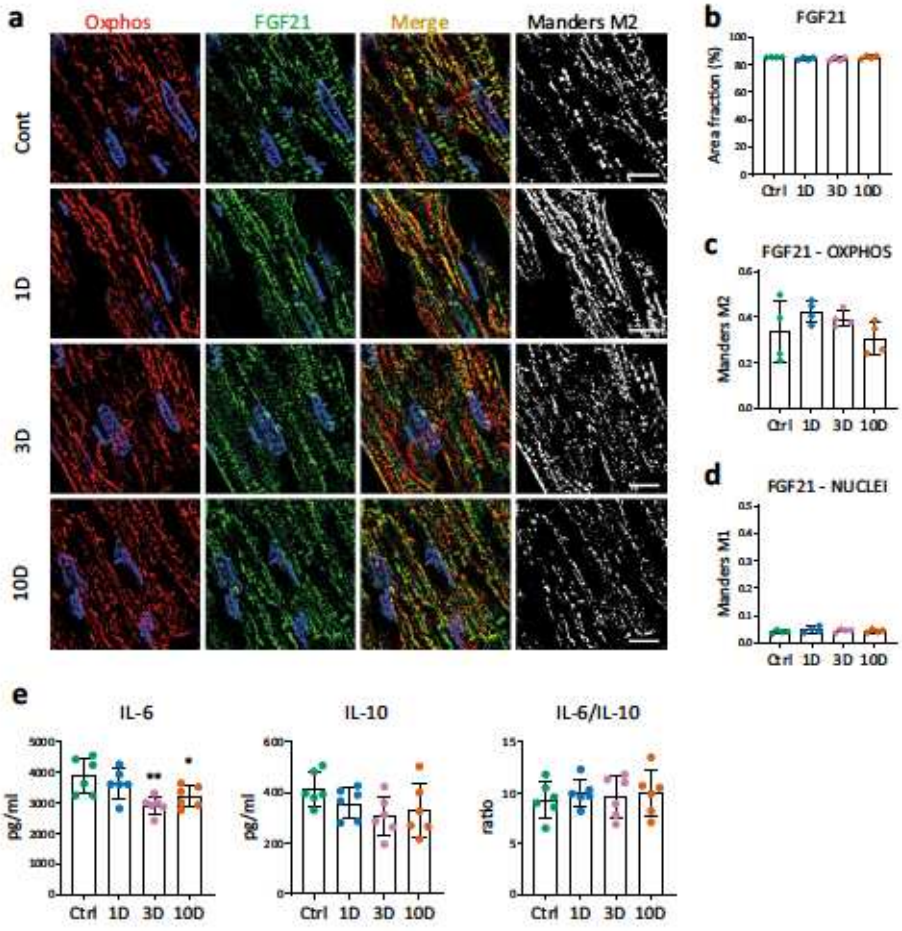

Figure 6. Inflammatory markers and expression of FGF21 in the left ventricle (LV) myocardium. (**a**) Representative images documenting spatial expression of FGF21 in control rats (Ctrl) and these exposed to 9 ± 1 °C for 1–3–10 days (1D, 3D, 10D). Co-localization of FGF21 (green) with the mitochondrial compartment (red; anti-OXPHOS IgGs) is shown in yellow-orange. Black and white images show corresponding colocalized pixels. Blue color indicates DAPI staining. (**b**) FGF21 density represented by the area fraction (%) of green positive signal. (**c**) Quantification of FGF21 colocalization with mitochondria was calculated as a Mander's M2 coefficient. (**d**) Quantification of FGF21 colocalization with nuclei was calculated as a Mander's M1 coefficient (n = 4; five ROIs for each sample. (**e**) Concentration of pro- and anti- inflammatory cytokines (IL-6, IL-10) and their ratio in LV homogenates. Data presented in graphs were analyzed by One-way ANOVA with Dunnett's multiple comparison test, values are means ± SD; *p < 0.05, **p < 0.01, ***p < 0.001 vs. Ctrl. Scale bars 10 µm.

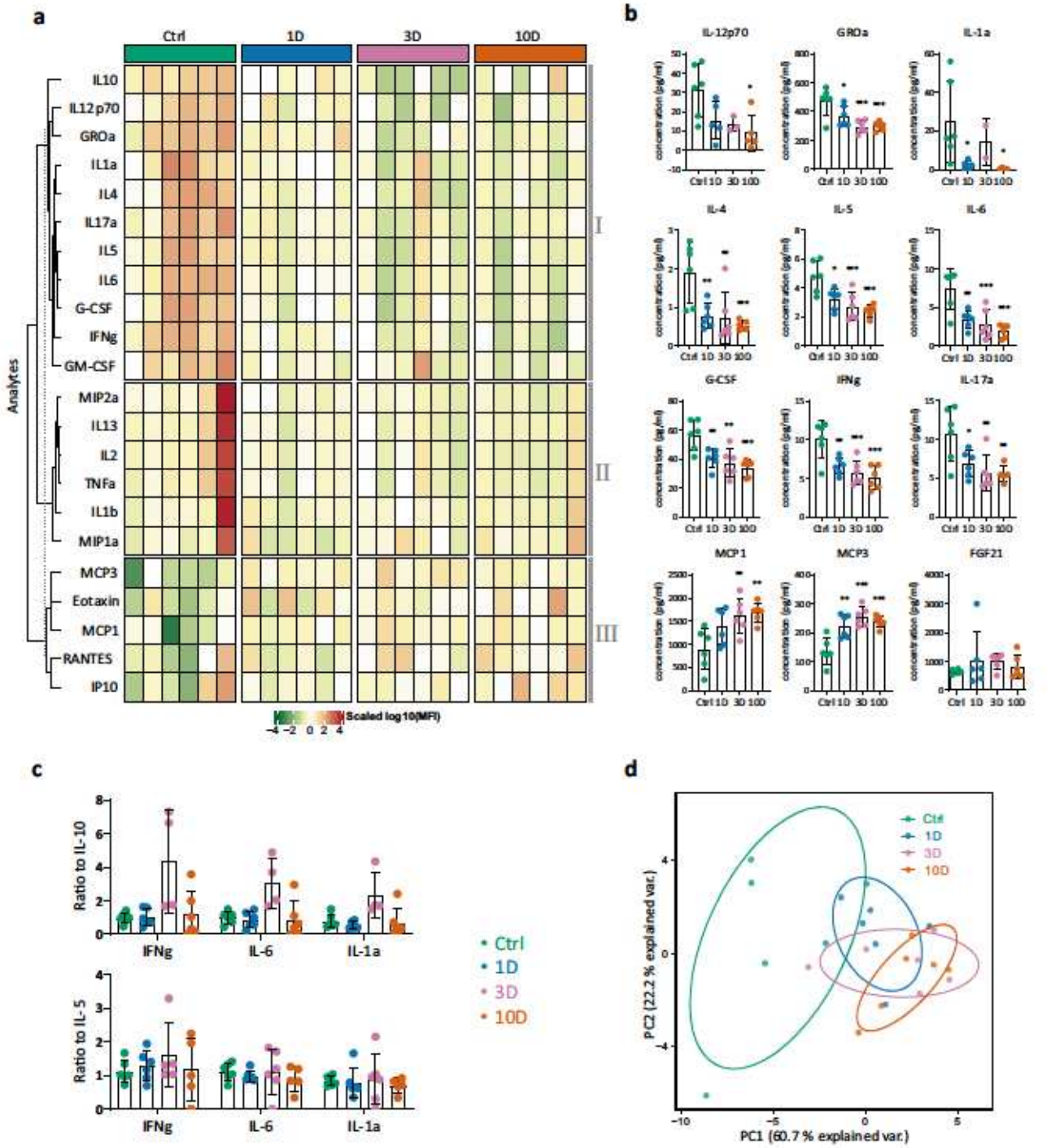

Figure 7. Multivariate analysis of cytokines and chemokines in arterial blood serum samples by Multiplex analysis from control rats (Ctrl) and rats exposed to 9 ± 1 °C for 1–3–10 days (1D, 3D, 10D). (**a**) The heatmap documents changes in the concentrations of 14 cytokines (G-CSF, GM-CSF, IFNg, IL-1α, IL-1β, IL-2, IL-4, IL-5, IL-6, IL-10, IL12p70, IL-13, IL-17A, TNFα) and 8 chemokines (Eotaxin, GROα, IP-10, MCP-1, MCP-3, MIP-1α, MIP-2, RANTES) expressed as scaled log10 (MFI) in three panels (I, II, III). (**b**) Significant changes in the analytes elicited by moderate cold exposure. (**c**) Inflammatory indexes calculated as the ratio of generally accepted pro-inflammatory IFNγ, IL-1α and IL-6, and anti-inflammatory IL-10 and IL-5 cytokines calculated from normalized values. (**d**) Multivariate analysis (PCA) of all analytes showing separation of the four experimental groups (Ctrl, green; 1D, blue; 3D, pink; 10D, orange) by first two principal components (PC1, PC2). The points represent individual samples, and ellipses 68% confidence interval for each group. The points represent individual samples, values are means ± SD; *p < 0.05, **p < 0.01, ***p < 0.001 vs. Ctrl. One-way ANOVA with Dunnett's multiple comparison test.

MCA process. The third cluster (III) manifests a trend of increased concentration, comprising only chemokines (eotaxin, IP-10, MCP-1, MCP-3, RANTES) of which only MCP-1 and MCP-3 reached significance (Fig. 7a, b).

As the first cluster (A) on the heatmap shows decline of both pro- and anti-inflammatory cytokines, we calculated the inflammatory index as the ratio of IFNγ, IL-1β, IL-6 to each of IL-10 and IL-5 from normalized values (Fig. 7c). Changes of the inflammatory index were not significant across the groups. Moreover, all inflammatory indexes tend to increase on day 3 when IL-10 was used as a denominator (Fig. 7c). PCA analysis shown in Fig. 7d clearly separates two clusters of the control (green) and day 10 group (orange), while the day 1 and day 3 groups overlap with other groups, manifesting a transient state of the immune response to cold during the early period of acclimation (Fig. 7d). The presented data document a significant shift to lower levels of key cytokines on day 10 of MCA, while the balance between pro- and anti-inflammatory cytokines remains unchanged between controls and experimental groups.

Discussion

Repeated exposure to mild cold has been presented in a few clinical trials as a successful therapeutic intervention in type II diabetes and obesity[7–9]. We have recently demonstrated an infarct size-limiting effect of chronic moderate cold exposure for 5 weeks at 8 ± 1 °C in rats, which persisted at least 2 weeks after the animals returned to control temperature[10,11]. Understanding the cellular and molecular processes during the early development of cold-elicited cardioprotective phenotype is important, especially considering potential therapeutic application. This requires a sensitive setting of the cold intensity and regimen considering an individual's health and constitution. Therefore, we aimed to determine whether the period of moderate acclimation required for cardioprotection could be further shortened and, if so, to characterize the relevant model.

In the present study we demonstrate for the first time that moderate cold acclimation achieved through exposure to 9 ± 1 °C for 3 and 10 days, but not for one day, suffices to reduce the infarct size, which distinguishes MCA from the effects of classic pre- or post-conditioning[10,11]. Both protective stages of MCA were accompanied by an increased mitochondrial resistance to Ca^{2+}-overload followed by β1-ARs desensitization, and increased compartmentalization of β3-ARs within transverse T-tubules. After 10 days of MCA, we observed a noticeable decrease in β2-ARs within the T-tubular system and in the phosphorylation of its downstream Akt^{Ser473} kinase. However, the expression and phosphorylation levels of PKA were not significantly altered. We propose that a fully acclimated phenotype is achieved under these conditions on day 10, as we observed BAT maturation at this time point of MCA, but not on day 3. The given phenotype involves AMPK activation in the heart, and we also found clustering of serum cytokines obtained by PCA analysis. For the specific signaling in cardiac tissue on day 3, MCA led to beneficial co-localizations of PKG with phospholamban on the sarcoplasmic reticulum and of HK2 with mitochondrial outer membrane. An anti-inflammatory effect was also evident in the LV homogenate. We did not observe any of the negative side effects reported for more severe cold conditions in rats (below 5 °C), such as systemic hypertension, LV hypertrophy, hypothermia, or adrenal gland hyperactivation which were described in previous studies[29]. The presented findings highlight the importance of determining the appropriate regimen of cold exposure with respect to the organism in order to achieve its beneficial effect. The duration of the protective action of short-term MCA after its cessation remains to be determined.

Adrenergic signaling, mitochondria, and AMPK recruitment during MCA

Our data suggest that a key point of the MCA-elicited cardioprotection is the enhanced mitochondrial resilience resulting from the shift in adrenergic signaling (β1-AR desensitization and enhancement of β3-AR in the T-tubular system) and AMPK activation. Trappanese et al. documented a link between β1-AR blockade and β3-AR coupling with nitric oxide-linked cGMP signaling[30]. Functional β3-ARs localize exclusively within the transverse T-tubules of healthy rat cardiomyocytes, and its dysregulation occurs in the failing heart[31]. Binding of catecholamines to β3-ARs induces negative inotropic and positive lusitropic effects via the inhibitory pathway of Gi/cGMP/PKG[32,33] and via the control of Ca^{2+} handling[34]. β3-AR/PKG-mediated moderation of Ca^{2+} transient currents can occur via NOS-dependent inhibition of L-type channels, attenuating excitation–contraction coupling[35]. Moreover, PKG-mediated phosphorylation of phospholamban improves Ca^{2+} uptake during cardiac myocyte relaxation[36]. Interestingly, while total Akt tended to decline, p-Akt^{Ser473} decreased significantly in the fully acclimated heart after 10 days of MCA. Recently, we reported that chronic cold exposure (5 weeks) did not alter Akt signaling, whereas the cardioprotection observed after 2 weeks of return to normothermic conditions required the activation of the Akt signaling pathway[10]. Concerning mitochondrial protection, we show here that increased translocation of HK2 to the outer mitochondrial membrane occurred on day 3 of MCA. The effect may improve mitochondrial coupling and reduce ROS production, thus preventing activation of apoptosis through opening of the MPT pore[37]. The HK2-mediated cardioprotective effect was documented under acute stress conditions such as pre-conditioning[38] or severe chronic hypoxia[39], but not under moderate regimens of chronic hypoxia[40]. It is noteworthy that PKG also prevents MPT pore opening via the activation of the mitoK(ATP) channel[41]. The presented data suggest differences in the cardioprotective targets in the early (3 days) and later stage (10 days) of MCA and indicate an important role for both PKG and HK2 in preservation of mitochondrial function during ischemia and reperfusion.

AMPK can be considered as another potential player in cold-induced cardioprotection in the present study, as after 10 days of MCA, the p-AMPK/AMPK ratio markedly increased. AMPK is known to exert pleotropic cytoprotective effects[42] and can be activated by phosphorylation or allosterically when the increased energy expenditure leads to imbalance of the ATP/AMP ratio through adrenergic or thyroid system signaling, or by nutrient-specific upstream signals controlling cell survival and regeneration, and mitochondrial biogenesis[43]. The loss of AMPK sensitivity to activating stimuli is related to ageing[44]. Cardioprotective activation of the AMPK signaling pathway was reported in mice subjected to exercise, and this effect was absent in hearts of β3-AR

knock-out mice[21,45]. Furthermore, both β3-AR and AMPK pathway prevents hypertrophic remodeling and fibrosis, while restoring the cellular energy balance[22,23,46,47]. Our findings align with the potential involvement of AMPK signaling in the protected cardiac phenotype induced by 10-day MCA without signs of hypertrophy.

Batokines FGF21 and IL-6

Brown adipose tissue is regulated by adrenergic signaling and is a potential player in cold-elicited cardioprotective phenotype due to its endocrine function. We characterized BAT maturation based on a significant increase in the BAT/BW ratio, mitochondrial biogenesis, UCP1-dependent respiration, and altered FGF21 spatial expression. In humans, the cold-adaptive phenotype has a beneficial effect on obese and diabetic patients even after 10 days of intermittent cold exposure (14–15 °C for 10 consecutive days)[3,4], which highlighting the clinical relevance of our model. The release of FGF21 from the liver and adipose tissue was reported to reduce cell death and to attenuate myocardial infarction in mice[48]. Additionally, it prevented hypertrophic stimuli via its anti-oxidant/anti-inflammatory action[49]. However, unlike in BAT, we did not observe increased FGF21 in serum, nor did we see changes in FGF21 spatial expression in heart tissue. Our finding suggests that FGF21 is unlikely to play a role in cardioprotection elicited by short-term MCA. Similarly, we can exclude a cardioprotective role of the IL-6 batokine, a key regulator of BAT growth, because its serum and heart tissue levels declined in both protective stages of MCA. Furthermore, acute ablation of BAT 2 h prior to the ischemic insult (considering 2-h half-life of FGF21), did not affect the infarct size-limiting effect (data not shown). Consequently, it appears unlikely that BAT plays a major role in the infarct size-limiting effect induced by MCA in our study. Current investigations into cold-therapy of diabetes, suggest that beneficial effects of CA may stem from tissues other than BAT, which is less abundant in humans[3].

Serum cytokines and chemokines

Moderate cold acclimation (MCA) exerts an impact on sympathetic nervous system, which is known to be a crucial regulator of immune responses especially during ischemic injury[15,50]. In the light of this, we have examined the effect of MCA on IL-6 and IL-10 in the LV cardiac tissue and conducted multiplex analyses of selected cytokines and chemokines in blood serum. We observed a significant reduction in IL-6 levels in the LV tissue. In the serum, MCA led to a decrease in pro-inflammatory T 1 cytokines (IL-17, IL-12p70, IL-6, IL-1β, IFNγ), and three anti-inflammatory T 2 cytokines (IL-4, IL-5, G-CSF). IL-17A participates in inflammation of blood vessels and cardiac cells and is also implicated in the pathogenesis of cardiovascular diseases that occur prematurely in chronic inflammatory disorders including atherosclerosis and myocardial infarction[51,52]. Likewise, while elevation of IL-6 is closely related to atherosclerosis, myocardial infarction, and heart failure, its transient increase also plays a role in tissue proliferation[53]. Activation of IFN-γ signaling pathways is thought to drive atherosclerosis, it is an important target for the prevention and treatment of cardiovascular diseases[54]. A marked decrease in IL-6 and IFN-γ corresponds to a decrease in heterodimeric IL-12p70, their direct regulator in innate adaptive responses[55]. Thus, the substantial downregulation of IL-17, IL-6 and IFN-γ suggests that short-term MCA mediates inflammation-suppressive immunomodulation that possesses a beneficial effect.

Of significant note, the calculated inflammatory ratios demonstrated that the balance between pro- and anti-inflammatory cytokines was maintained at equal level in the completely acclimated rats on day 10 of MCA. While the main players in T 1 pro-inflammatory responses were significantly suppressed by the MCA regimen, the chemotactic cytokines MCP-1 and MCP-3 were upregulated. MCP-1, monocyte chemotactic protein, contributes to routine immunological surveillance[56], and MCP-3 was shown to stimulate the migration of circulating angiogenic cells and promote angiogenesis, suggesting its role in the cardiac repair processes[57].

Regarding inflammatory responses in cardiac tissue, the decline in IL-6 indicates a moderate anti-inflammatory effect of MCA in the heart. It is known that acute I/R insult increases pro-inflammatory T 1 cytokines, as well as several chemokines in the heart tissue, levels of which are critical for subsequent cardiac remodeling and tissue repair[52,58,59]. In this context, the increased whole-body pro-inflammatory status observed during aging and various pathophysiological complications such as obesity and metabolic syndrome which often accompany cardiovascular diseases, might impair the healing process of the injured heart[60]. Moreover, acute coronary syndrome and atherosclerosis are accompanied by asignificant pro-inflammatory T 1/T 2 imbalance[61]. Therefore, we speculate that the MCA-elicited decline of predominantly pro-inflammatory cytokines, while maintaining the balance of the T 1/T 2 ratio, reduces the likelihood of an inflammation burst, thereby potentially contributing to the cardioprotective effect. Notably, the combination of cold exposure training with a breathing exercise robustly attenuates the inflammatory response in healthy young men[62]. However, repeated immersion in cold water (14 °C for 1 h/day, 6 week) exhibited a slight stimulatory effect on the T 1-linked immune system of trained young men[63]. The given data suggests that the intensity and regimen of CA plays pivotal role in the immune response. Further in-depth studies are required in this area to fully comprehend the implications of the immune system in the context of MCA.

Summary

The presented data provide a comprehensive overview of the impact of continuous exposure to moderate cold on β-adrenergic signaling in the left myocardium as well as a systemic profile of cytokines/chemokines during the acute and early phases of the exposure.

In this study we demonstrate that short-term moderate cold exposure enhances myocardial tolerance to I/R injury in rats within as early as 3 days without any apparent negative side effects such as hypertension or myocardial hypertrophy. The cold-elicited cardioprotective effect is accompanied by a reduction in the total number of adrenergic receptors in the membrane fraction, primary involving β1-ARs. Additionally, there is an attenuation of β2-ARs/Akt signaling and reinforcement of the minor subtype of β3-ARs/PKG/AMPK signaling.

These observations suggest that moderate cold exposure leads to modulation of both stimulatory and inhibitory adrenergic pathways contributing to its cardioprotective effect. At the systemic level, our findings revealed a significant shift in the immune status after 10 days of moderate cold exposure implying an anti-inflammatory and immunosuppressive effect.

Taken together, short-term MCA is a safe, non-hypothermic intervention that stimulates endogenous protective pathways not only in the heart but also in the whole organism. It prepares the organism to better cope with acute oxygen deprivation. A detailed understanding of the underlying mechanisms of MCA is a prerequisite for its potential application in future clinical practice.

Materials and methods

Animals, cold exposure protocol, and ischemia–reperfusion injury

Male Wistar rats (12-week-old, 300–350 g body weight, specific-pathogen-free (SPF); from Velaz, s.r.o., Prague, Czech Republic; e.g. inclusion criteria for all experiments) were housed in pairs in well-bedded cages to minimize environmental and social stress. All experiments were performed in the "Winter-Spring" season (November till April) with 12/12 light/dark cycle. We took special care to minimize potential confounders. The animals had free access to water and standard diet (Altromin mod.1324, Velaz s.r.o). Rats were randomly divided into four groups. Three experimental groups were exposed continuously to 9 ± 1 °C for 1, 3 and 10 days (start and end of experiment was at 8 a.m.). The temperature was set below the threshold of shivering thermogenesis[28]. The control group was kept at 24 ± 1 °C throughout experiment. At the end of cold exposure, all animals were anesthetized (thiopental, 60 mg/kg; i.p.) at the respective temperature to avoid an acute thermoregulatory response. At the end of each experiment, hearts were excised under deep anesthesia for further analyses. The number of animals per group ("n") and exclusion criteria are indicated in the respective methods for each experiment when applied.

Cardiac ischemic tolerance

Anesthetized animals (n = 16 per group) were intubated and ventilated (Ugo Basile, Italy) at 60–70 strokes/min (tidal volume of 1.2 ml per 100 g of body weight). Blood pressure in the cannulated carotid artery and a single lead electrocardiogram were recorded using PowerLab and LabChart Pro software (ADInstruments, Australia). Left thoracotomy was performed as follows: a silk braided suture 5/0 (Chirmax s.r.o.) was placed around the left anterior descending coronary artery about 1–2 mm distal to its origin. After a 15-min stabilization, regional myocardial ischemia was induced by tightening the suture through a polyethylene tube. After a 20-min occlusion period, the ligature was released and the chest closed, air was removed from the thorax, and spontaneously breathing animals were maintained under deep anesthesia for 3 h. Then, hearts were excised and washed by perfusion with saline via the aorta. The area at risk (AR) was delineated by perfusion with 5% potassium permanganate when ligature was re-tightened and frozen at − 20 °C as described[10,11,64]. Frozen hearts were cut into 1 mm thick slices and stained with 1% 2,3,5-triphenyltetrazolium chloride (Merck, pH 7.4 and 37 °C) for 30 min, then fixed by immersion in a to 4% paraformaldehyde solution[64]. After 3 days, both sides of the slices were photographed. The infarct size (IS), and the size of the AR and the left ventricle were determined using Graphic Cell Analyzer software[65]. Exclusion criteria for the I/R protocol included the occurrence of cardiac arrhythmias during the stabilization phase, animal death during the experiment, or unsuccessful staining. Based on the above criteria, four animals/hearts were excluded from each experimental group.

Echocardiography

In a separate group of animals (n = 5), in vivo heart imaging was performed prior to and after the acclimation using multimodal Vevo3100/LAZR-X Imaging platform (FUJIFILM VisualSonics, Inc., Toronto, Canada) as follows. Anesthetized animals (isoflurane 3%, 1.2 l/min for initiation and 1.5% for maintenance of anesthesia; Baxter S.A.Bd, Belgium) were placed on a heating pad (up to 37 °C) and connected to electrodes for monitoring the ECG and respiration) using the MX201 transducer (15 MHz frequency). Heart dimensions and function were evaluated by means of the parasternal left ventricle (LV) long-axis view. Rat cardiology transducer and M-mode echocardiography were used (M-mode gain set to 50 dB, B-mode gain 30 dB). The transducer imaging range was set from 6 to 26 mm. the EKV mode acquisition and process style were standard, the frame rate was 1000 Hz, and PSLAX was pre-set. After monitoring, animals had a rest for 4 days to recover from anesthesia and were then exposed to MCA (9 °C) for 10 days, and the whole imaging procedure was repeated. The left ventricular stroke volume (LVSV), ejection fraction (LVEF), fractional shortening (LVFS) and cardiac output (CO) were evaluated using the Vevo lab software. No data were excluded from the analyses.

Isolation of mitochondria

Hearts from another group of animals were excised from anesthetized rats (n = 6) (thiopental, 60 mg/kg) and briefly washed in ice-cold saline. The left and right ventricles and the septum were separated on ice. Immediately after that, interscapular BAT was isolated and properly cleaned from other tissues on ice-cold plate. Mitochondrial fractions were freshly isolated from both fresh LV and BAT as described previously[11,66]. The free LV and BAT tissues were homogenized at 0 °C by a Teflon–glass homogenizer as 10% and 5% homogenate, respectively in a medium containing 250 mM sucrose, 10 mM Tris/HCl, 2 mM EGTA and 0.5 mg/ml of fatty acid-free BSA, pH 7.2. The homogenate was centrifuged for 10 min at 600*g*, and the supernatant was centrifuged for 10 min at 10,000*g*. The mitochondrial sediment was washed twice in a sucrose medium without EGTA and BSA by centrifugation for 10 min at 10,000*g*. Pellets of washed mitochondria were re-suspended in 0.5 ml of 250 mM sucrose, 10 mM Tris/HCl, pH 7.2.

Mitochondrial swelling—cardiac tissue

Fresh myocardial LV mitochondria were tested for calcium sensitivity using mitochondrial swelling as indicated by a decrease in absorbance at 520 nm, measured with a Perkin-Elmer Lambda spectrophotometer at 30 °C in a swelling medium (10 mM HEPES, 65 mM KCl, 125 mM sucrose, 5 mM succinate and 1 mM KH_2PO_4, pH 7.2) as previously described[11,66]. Briefly, isolated mitochondria (~ 0.4 mg of protein) were added to 1 ml of the medium to achieve absorbance of approximately 1. After 1 min of pre-incubation, the swelling medium containing 10 mM $CaCl_2$ solution was added to reach a final concentration of 200 µM, and absorbance was read for 5 min at 1-s intervals. The maximum swelling rate obtained by deriving the swelling curve is expressed as the change in absorbance (ΔA520/1 s) and the moving average of the maximum rate was evaluated as a parameter of mitochondrial membrane permeability (MPT) pore stability. No data were excluded from the analyses.

UCP-dependent respiration—brown adipose tissue

BAT mitochondria were assessed for UCP1-dependent respiration in freshly isolated samples using the O2k-respirometer (Oroboros Instruments, Innsbruck, Austria). All assays were conducted in the K-medium (10 mM Tris, 80 mM KCl, 3 mM $MgCl_2$, 5 mM KH_2PO_4, 0.5 mM EDTA) at 25 °C. UCP1-dependent respiration was directly evaluated by titration of substrates (5 mM pyruvate, 1.5 mM octanoyl-l-carnitine, 10 mM glutamate, 2 mM malate, 10 mM succinate) followed by titration of the UCP1 inhibitor ADP (10–15 mM) and the ATP synthase inhibitor oligomycin (2 µg/ml)[67]. No data were excluded from the analyses.

Cardiac tissue fractionation

Hearts from another group of animals (n = 6) were excised after anesthesia (thiopental, 60 mg/kg) and briefly washed in ice-cold saline. The left and right ventricles and the septum were separated on ice within seconds and snap-frozen in liquid nitrogen, weighed, and stored in liquid nitrogen until use. The free walls of LVs were fractionated for further analyses of β-AR binding by radio-immunoassay and western blotting as follows[11,68]. Each frozen sample was placed in five volumes of ice-cold TMES buffer (20 mM Tris–HCl, 3 mM $MgCl_2$, 1 mM EDTA, 250 mM sucrose; pH 7.4) containing protease and phosphatase inhibitors (cOMPLETE and PhosSTOP, Merck), cut into small pieces and homogenized on ice using the Ultra-Turrax (IKA, Germany) (24,000 rpm, 15 s), and followed by glass homogenizer with motor-driven Teflon pestle (1200 rpm, 2 min). Aliquots of each homogenate sample were stored in liquid nitrogen for further analyses. The homogenate was centrifuged (2100*g*, 10 min, 4 °C, Hettich Universal 320R; Hettich, Germany). The nuclear-free supernatant was collected, and the pellet homogenized in the same volume of TMES buffer and centrifuged again. The supernatants were combined and centrifuged (50,000*g*, 30 min, 4 °C, Beckman Optima L-90K, rotor Ti50, Beckman, USA). The pellet (crude membrane fraction) was homogenized in TMES buffer without sucrose, and aliquots were stored at − 80 °C until use. Protein concentration was assessed using the Bradford method (Merck).

β-Adrenoceptor binding radio-immunoassay

The total number of myocardial β-ARs was determined by the radioligand binding assay with the β-AR antagonist [3H]dihydroalprenolol ([3H]DHA) as described previously[11,69]. In brief, samples of the crude membrane fraction (containing 150 µg protein) were incubated in the medium (total volume of 0.2 ml) containing 50 mM Tris–HCl, 10 mM MgCl2 and 1 ascorbic acid at pH 7.4 along with the β-AR antagonist [3H]DHA (ARC, USA) in at decreasing concentrations from 6 to 0.19 nM. The incubation was carried out at 37 °C for 1 h. The reaction was terminated by adding 3 ml of ice-cold washing buffer (50 mM Tris–HCl, 10 mM $MgCl_2$; pH 7.4), followed by filtration through a GF/C filter pre-soaked for 1 h with 0.3% polyethylenimine. The filter was washed twice with 3 ml of ice-cold washing buffer. After adding 4 ml of scintillation cocktail EcoLite (MP Biomedicals, USA), the radioactivity retained on the filter was assessed by liquid scintillation counting for 5 min. Non-specific binding (background signal) was defined as the signal that was not displaced by 10 µM β-propranolol, representing approximately 40% of the totally bound radioligand. Binding characteristics of β-ARs (Bmax and Kd) in the crude membrane fraction were calculated as previously described and statistically analyzed using One site-specific binding equation, in GraphPad Prism 9 software. All Bmax and Kd values obtained through nonlinear regression analysis of samples from individual animals were included. No exclusion criteria were applied to the results of individual animals. Addressing the original data processing, the following exclusion criteria were applied. For total and nonspecific binding, data points that did not fall on the curve of the nonlinear and linear regression analyzes, respectively, were subjected to review, and outliers that deviated from the mean by more than 25% were excluded.

Western blot analysis

Individual LV (n = 5–6 per group) samples, diluted in Laemmli sample buffer (BioRad), of from the crude membrane fraction, nuclei-free supernatant and mitochondrial fraction from each group (20–30 µg, 20 µg and 30 µg protein per lane, respectively) were resolved by sodium dodecyl sulfate electrophoresis on 10–12% polyacrylamide gels at a constant voltage of 200 V using Mini-Protean Tetra Cell (Bio-Rad). The gel-resolved proteins were electro-transferred onto the nitrocellulose membrane (0.2 µm pore size, BioRad) at a constant voltage of 100 V and 350 mA current for 1 h using Mini Trans-Blot Module (Bio-Rad) according to manufactures instructions. The nitrocellulose membranes (0.22 µm pore, BioRad) were then blocked with 5% non-fat milk in Tris-buffered saline for 1 h, and incubated overnight at 4 °C with the following polyclonal antibodies, according to manufacturer's instructions: β2-Ars (bs-0947R, Bioss, USA), β3-Ars (bs-1063R), Gs, Gi1/2, and Gi3 (RCS polyclonal antibody)[70] for the crude membrane fraction, AMPK (2532, Cell Signaling, USA), p-AMPK$^{\alpha\ r172}$ (sc-33524, Santa Cruz, USA), PKA (sc-365615), pPKA (sc-32968), PKG (C8A4, Cell Signaling) for the nuclei-free supernatant, and HK1 (sc-28885), HK2 (sc-6521) for the mitochondrial fraction. After washing, membranes

were incubated with secondary HRP-conjugated anti-rabbit (A9169 or A0645, Merck), anti-mouse (sc-2371) or anti-goat antibody (AP180P). Protein bands were visualized with the ECL SuperSignal substrate (34075, Thermo Fisher Scientific, USA) using the LAS-4000 imaging system (Fujifilm, Japan). The intensity of protein bands was quantified densitometrically using ImageJ[71]. At least three samples from each group were run on the same gel in technical duplicates, quantified on the same membrane, and normalized to total protein content loaded per lane as determined by Ponceau S (Merck) staining. Prestained protein ladders (BioRad) were used as molecular weight markers. The accuracy and reproducibility of the chemiluminescence signal were validated by loading samples at ascending concentrations of 20 to 30 µg protein per lane. In the original data processing, exclusion criteria were sporadically applied when a normalized value of the triplicate in a gel differed by at least half an order of magnitude.

Quantitative immunofluorescence microscopy

In separate animal groups (n = 5 per group), hearts were excised from anesthetized rats, relaxed by perfusion with the relaxation Tyrode solution and fixed with freshly prepared 4% formaldehyde solution using the Langendorff apparatus. LV samples were treated aspreviously reported[39,72]. Similarly, pieces of isolated BAT (1 mm^3) were fixed with 4% formaldehyde, cryoprotected by 20% sucrose, frozen and stored at −80 °C. Sections (5–7 µm) of both BAT and LV samples were cut using a cryostat (Leica CM3050, Leica microsystems, Germany), rehydrated in PBS, permeabilized in ice-cold methanol, and incubated (5 min) in 1% SDS in PBS for antigen retrieval. Sections were incubated for 80 min in the blocking solution at room temperature (10% donkey serum, 10% goat serum, 0.3% Triton X-100, 0.3 M glycine in PBS), and incubated with the following primary antibodies at 4 °C overnight: UCP1 (ab-23841, Abcam, UK) and FGF21 (ab-171941) for BAT, β2-AR (bs-0947R), β3-AR (bs-1063R), HK1 (ab-150423), and HK2 (ab-78259) and PKG1 (C8A4, Cell Signaling) for the LV, and then with the secondary donkey anti-rabbit IgG AlexaFluor488 conjugate (A21206, ThermoFisher Scientific) for 1 h at room temperature. The fluorescence marker for mitochondria was the anti-OXPHOS Ab cocktail (ab-110412), while for sarcolemma, and T-tubules we used the wheat germ agglutinin (WGA) Alexa-647 conjugate (W-32466, ThermoFisher Scientific). Additionally, for the sarcoplasmic reticulum we used anti-phospholamban (ab-2865). Sections were mounted in ProLong Gold Antifade Reagent with DAPI (Invitrogen). Images were captured from at least 5 randomly selected fields of view (FOV) for each section using a wide-field inverted microscope (NikonTi2) equipped with a set of LED illumination for fluorescence imaging (Nikon, Tokyo, Japan). Images were deconcolved and pre-processed using the Nikon Microscope Imaging Software (NIS-Elements). The extent of co-localization was calculated using the thresholded Manders M1 or M2 coefficient[73] through the Colocalization Threshold plug-in in FIJI software[74]. No data were excluded from the analyses and any missing values in the raw dataset were a result of the colocalization algorithm.

Multiplex and ELISA analysis of blood serum and heart homogenate

Rat serum samples (n = 6 per group) were collected and stored in liquid nitrogen. Prior to analysis, they were thawed on ice and centrifuged (10,000*g*, 10 min, 4 °C) for pre-cleaning. Concentrations of 22 cytokines (G-CSF, GM-CSF, IFNγ, IL-1α, IL-1β, IL-2, IL-4, IL-5, IL-6, IL-10, IL-12p70, IL-13, IL-17A, TNFα) and chemokines (Eotaxin, GROα, IP-10, MCP-1, MCP-3, MIP-1α, MIP-2, RANTES) were analyzed using the Cytokine & Chemokine 22-Plex Rat ProcartaPlex™ Panel (EPX220-30122-901, ThermoFisher Scientific). Serum samples were diluted at a 1:1 ratio with the Assay Diluent to minimize matrix effects. The same diluent was used as a blank and for the preparation of calibration standards. Reverse pipetting was employed for high accuracy in all liquid handling steps. All samples, standards and blanks were analyzed in two technical replicates following the manufacturer's instructions. The fluorescence intensities of at least 100 beads per analyte were recorded using the Luminex 200™ analyzer with the xPonent software build 3.1.871.0 (Luminex Corp.) properly calibrated according to the manufacturer's instructions. No data were excluded from the analyses. Sporadic missing values in the raw dataset were designated as *n.a.* outputs from the reader.

Raw data were processed in R statistical environment version 4.1.2[75] using drLumi package[76]. The median fluorescence intensity (MFI) for Luminex xMAP data and absorbance for FGF21 ELISA data were used for standard curve fitting and quantitation of cytokine/chemokine concentrations as previously described[77]. Concentrations or MFI/absorbances of two technical replicates of each sample were averaged before further statistical analysis.

Concentration of FGF21 in rat blood serum and IL-6, and IL-10 in LV nuclear free supernatant were determined using an ELISA kit (ab-223589; BMS625, ThermoFisher Scientific, ab100764) following the manufacturer´s instructions with the following modifications: Serum was diluted 1:1 with Sample Diluent NS (ab-193972), and 850 µg and 425 µg of LV protein were loaded per well for IL-10 and IL-6 analyses, respectively. Kinetic evaluation of absorbance at 600 nm was performed for 20 min in 30 s intervals, with shaking between reads (Synergy microplate reader, Biotek, USA). After a 20-min interval, 100 µl of Stop Solution was added to each well and endpoint absorbance at 450 nm was measured using the same instrument. No data were excluded from the analyses.

Statistical analysis

The sample size of experimental animals was statistically estimated using the resource equation approach and adjusted in accordance with ethical standards for animal experimentation. For the analysis of infarct size, twelve hearts were included in each group. Mitochondrial fractions from half of the six LV samples were used for swelling analysis. In each group, six whole LVs were fractioned and used for WB analyses, ELISA, and the receptor binding assay. For quantitative immunofluorescence analysis, samples from five hearts per group were employed. Echocardiography involved five animals per group. Statistical analyses were conducted using the GraphPad Prism 8 software (GraphPad, San Diego, CA). The distribution of data was analyzed by Shapiro–Wilk and Kolmogorov–Smirnov normality tests. The identification of outliers was carried out using the ROUT (Robust

regression and Outlier removal) method with a ROUT coe cient set at Q = 1%. For parametric data, one-way ANOVA with Dunnett's multiple comparison test was employed to identify signi cant di erences between the means of individual groups. e signi cance level of p 0.05 was considered statistically signi cant. Data are presented as means ± SD. To visualize the levels of analyzed cytokines and chemokines in six serum samples per group, the raw MFI values from Luminex measurement were log10 transformed. All values were further scaled and centered, and the heatmap was constructed using the R package ComplexHeatmap[78]. Using the same data matrix, principal component analysis (PCA) was also performed to identify the major contributors to di er-ences among experimental groups. e rst two principal components (PC1) and (PC2) were visualized using the R package ggbiplot[79].

Limitation of the study

It should be mentioned, however, that the smaller number of samples (n = 5) in some analyses could be considered a certain limitation of the study.

Ethics statement

e study is reported in accordance with ARRIVE guidelines of animal research. Animals were handled in accordance with the Guide for the Care and Use of Laboratory Animals published by the US National Institutes of Health (NIH Publication, 8th edition, revised 2011). e experimental protocol was approved by the Animal Care and Use Committee of the Faculty of Science, Charles University and Ministry of Education, Youth and Sport, Prague, Czech Republic, No. MSMT-12457/2021-3.

Data availability

e datasets generated and analyzed during the current study are available in the FigShare public repository under the doi number https://doi.org/10.6084/m9.gshare.23301260.

Received: 4 July 2023; Accepted: 4 October 2023
Published online: 25 October 2023

References

1. Heusch, G. Critical issues for the translation of cardioprotection. *Circ. Res.* **120**, 1477–1486 (2017).
2. Paradies, V., Chan, M. H. H. & Hausenloy, D. J. Strategies for reducing myocardial infarct size following STEMI. *Primary Angioplasty* 307–322. https://pubmed.ncbi.nlm.nih.gov/31314426/ (2018).
3. Hanssen, M. J. W. *et al.* Short-term cold acclimation improves insulin sensitivity in patients with type 2 diabetes mellitus. *Nat. Med.* **21**, 863–865 (2015).
4. Hanssen, M. J. W. *et al.* Short-term cold acclimation recruits brown adipose tissue in obese humans. *Diabetes* **65**, 1179–1189 (2016).
5. KralovaLesna, I., Rychlikova, J., Vavrova, L. & Vybiral, S. Could human cold adaptation decrease the risk of cardiovascular disease?. *J. erm. Biol.* **52**, 192–198 (2015).
6. Sun, Z. & Cade, R. Cold-induced hypertension and diuresis. *J. erm. Biol.* **25**, 105–109 (2000).
7. ClinicalTrials.gov. *Chronic Cold Exposure and Energy Metabolism in Humans*. https://beta.clinicaltrials.gov/study/NCT01730105 (U. S. National Library of Medicine, 2022).
8. ClinicalTrials.gov. *e E ect of Cold Exposure on Energy Expenditure*. https://beta.clinicaltrials.gov/study/NCT05107570 (U. S. National Library of Medicine, 2022).
9. ClinicalTrials.gov. *Cold Acclimation as a Modulator of Brown Adipose Tissue Function in Adults with Obesity* (*MOTORBAT*). https://beta.clinicaltrials.gov/study/NCT05468151 (U. S. National Library of Medicine, 2022).
10. Tibenska, V. *et al.* e cardioprotective e ect persisting during recovery from cold acclimation is mediated by the b2-adrenoceptor pathway and Akt activation. *J. Appl. Physiol.* **130**, 746–755 (2021).
11. Tibenska, V. *et al.* Gradual cold acclimation induces cardioprotection without a ecting -adrenergic receptor-mediated adenylyl cyclase signaling. *J. Appl. Physiol.* **128**, 1023–1032 (2020).
12. Le owitz, R. J., Rockman, H. A. & Koch, W. J. Catecholamines, cardiac -adrenergic receptors, and heart failure. *Circulation* **101**, 1634–1637 (2000).
13. Scanzano, A. & Cosentino, M. Adrenergic regulation of innate immunity: A review. *Front. Pharmacol.* **6**, 1–18 (2015).
14. Grisanti, L. A. *et al.* 2-Adrenergic receptor-dependent chemokine receptor 2 expression regulates leukocyte recruitment to the heart following acute injury. *Proc. Natl. Acad. Sci. USA* **113**, 15126–15131 (2016).
15. Grisanti, L. A. *et al.* Leukocyte-expressed 2-adrenergic receptors are essential for survival a er acute myocardial injury. *Circulation* **134**, 153–167 (2016).
16. Brodde, O. E., Michel, M. C., Brodde, O. E. & Michel, M. C. Adrenergic and muscarinic receptors in the human heart. *Pharmacol. Rev.* **51**, 651–689 (1999).
17. Barki-Harrington, L., Perrino, C. & Rockman, H. A. Network integration of the adrenergic system in cardiac hypertrophy. *Cardiovasc. Res.* **63**, 391–402 (2004).
18. Lohse, M. J., Engelhardt, S. & Eschenhagen, T. What is the role of -adrenergic signaling in heart failure?. *Circ. Res.* **93**, 896–906 (2003).
19. Balligand, J. L. Cardiac salvage by tweaking with beta-3-adrenergic receptors. *Cardiovasc. Res.* **111**, 128–133 (2016).
20. Micova, P. *et al.* Chronic intermittent hypoxia affects the cytosolic phospholipase A2 /cyclooxygenase 2 pathway via 2-adrenoceptor-mediated ERK/p38 stimulation. *Mol. Cell. Biochem.* **423**, 151–163 (2016).
21. Barr, L. A. *et al.* Exercise training provides cardioprotection by activating and coupling endothelial nitric oxide synthase via a 3-adrenergic receptor-AMP-activated protein kinase signaling pathway. *Med. Gas Res.* **7**, 1–8 (2017).
22. Belge, C. *et al.* Enhanced expression of 3-adrenoceptors in cardiac myocytes attenuates neurohormone-induced hypertrophic remodeling through nitric oxide synthase. *Circulation* **129**, 451–462 (2014).
23. Dubois-Deruy, E. *et al.* Beta 3 adrenoreceptors protect from hypertrophic remodelling through AMP-activated protein kinase and autophagy. *ESC Hear. Fail.* **7**, 920–932 (2020).
24. Sentis, S. C., Oelkrug, R. & Mittag, J. yroid hormones in the regulation of brown adipose tissue thermogenesis. *Endocr. Connect.* **10**, R106–R115 (2021).
25. Nedergaard, J., Wang, Y. & Cannon, B. Cell proliferation and apoptosis inhibition: Essential processes for recruitment of the full thermogenic capacity of brown adipose tissue. *Biochim. Biophys. Acta-Mol. Cell Biol. Lipids* **1864**, 51–58 (2019).
26. Hanssen, M. J. W. *et al.* Serum FGF21 levels are associated with brown adipose tissue activity in humans. *Sci. Rep.* **5**, 1–8 (2015).

27. Villarroya, J. *et al.* New insights into the secretory functions of brown adipose tissue. *J. Endocrinol.* **243**, R19–R27 (2019).
28. Lømo, T., Eken, T., Bekkestad Rein, E. & Njå, A. Body temperature control in rats by muscle tone during rest or sleep. *Acta Physiol.* **228**, 1–26 (2020).
29. Shechtman, O., Fregly, M. J. & Papanek, P. E. Factors a□ecting cold-induced hypertension in rats. *Proc. Soc. Exp. Biol. Med.* **195**, 364–368 (1990).
30. Trappanese, D. M. *et al.* Chronic □1-adrenergic blockade enhances myocardial □3-adrenergic coupling with nitric oxide-cGMP signaling in a canine model of chronic volume overload: New insight into mechanisms of cardiac bene□t with selective □1-blocker therapy. *Basic Res. Cardiol.* **110**, 1–26 (2015).
31. Schobesberger, S. *et al.* □-Adrenoceptor redistribution impairs NO/cGMP/PDE2 signalling in 4 failing cardiomyocytes. *Elife* **9**, 1–15 (2020).
32. Gauthier, C. *et al.* □ e negative inotropic e□ect of □3-adrenoceptor stimulation is mediated by activation of a nitric oxide synthase pathway in human ventricle. *J. Clin. Invest.* **102**, 1377–1384 (1998).
33. Mongillo, M. *et al.* Compartmentalized phosphodiesterase-2 activity blunts □-adrenergic cardiac inotropy via an NO/cGMP-dependent pathway. *Circ. Res.* **98**, 226–234 (2006).
34. Farah, C., Michel, L. Y. M. & Balligand, J. L. Nitric oxide signalling in cardiovascular health and disease. *Nat. Rev. Cardiol.* **15**, 292–316 (2018).
35. Cheng, H. J. *et al.* Upregulation of functional □3-adrenergic receptor in the failing canine myocardium. *Circ. Res.* **89**, 599–606 (2001).
36. Jin, C. Z. *et al.* Neuronal nitric oxide synthase is up-regulated by angiotensin II and attenuates NADPH oxidase activity and facilitates relaxation in murine le□ ventricular myocytes. *J. Mol. Cell. Cardiol.* **52**, 1274–1281 (2012).
37. Calmettes, G. *et al.* Hexokinases and cardioprotection. *J. Mol. Cell. Cardiol.* **78**, 107–115 (2015).
38. Halestrap, A. P., Pereira, G. C. & Pasdois, P. □ e role of hexokinase in cardioprotection—Mechanism and potential for translation. *Br. J. Pharmacol.* **172**, 2085–2100 (2015).
39. Waskova-Arnostova, P. *et al.* Cardioprotective adaptation of rats to intermittent hypobaric hypoxia is accompanied by the increased association of hexokinase with mitochondria. *J. Appl. Physiol.* **119**, 1487–1493 (2015).
40. Waskova-Arnostova, P. *et al.* Chronic hypoxia enhances expression and activity of mitochondrial creatine kinase and hexokinase in the rat ventricular myocardium. *Cell. Physiol. Biochem.* **33**, 310–320 (2014).
41. Costa, A. D. T. & Garlid, K. D. Intramitochondrial signaling: Interactions among mitoKATP, PKC□, ROS, and MPT. *Am. J. Physiol.-Heart Circ. Physiol.* **295**, H874–H882 (2008).
42. Li, X. *et al.* AMPK: A therapeutic target of heart failure—Not only metabolism regulation. *Biosci. Rep.* **39**, 1–13 (2019).
43. Marino, A. *et al.* AMP-activated protein kinase: A remarkable contributor to preserve a healthy heart against ROS injury. *Free Radic. Biol. Med.* **166**, 238–254 (2021).
44. Salminen, A. & Kaarniranta, K. AMP-activated protein kinase (AMPK) controls the aging process via an integrated signaling network. *Ageing Res. Rev.* **11**, 230–241 (2012).
45. Calvert, J. W. *et al.* Exercise protects against myocardial ischemia-reperfusion injury via stimulation of □3-adrenergic receptors and increased nitric oxide signaling: Role of nitrite and nitrosothiols. *Circ. Res.* **108**, 1448–1458 (2011).
46. Hermida, N. *et al.* Cardiac myocyte □3-adrenergic receptors prevent myocardial □brosis by modulating oxidant stress-dependent paracrine signaling. *Eur. Heart J.* **39**, 888–898 (2018).
47. Horman, S., Beauloye, C., Vanoverschelde, J. L. & Bertrand, L. AMP-activated protein kinase in the control of cardiac metabolism and remodeling. *Curr. Heart Fail. Rep.* **9**, 164–173 (2012).
48. Liu, S. Q. *et al.* Endocrine protection of ischemic myocardium by FGF21 from the liver and adipose tissue. *Sci. Rep.* **3**, 1–11 (2013).
49. Planavila, A. *et al.* Fibroblast growth factor 21 protects against cardiac hypertrophy in mice. *Nat. Commun.* **4**, 1–12 (2013).
50. Mann, D. L. Innate immunity and the failing heart: □ e cytokine hypothesis revisited. *Circ. Res.* **116**, 1254–1268 (2015).
51. Robert, M. & Miossec, P. E□ects of interleukin 17 on the cardiovascular system. *Autoimmun. Rev.* **16**, 984–991 (2017).
52. Mills, K. H. G. IL-17 and IL-17-producing cells in protection versus pathology. *Nat. Rev. Immunol.* **23**, 38–54 (2023).
53. Kanda, T. & Takahashi, T. Interleukin-6 and cardiovascular diseases. *Jpn. Heart J.* **45**, 183–193 (2004).
54. Elyasi, A. *et al.* □ e role of interferon-□ in cardiovascular disease: An update. *In□amm. Res.* **69**, 975–988 (2020).
55. Trinchieri, G. Interleukin-12 and the regulation of innate resistance and adaptive immunity. *Nat. Rev. Immunol.* **3**, 133–146 (2003).
56. Deshmane, S. L., Kremlev, S., Amini, S. & Sawaya, B. E. Monocyte chemoattractant protein-1 (MCP-1): An overview. *J. Interf. Cytokine Res.* **29**, 313–325 (2009).
57. Bousquenaud, M. *et al.* Monocyte chemotactic protein 3 is a homing factor for circulating angiogenic cells. *Cardiovasc. Res.* **94**, 519–525 (2012).
58. Liu, J. *et al.* Eosinophils improve cardiac function a□er myocardial infarction. *Nat. Commun.* **11**, 1–15 (2020).
59. Sharma, H. S. & Das, D. K. Role of cytokines in myocardial ischemia and reperfusion. *Mediators In□amm.* **6**, 175–183 (1997).
60. Henein, M. Y., Vancheri, S., Longo, G. & Vancheri, F. □ e role of in□ammation in cardiovascular disease. *Int. J. Mol. Sci.* **23**, 1–23 (2022).
61. Szodoray, P. *et al.* □ 1/□ 2 imbalance, measured by circulating and intracytoplasmic in□ammatory cytokines—Immunological alterations in acute coronary syndrome and stable coronary artery disease. *Scand. J. Immunol.* **64**, 336–344 (2006).
62. Zwaag, J., Naaktgeboren, R., Van Herwaarden, A. E., Pickkers, P. & Kox, M. □ e e□ects of cold exposure training and a breathing exercise on the in□ammatory response in humans: A pilot study. *Psychosom. Med.* **84**, 457–467 (2022).
63. Janský, L. *et al.* Immune system of cold-exposed and cold-adapted humans. *Eur. J. Appl. Physiol. Occup. Physiol.* **72**, 445–450 (1996).
64. Kasparova, D. *et al.* Cardioprotective and nonprotective regimens of chronic hypoxia diversely a□ect the myocardial antioxidant systems. *Physiol. Genomics* **47**, 612–620 (2015).
65. Parulek, J., Srámek, M., Cerveanský, M., Novotová, M. & Zahradník, I. A cell architecture modeling system based on quantitative ultrastructural characteristics. *Methods Mol. Biol.* **500**, 289–312 (2009).
66. Necká□ J. *et al.* Selective replacement of mitochondrial DNA increases the cardioprotective e□ect of chronic continuous hypoxia in spontaneously hypertensive rats. *Clin. Sci.* **131**, 865–881 (2017).
67. Porter, C. *et al.* Human and mouse brown adipose tissue mitochondria have comparable UCP1 function. *Cell Metab.* **24**, 246–255 (2016).
68. Hahnova, K. *et al.* □-Adrenergic signaling in rat heart is similarly a□ected by continuous and intermittent normobaric hypoxia. *Gen. Physiol. Biophys.* **35**, 165–173 (2016).
69. Klevstig, M. *et al.* Transgenic rescue of defective Cd36 enhances myocardial adenylyl cyclase signaling in spontaneously hypertensive rats. *P□ugers Arch. Eur. J. Physiol.* **465**, 1477–1486 (2013).
70. Ihnatovych, I. *et al.* Maturation of rat brain is accompanied by di□erential expression of the long and short splice variants of G(s) alpha protein: identi□cation of cytosolic forms of G(s)alpha. *J. Neurochem.* **79**, 88–97 (2001).
71. Schneider, C. A., Rasband, W. S. & Eliceiri, K. W. NIH Image to ImageJ: 25 years of image analysis. *Nat. Methods* **9**, 671–675 (2012).
72. Kohutova, J. *et al.* Anti-arrhythmic cardiac phenotype elicited by chronic intermittent hypoxia is associated with alterations in connexin-43 expression, phosphorylation, and distribution. *Front. Endocrinol. (Lausanne)* **9**, 1–10 (2019).
73. Manders, E. M. M., Verbeek, F. J. & Aten, J. A. Measurement of co-localization of objects in dual-colour confocal images. *J. Microsc.* **169**, 375–382 (1993).
74. Schindelin, J. *et al.* Fiji: An open-source platform for biological-image analysis. *Nat. Methods* **9**, 676–682 (2012).

75. R Core Team. *R: A Language and Environment for Statistical Computing*. https://www.r-project.org/ (R Foundation for Statistical Computing, 2021).
76. Sanz, H. *et al.* drLumi: An open-source package to manage data, calibrate, and conduct quality control of multiplex bead-based immunoassays data analysis. *PLoS One* **12**, 1–18 (2017).
77. KupcovaSkalnikova, H., VodickovaKepkova, K. & Vodicka, P. Luminex xMAP assay to quantify cytokines in cancer patient serum. *Methods Mol. Biol.* **2108**, 65–88 (2020).
78. Gu, Z., Eils, R. & Schlesner, M. Complex heatmaps reveal patterns and correlations in multidimensional genomic data. *Bioinformatics* **32**, 2847–2849 (2016).
79. Vu, V. Q. *GitHub—vqv/ggbiplot: A Biplot Based on ggplot2*. https://github.com/vqv/ggbiplot (2011).

Acknowledgements

is work has been supported by the Charles University Grant Agency (GAUK 37232), PK and FG acknowledge support by the project "Grant Schemes at CU" (reg. no. CZ.02.2.69/0.0/0.0/19_073/0016935). Charles University Institutional Research Fund (SVV-260683). FK acknowledge support by the project National Institute for Research of Metabolic and Cardiovascular Diseases (Program EXCELES, Project No. LX22NPO5104)—funded by the European Union—Next Generation EU. Microscopy co-nanced by the Czech-BioImaging large RI project LM2018129. Computational resources were supplied by the project "e-Infrastruktura CZ" (e-INFRA LM2018140) provided within the program Projects of Large Research, Development and Innovations Infrastructure.

Author contributions

A.M. O.N., F.K. and J.Z. are responsible for the conception or design of the research. A.M., P.K., B.E., F.G., D.H., V.Z., P.M. P.Ve., V.T., P.Vo., L.H., B.S.B., M.S., and J.Z. performed the experiments and analyzed the data. B.E., D.H., O.N., J.No, P.Vo., J.Ne., F.K. and J.Z. interpreted the results of the experiments. B.E., P.Vo., D.H. and J.Z. prepared graphs and gures. B.E., P.Vo. and J.Z. performed statistical analyses and nal design of all gures in the Adobe Ilustrators. A.M. J.Z., and O.N. dra ed the manuscript; J.Ne., J.No., and F.K. edited and revised the manuscript; all authors approved the nal version of the manuscript.

Competing interests

e authors declare no competing interests.

Additional information

Correspondence and requests for materials should be addressed to J.M.Z.

Reprints and permissions information is available at www.nature.com/reprints.

Publisher's note Springer Nature remains neutral with regard to jurisdictional claims in published maps and institutional a liations.

J Appl Physiol 130: 746–755, 2021.
First published December 18, 2020; doi:10.1152/japplphysiol.00756.2020

american physiological society

JOURNAL OF APPLIED PHYSIOLOGY

RESEARCH ARTICLE

Physiology of Thermal Therapy

The cardioprotective effect persisting during recovery from cold acclimation is mediated by the β_2-adrenoceptor pathway and Akt activation

Veronika Tibenska,[1]* Aneta Marvanova,[1]* Barbara Elsnicova,[1] Lucie Hejnova,[1] Pavel Vebr,[1] Jiri Novotný,[1] Frantisek Kolar,[2] Olga Novakova,[1,2] and Jitka M. Zurmanova[1]

[1]*Department of Physiology, Faculty of Science, Charles University, Prague, Czech Republic and* [2]*Institute of Physiology of the Czech Academy of Sciences, Prague, Czech Republic*

Abstract

The infarct size-limiting effect elicited by cold acclimation (CA) is accompanied by increased mitochondrial resistance and unaltered β_1-adrenergic receptor (AR) signaling persisting for 2 wk at room temperature. As the mechanism of CA-elicited cardioprotection is not fully understood, we examined the role of the salvage β_2-AR/G_i/Akt pathway. Male Wistar rats were exposed to CA (8°C, 5 wk), whereas the recovery group (CAR) was kept at 24°C for additional 2 wk. We show that the total number of myocardial β-ARs in the left ventricular myocardium did not change after CA but decreased after CAR. We confirmed the infarct size-limiting effect in both CA and CAR groups. Acute administration of β_2-AR inhibitor ICI-118551 abolished the protective effect in the CAR group but had no effect in the control and CA groups. The inhibitory $G_i\alpha_{1/2}$ and $G_i\alpha_3$ proteins increased in the membrane fraction of the CAR group, and the phospho-Akt (Ser^{473})-to-Akt ratio also increased. Expression, phosphorylation, and mitochondrial location of the Akt target glycogen synthase kinase (GSK-3β) were affected neither by CA nor by CAR. However, GSK-3β translocated from the Z-disk to the H-zone after CA, and acquired its original location after CAR. Our data indicate that the cardioprotection observed after CAR is mediated by the β_2-AR/G_i pathway and Akt activation. Further studies are needed to unravel downstream targets of the central regulators of the CA process and the downstream targets of the Akt protein after CAR.

NEW & NOTEWORTHY Cardioprotective effect of cold acclimation and that persisting for 2 wk after recovery engage in different mechanisms. The β_2-adrenoceptor/G_i pathway and Akt are involved only in the mechanism of infarct size-limiting effect occurring during the recovery phase. GSK-3β translocated from the Z-line to the H-zone of sarcomeres by cold acclimation returns back to the original position after the recovery phase. The results provide new insights potentially useful for the development of cardiac therapies.

β 2-adrenergic signaling; cardioprotection; cold acclimation; glycogen synthase kinase-3β; protein kinase B/Akt

INTRODUCTION

Despite intensive research, acute myocardial infarction remains a leading cause of death and disability. New approaches are therefore needed to reduce myocardial infarct size and its severity. Recently, it was reported that cold acclimation (CA) possesses an infarct size-limiting effect (1, 2). We have documented that exposure of rats to 5 wk of gradual mild cold acclimation (CA), followed by 2 wk of recovery resulted in reduction of myocardial infarct size without apparent side effects such as hypertension or hypertrophy. We suggested that β-adrenergic signaling plays a significant role in the development of cardioprotection triggered by CA, but its mechanism is not known (1).

There are three subtypes of β-adrenoceptors (β-ARs) in the ventricular myocardium, β_1-ARs, β_2-ARs, and β_3-ARs (3). The predominant β_1-ARs, coupled to $G_s\alpha$ are required for hormone-stimulated cAMP generation by adenylyl cyclase, which stimulates the activity of PKA. Acute activation of PKA results in phosphorylation of target proteins and promotes positive inotropic and lusitropic effects; its persistent activation is, however, detrimental (4). Our recent study showed that cold-induced cardioprotection implies an unaltered β_1-AR/adenylyl cyclase/cAMP pathway, including stable levels of phosphorylated PKA and G_s. We confirmed the finding by acute administration of β_1-AR antagonist (metoprolol), which did not affect the CA-elicited cardioprotection. Simultaneously, increased β_2-AR translocation to the

* V. Tibenska and A. Marvanova contributed equally to this work.
Correspondence: J. M. Zurmanova (jitka.zurmanova@natur.cuni.cz).
Submitted 2 September 2020 / Revised 15 December 2020 / Accepted 15 December 2020

membrane fraction was observed after CA, and it remained upregulated for 2 wk of recovery at 24°C following CA (1).

It is known that β_2-ARs, unlike β_1-ARs, signal via both G_s and G_i proteins (5). Thus, β_2-ARs can activate not only G_s/cAMP-dependent PKA signaling pathways but also G_i protein-dependent pathways. This includes, for example, phosphoinositide-3-kinase/protein kinase B (PI3K/Akt) (6) and cytosolic phospholipase A_2 that dampen the β_2-AR/cAMP/PKA signaling in the heart in a pertussis toxin-sensitive manner (7, 8). Activation of β_2-ARs is implicated in the cardioprotective effect of preconditioning (9), and both downstream kinases, PKA and Akt, were found to play an important role in this process (10). Phosphorylation of Ser^{473} of Akt is believed to be a crucial step in its activation, since it stabilizes the kinase domain in its active conformation (11). The β_2-AR/G_i/PI3K/Akt signaling axis that promotes cell survival (12) has been repeatedly reported to be cardioprotective (13–15). The Akt-elicited antiapoptotic effect is mediated mainly via mitochondria by inhibition of the mitochondrial permeability transition pore (mPTP) opening, presenting a key terminal effector of cardioprotection and cell death (16, 17).

In the present study, we examined the role of β_2-AR/G_i signaling and the possible involvement of Akt kinase in the CA-elicited infarct size-limiting effect. The results of our study indicate that the β_2-AR pathway plays a protective role in cardioprotection during the recovery phase after CA.

METHODS

Cold Acclimation and Ischemia-Reperfusion Injury

The cold acclimation and ischemia-reperfusion protocol was performed as previously described (1). Male Wistar rats (7-wk old, 200 g body weight, Velaz, Prague, Czech Republic) were housed in pairs in well-bedded cages to minimize environmental and social stress. All experiments were performed in the "winter-spring" season (from November to April). The animals were handled in accordance with the National Institutes of Health Guide for the Care and Use of Laboratory Animals (NIH Publication, 8th ed., Revised 2011). The experimental protocol was approved by the Animal Care and Use Committee of the Faculty of Science, Charles University, Prague, Czech Republic.

Rats divided into two experimental groups were acclimated to 8 ± 1°C for 8 h/day during the 1st wk and then for 24 h/day during the following 4 wk, either without (CA, n = 24) or with 2 wk of recovery at 24 ± 1°C (CAR, n = 24). The control group (n = 24) was kept at 24 ± 1°C during the whole experiment. At the end of acclimation, the animals were anesthetized (thiopental, 60 mg/kg) at the respective acclimation temperature to prevent acute thermoregulatory response. Twelve animals from each group were treated after anesthesia by the β_2-AR selective inhibitor ICI-118551 (Sigma-Aldrich; dissolved in saline), which was administered intraperitoneally at 1 mg/kg of body weight 20 min before coronary occlusion. The same volume of saline was administered in the respective control subgroups. Anesthetized animals were intubated, connected to a rodent ventilator (Ugo Basile, Italy), and ventilated at 60–70 strokes/min (tidal volume of 1.2 mL per 100 g of body weight). Systemic blood pressure was monitored by cannulation of the carotid artery and a single-lead electrocardiogram was recorded using PowerLab and LabChart Pro software (ADInstruments). The rats were subjected to left thoracotomy, followed by 10 min stabilization, left coronary artery occlusion for 20 min, and subsequent 3-h reperfusion. Then the hearts were excised, and the area at risk was delineated by perfusion with 5% potassium permanganate. Frozen hearts were cut to 1-mm thick slices and infarct size was visualized by staining with 1% 2,3,5-triphenyltetrazolium chloride (Sigma-Aldrich) as described previously (18). Infarct size and area at risk were quantified by the Graphic Cell Analyzer software (19).

Homogenate and Crude Membrane Fraction Preparation

Hearts from individual groups of animals (n = 8) were collected under the same conditions. Briefly, hearts were excised from anesthetized rats (thiopental, 60 mg/kg) and quickly washed in ice-cold saline. Left and right ventricles and the septum were separated. The left ventricle (LV) free wall was snap-frozen in liquid nitrogen, weighed, and stored in liquid nitrogen until use as described previously (20). Each frozen LV sample was placed in five volumes of ice-cold TMES buffer (20 mM Tris-HCl, 3 mM $MgCl_2$, 1 mM EDTA, 250 mM sucrose; pH 7.4) containing protease and phosphatase inhibitors (cOMPLETE and PhosSTOP, Sigma-Aldrich), cut into small pieces, and homogenized on ice using an Ultra-Turrax (IKA, 24,000 rpm, 15 s), and a glass homogenizer with a motor-driven Teflon pestle (1,200 rpm, 2 min). Aliquots of homogenate from each sample were stored in liquid nitrogen for further analyses. The homogenate was centrifuged (2,100 rpm, 10 min, 4°C, Hettich Universal 320R, Hettich, Germany). The supernatant was collected, and the pellet was homogenized in the same volume of TMES and centrifuged again. Both supernatants were mixed and centrifuged (23,500 rpm, 30 min, 4°C, Beckman Optima L-90K, rotor Ti 50.2 Beckman). The pellet (crude membrane fraction) was homogenized in TMES buffer without sucrose (13), and stored the aliquots at −80°C until use. Protein concentration was assessed using the Bradford protein assay (Sigma-Aldrich).

β-Adrenoreceptor Binding Assay

The total number of myocardial β-ARs was determined by the radioligand binding assay with the β-AR antagonist [^{3}H]CGP-12177 as previously described (21). Briefly, samples of crude membrane fraction (100 μg protein) were incubated in the medium (total volume of 0.5 mL) containing 50 mM Tris-HCl, 10 mM $MgCl_2$, and 1 mM ascorbic acid at pH 7.4 with the β-AR antagonist [^{3}H]CGP 12177 (ARC) in descending concentrations from 5 nM to 0.15 nM at 37°C for 1 h. The reaction was terminated by adding 3 mL of ice-cold washing buffer (50 mM Tris-HCl and 10 mM $MgCl_2$; pH 7.4) and subsequent filtration through GF/C filter pre-soaked for 1 h with 0.3% polyethyleneimine. The filter was washed twice with 3 mL of ice-cold washing buffer. After addition of 4 mL scintillation cocktail EcoLite (MP Biomedicals), radioactivity retained on

Table 1. *Basic parameters*

	Control Group	Cold Acclimated Group	Cold Acclimated + Recovery Group
Number of animals/group	12	12	12
Body weight, g	436 ± 6	403 ± 4†	466 ± 5†
Brown adipose tissue, mg	371 ± 27	704 ± 31†	622 ± 31†
Brown adipose tissue/body weight	0.86 ± 0.07	1.75 ± 0.08†	1.33 ± 0.06†
Heart weight, mg	1013 ± 38	1003 ± 45	1137 ± 31
Left ventricle/body weight	1.32 ± 0.07	1.34 ± 0.11	1.45 ± 0.06
Right ventricle/body weight	0.47 ± 0.02	0.55 ± 0.02*	0.48 ± 0.01
Heart weight/body weight	2.32 ± 0.08	2.49 ± 0.11	2.44 ± 0.07

Values are means ± SE. *$P < 0.01$; †$P < 0.001$ vs. control.

the filter was assessed by liquid scintillation counting for 5 min. Nonspecific binding (background signal) was defined as the signal that was not displaced by 10 μM L-propranolol. It represented ~30% of the totally bound radioligand. The proportion of β_2-ARs (% of total β-ARs) in the crude membrane fraction was determined using a competitive binding assay with the β_2-AR selective antagonist ICI-118551. Crude membrane samples were incubated with 1 nM [^{3}H] CGP 12177 at increasing concentrations of the selective β_2-AR antagonist ICI-118551 (10^{-10}–10^{-4} M). Binding characteristics (B_{max} and K_d) and the percentage of β_2-ARs in the membrane fraction were calculated and statistically analyzed using GraphPad Prism 8 software.

Western Blot Analysis

Individual samples (n = 8) of crude membrane fractions from each group (20 μg protein/lane) were resolved by SDS-PAGE using 12% polyacrylamide gel at constant voltage (200 V) and Mini-Protean Tetra Cell (Bio-Rad), and subsequently blotted onto nitrocellulose membranes (0.2-μm pore size; Bio-Rad) at constant voltage of 100 V for 90 min using the Wet Blot Module (Bio-Rad) as previously described (22). After blocking with 5% nonfat milk in Tris-buffered saline (20 mM Tris-HCl, 0.5 M NaCl, and 0.05% Tween 20) for 1 h, the membranes were incubated overnight at 4°C with polyclonal antibodies against $G_i\alpha_{1/2}$, $G_i\alpha_3$ [RCS antibody (23)], and Akt (sc-8312, Santa Cruz Biotechnology) or phosphorylated (p-)Akt (Ser^{473}) (no. 9271S, Cell Signaling), GSK-3β (sc-9166), and mouse monoclonal anti-p-GSK-3β (Ser^9) (sc-373800). The membranes were then washed and incubated with HRP-conjugated anti-rabbit antibody (A9169, Sigma-Aldrich) or HRP-conjugated anti-mouse antibody (no. 31432, Invitrogen). Protein bands were visualized by enhanced chemiluminescence (ECL) substrate SuperSignal West Dura Extended Duration Substrate (ThermoFisher Scientific) using the LAS-4000 imaging system (Fujifilm). Protein band intensity was quantified densitometrically using Quantity One Software (Bio-Rad). At least four samples from each group were always run on the same gel, quantified on the same membrane, and normalized to the total protein content per lane determined by Ponceau S staining, β-actin and GAPDH were used as a loading control in crude membrane fractions and homogenates, respectively. The accuracy and reproducibility of the chemiluminescence signal was validated by loading samples in ascending concentrations of 10 – 40 μg protein/lane, and each determination was performed at least three times. All figures show representative images of individual Western blots.

Quantitative Fluorescence Microscopy

In separate groups (n = 5), hearts were excised from anesthetized rats, relaxed by Tyrode solution and fixed with freshly prepared 4% formaldehyde using the Langendorff apparatus as reported (24, 25). The LV was then separated, frozen in liquid nitrogen, and stored at −80°C. All samples were collected under the same conditions. Sections (5–7 μm) were cut using a cryostat (Leica CM3050, Leica Microsystems), rehydrated in PBS, permeabilized in ice-cold methanol, and shortly incubated in 1% SDS in PBS for antigen retrieval. Sections were incubated for 80 min with blocking solution at room temperature (10% donkey serum, 10% goat serum, 0.3% Triton X-100, and 0.3 M glycin in PBS), and stained with rabbit monoclonal anti-p-GSK-3β (Ser^9) (D85E12, Cell Signaling Technology), or mouse monoclonal anti-GSK-3β (sc-377213), or mouse monoclonal anti-p-GSK-3β (Ser^9) (sc-373800) and subsequently with anti-rabbit IgG Alexa Fluor 488 (A21206, Life Technologies) or anti-mouse IgG-Alexa Fluor 647 (A21235, Life Technologies), respectively. To analyze subcellular localization of p-GSK-3β and its colocalization with mitochondria, or thin filaments in the I-band, sections were stained with both mouse anti-OXPHOS antibody cocktail (ab110412, Abcam) and anti-mouse IgG Alexa Fluor 647 or Alexa Fluor 488

Table 2. *Hemodynamic parameters*

	Baseline	Ischemia	Reperfusion
Number of animals/group	12	12	12
Heart Rate, beats/min			
Control			
Untreated	374 ± 6	363 ± 6	359 ± 7
ICI-118551	380 ± 9	369 ± 8	366 ± 6
Cold acclimation			
Untreated	369 ± 15	350 ± 15	346 ± 15
ICI-118551	368 ± 6	354 ± 10	357 ± 11
Recovery			
Untreated	374 ± 9	369 ± 12	361 ± 10
ICI-118551	359 ± 9	344 ± 8	343 ± 8
Blood Pressure, mmHg			
Control			
Untreated	82 ± 8	77 ± 7	71 ± 5
ICI-118551	75 ± 8	65 ± 5	58 ± 4
Cold acclimation			
Untreated	78 ± 7	66 ± 4	59 ± 4
ICI-118551	71 ± 7	65 ± 4	65 ± 5
Recovery			
Untreated	80 ± 6	71 ± 6	67 ± 4
ICI-118551	72 ± 7	65 ± 5	60 ± 4

Values are means ± SE. ICI-118551, β_2-AR selective antagonist.

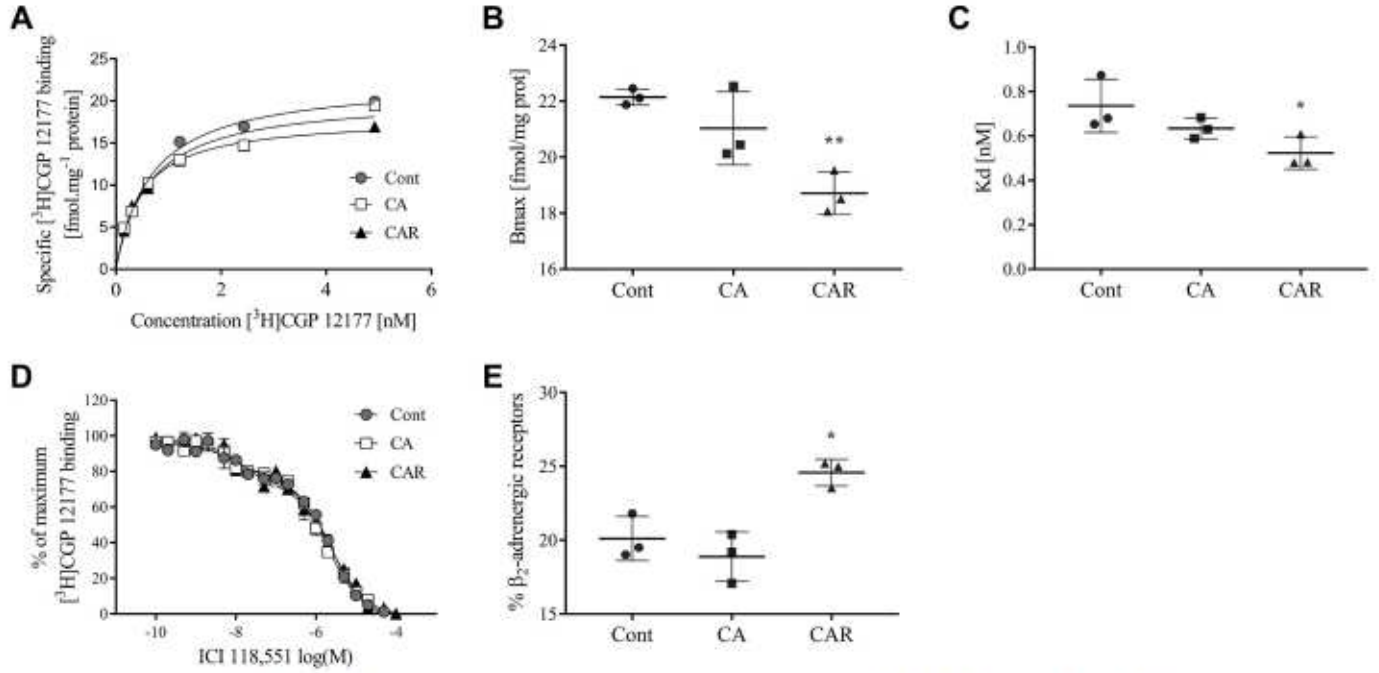

Figure 1. Effect of cold acclimation (CA) on the total number of β-adrenergic receptors (β-ARs) and the β_2-AR proportion in the crude plasma membrane fractions from left ventricles of control rats (Cont) and those acclimated for 5 wk to cold (CA) and subsequently recovered for 2 wk at 24°C (CAR). Representative saturation binding curves (*A*), total number of β-ARs (*B*), and receptor affinity (*C*). *D*, *E*: proportions of the β_2-AR subtype were assessed using competitive displacement of [^{3}H]CGP12177 by the β_2-AR-selective antagonist ICI-118551. Plotted data represent means ± SD of three separate experiments performed in triplicate ($n = 6$ in each group, males). Data were analyzed by nonlinear regression according to a one-site saturation equation (*A*) or two-site competition equation (*C*) and one-way ANOVA with Dunnett's multiple comparisons test (*B*, *D*, and *E*). $^*P < 0.05$ and $^{**}P < 0.01$ vs. Cont.

phalloidin (A22287, Life Technologies). Sections were mounted in ProLong Gold Antifade Reagent with DAPI (Invitrogen). Images taken from at least five randomly selected positions of each section were scanned sequentially using a wide-field inverted fluorescence microscope (IX2-UCB, Olympus). Each position was optically sectioned at 0.5-μm steps resulting in ~8–12 *Z*-stack layers, depending on the specimen thickness. Images were processed in Nikon Microscope Imaging Software (NIS-Elements, Japan). Colocalization analyses were performed as previously described (1) using ImageJ software (26).

Statistical Analysis

Statistical analysis was performed using the GraphPad Prism 8 software (GraphPad). The distribution of data was analyzed by Shapiro–Wilk and Komogorov–Smirnov normality tests. For parametric data, one-way ANOVA with Dunnett's multiple comparison test was used to identify significant differences between mean values of individual groups. Two-way ANOVA with Dunnett's multiple comparison test (effect of low temperature and/or ischemia-reperfusion) and Sidak's multiple comparison test (effect of ICI-118551) was used for

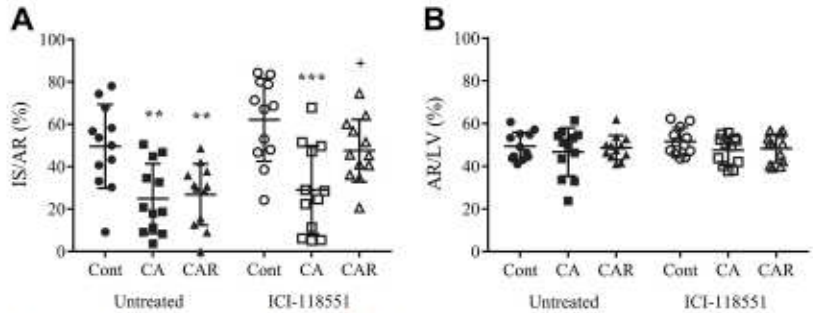

Figure 2. Effect of β_2-adrenergic receptor (β_2-AR) antagonist on cold acclimation (CA)-elicited cardioprotection. Infarct size (IS) was expressed as a percentage of area at risk (AR; *A*) and AR normalized to the left ventricle (LV; *B*) in control rats (Cont; circles) and those acclimated for 5 wk to cold (CA; squares) and subsequently recovered for 2 wk at 24°C (CAR; triangles). Empty symbols show the effect the β_2-AR inhibitor ICI-118551 (1 mg/kg body wt, $n = 12$ in each group, males). Data were analyzed by two-way ANOVA with Dunnett's multiple comparisons test (effect of low temperature and/or ischemia-reperfusion) and with Sidák's multiple comparisons test (effect of ICI-118551). Values are means ± SD. $^{**}P < 0.01$ and $^{***}P < 0.01$ vs. Cont; $+P < 0.05$ vs. untreated.

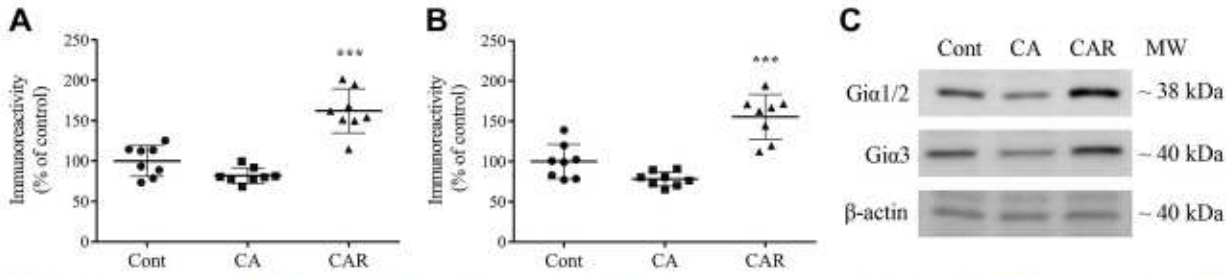

Figure 3. Effect of cold acclimation (CA) on expression of myocardial G_i proteins. Relative protein levels of $G_i\alpha_{1/2}$ (*A*) and $G_i\alpha_3$ (*B*) were determined in the crude membrane fraction ($n = 8$, males) from control rats (Cont) and those acclimated for 5 wk to cold (CA) and subsequently recovered for 2 wk at 24°C (CAR). *C*: images of representative membranes for Western blot analysis of $G_i\alpha_{1/2}$, $G_i\alpha_3$, and β-actin as a loading control. Data were analyzed by one-way ANOVA with Dunnett's multiple comparisons test. Values are means ± SD. $^{***}P < 0.001$ vs. Cont.

data from the β_2-AR inhibitor experiment. Data were considered statistically significant at $P < 0.05$.

RESULTS

Proper acclimation to low temperature was confirmed by significantly increased weight of brown adipose tissue (BAT) after CA (by 90% compared with controls; Table 1). The increase in BAT weight persisted even after cessation of CAR (by 62%).

Body weight of the CA group animals was slightly but significantly lower (8%) compared with controls, and body weight of CAR group (2-wk older animals) increased by 12%. Heart weight and the ratio of heart/body weight did not differ between the groups (Table 1), which excludes potential heart hypertrophy. Consistent with this, baseline values of mean arterial blood pressure and heart rate were affected neither by CA nor by CAR. Acute administration of a specific β_2-AR inhibitor had no effect on hemodynamic parameters (Table 2).

To evaluate the role of β-ARs in cardioprotection elicited by CA, we assessed the number of total β-ARs. Analysis of saturation binding curves (Fig. 1*A*) indicated that the total number of β-ARs did not change as a result of CA but decreased by ~16% after CAR (Fig. 1*B*). In parallel, the binding affinity of [^{3}H]CGP 12177 to β-ARs somewhat increased after CAR, which was reflected by a 29% drop in the value of K_d (Fig. 1*C*). The ratio of β_1- and β_2-ARs was not affected by CA, but the β_2-AR fraction increased from 20% to 25% after 2 wk recovery (Fig. 1, *D* and *E*).

We next evaluated an extent of myocardial infarction in the presence of β_2-AR selective inhibitor ICI-118551 in order to confirm or exclude the role of β_2-AR in CA-elicited cardioprotection. Infarct size represented 50% of the area at risk in control rats. CA reduced infarct size to 25% and the protection persisted in the CAR group (to 27%). Administration of β_2-AR inhibitor abolished the protective effect in the CAR group, but it had no significant effect in the control and CA groups (Fig. 2*A*). These results confirm a role of β_2-ARs in the infarct-size lowering effect of CAR but not that of CA. The average area at risk normalized to the LV (AR/LV) was 47%–52%, and it did not differ among the groups (Fig. 2*B*).

Subsequent analysis of the β_2-AR downstream pathway showed that, when compared with the control group, the protein level of $G_i\alpha_{1/2}$ and $G_i\alpha_3$ in the crude membrane fraction increased after CAR by 62% and 55%, respectively (Fig. 3, *A* and *B*). Interestingly, we found that after CAR the level of the Akt protein decreased by 17%, whereas phosphorylation of p-Akt (Ser^{473}) increased by 27%. Intriguingly, the p-Akt (Ser^{473})-to-Akt ratio increased by 50% in the CAR group (Fig. 4, *A*–*C*).

In the next set of experiments, GSK-3β, a target of Akt that regulates the mitochondrial proapoptotic pathway, was assessed. However, neither the protein nor its form phosphorylated on Ser^9 was affected by CA (Fig. 5, *A*–*D*). Fluorescent signal of p-GSK-3β (Ser^9) appeared mostly in transversal stripes in longitudinal sections of LVs, and we did not observe any differences in the colocalization of p-GSK-3β (Ser^9) with mitochondria among the groups (Fig. 5, *E* and *F*).

Analysis of total GSK-3β localization in sarcomeres revealed its translocation from the middle of I-band (Z-disk) to the H-zone after CA, which was reversed after CAR (Fig. 5*G*), and this was confirmed by a significant decrease in the colocalization of GSK-3β with phalloidin after CA but not

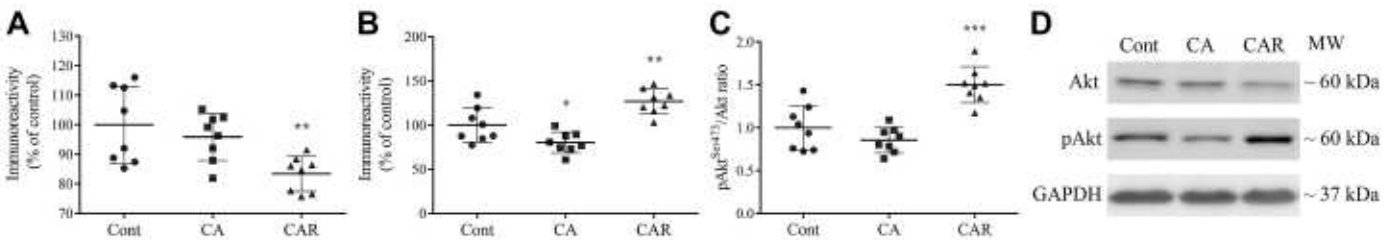

Figure 4. Effect of cold acclimation (CA) on myocardial protein kinase B (Akt) expression and phosphorylation (p-Akt^{Ser473}). Relative protein levels of Akt (*A*), p-Akt^{Ser473} (*B*), and the p-Akt^{Ser473}-to-Akt ratio (*C*) were determined in the crude membrane fraction ($n = 8$, males) from control rats (Cont) and those acclimated for 5 wk to cold (CA) and subsequently recovered for 2 wk at 24°C (CAR). *D*: images of representative membranes for Western blot analysis of Akt, Akt^{Ser473}, and GAPDH as a loading control. Data were analyzed by one-way ANOVA with Dunnett's multiple comparisons test. Values are means ± SD. $^{*}P < 0.05$ and $^{***}P < 0.0001$ vs. Cont.

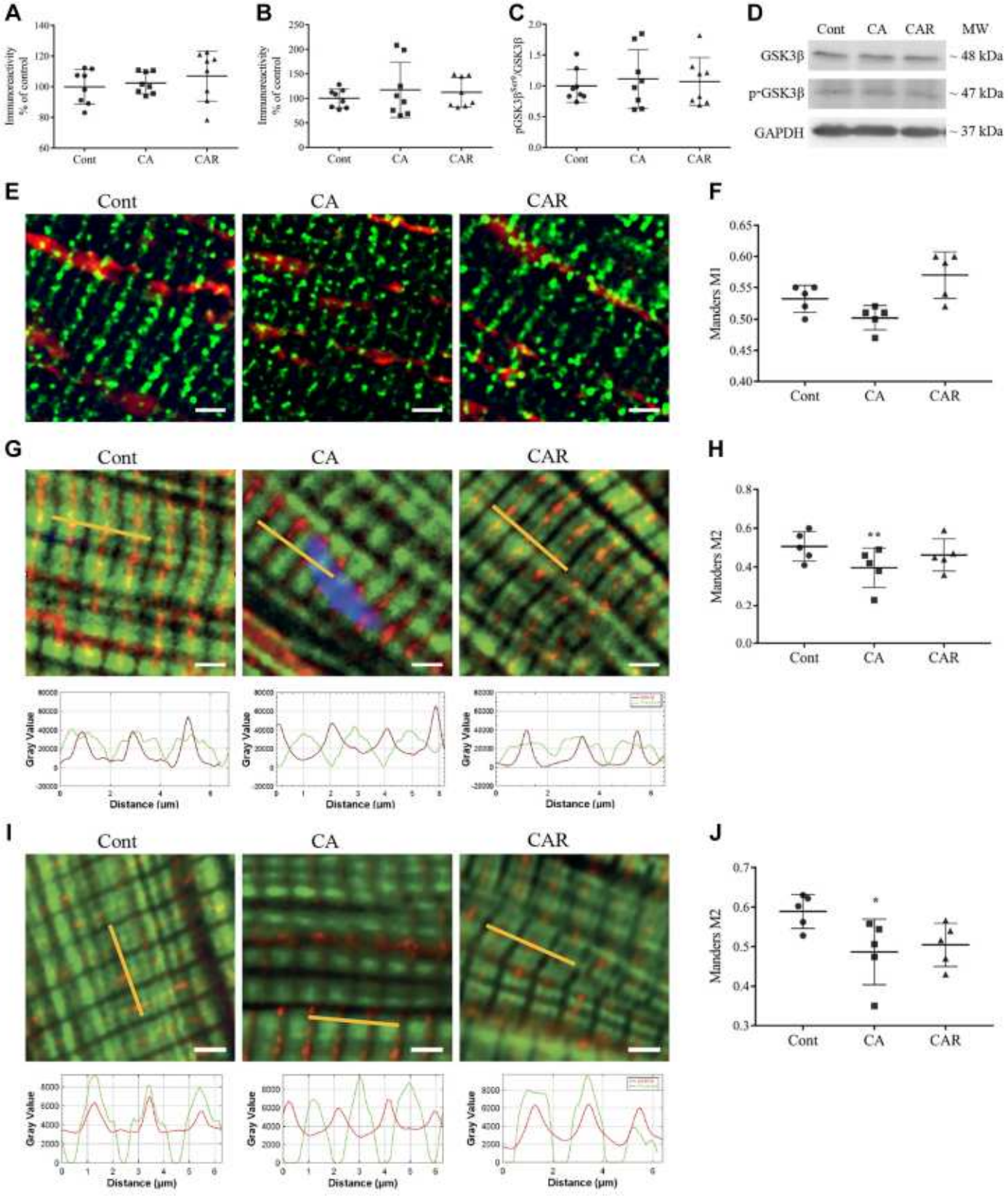

CAR (Fig. 5*H*). Application of another GSK-3β antibody (anti-mouse monoclonal sc-377213) confirmed this unexpected observation (data not shown). Analysis of p-GSK-3β (Ser^9) localization detected similar translocation pattern to the total GSK-3β (Fig. 5, *I* and *J*). The role of GSK-3β translocation in CA is unclear at present, and we are pursuing experiments to resolve this issue.

DISCUSSION

The present study builds on a recent observation that cardioprotection is induced by mild CA that persists for at least 2-wk period of normothermic recovery with a possible role of β_2-ARs in the mechanism (1). Here, we show that the mechanism of the infarct size-limiting effect elicited by CA is not identical when analyzed immediately after CA and after CAR. A competitive receptor-binding assay demonstrated increased proportion of β_2-AR within total β-AR in crude myocardial membrane fraction after CAR but not after CA. This effect was confirmed by acute administration of the specific β_2-AR inhibitor ICI-118551, which abolished the infarct size-lowering effect persisting after CAR, but not that elicited by CA.

The observed increase in the β_2-AR-to-β_1-AR ratio after CAR is apparently a result of upregulation of β_2-ARs and downregulation of β_1-ARs. The increased β_2-/β_1-AR ratio under stress conditions may be involved in the protection of the heart against damage caused by overstimulation, since the β_2-AR-subtype couples to both G_s and G_i proteins (27, 28). As we demonstrated previously, the G_s/adenylyl cyclase/PKA pathway remained unaltered in both the CA and CAR groups (1). Hence, in the present study we focused on the G_i/Akt pathway downstream of β_2-AR. Expression of $G_i\alpha$ proteins (Giα1/2 and Giα3) markedly increased after CAR, and this was reflected by activation of Akt; the p-Akt-to-Akt ratio increased considerably in this group. Activation of the β_2-AR/G_i/Akt pathway is related to intracellular signaling associated with antiapoptotic effects and improved cell survival (12, 29), which have been repeatedly reported as cardioprotective (13, 14, 30). Activated Akt phosphorylates several regulatory proteins, including caspase-9, Bcl-2-family proteins, and GSK-3β (31). Akt-mediated phosphorylation inactivates caspase-9, resulting in suppression of mitochondria-dependent apoptosis (32). Moreover, inactivation of the proapoptotic protein Bad by phosphorylation contributes to stabilization of outer mitochondrial membrane. Akt also inhibits a conformational change of the proapoptotic Bax protein and its translocation to mitochondria (33). Hexokinase 2, phosphorylated on Thr^{472} by Akt, increases its association with the outer mitochondrial membrane, which maintains mitochondrial membrane potential by preferential ADP supply to complex V and prevents association of the proapoptotic Bax protein with the voltage-dependent anion channel (25, 34).

Akt activation can protect mitochondria and prevent release of proapoptotic proteins, i.e., cytochrome *c* or the apoptosis-inducing factor (35), which restrain increase in oxidative stress and lower the probability of mPTP opening (36). As we demonstrated previously, both CA and CAR lead to increased mitochondrial resistance to Ca^{2+} overload (1). This suggests that active Akt can contribute to the cardioprotective effect elicited by CAR via increasing the resistance of mPTP to Ca^{2+}-overload. Nevertheless, our data suggest that mitochondrial protection in CA and CAR groups involves different mechanisms, whose precise delineation is a subject of our further studies.

In this study, we also focused on GSK-3β, a key component of the PI3K/Akt pathway, which may contribute to mPTP opening when translocated to mitochondria (37). The prosurvival PI3K/Akt signaling negatively regulates GSK-3β and thus may participate in mitochondria-linked cardioprotection (38–41). We have observed, however, that expression, phosphorylation, and location of GSK-3β in the mitochondrial compartment were affected neither by CA nor by CAR. This finding may exclude GSK-3β as an Akt target in the CA-elicited cardioprotective mechanism related to prevention of mPTP opening.

Importantly, a detailed inspection of the striated distribution pattern of GSK-3β in longitudinal sections of LVs revealed its translocation from the Z-disk to the H-zone compartment after CA and back to the original position during the recovery phase. To the best of our knowledge, this phenomenon has not been reported to date. There is strong evidence that GSK-3β-targeted proteins located mostly within the Z-disk of the sarcomere mediate the increase in myofilament Ca^{2+} sensitivity in the failing heart when the kinase is rephosphorylated during cardiac resynchronization therapy (42, 43). This phosphorylation is accompanied by restoration of contractility. Interestingly, Akt was excluded as an upstream kinase in this process (42). In line with this, our data suggest that the CA-elicited translocation of GSK-3β to the H-band occurs in an Akt-independent manner (as Akt is activated only after CAR). To the best of our knowledge, there is no data suggesting that GSK-3β phosphorylates its substrate proteins within the central part of the H-band, i.e., the M-line. However, a possible candidate is myosin binding

Figure 5. Effect of cold acclimation (CA) on myocardial glycogen synthase kinase-3β (GSK-3β) expression, phosphorylation (p-GSK-3β^{Ser9}), and location. Relative protein levels of total GSK-3β (*A*), p-GSK-3β^{Ser9} (*B*), and the p-GSK-3β^{Ser9}-to-total-GSK3β ratio (*C*) were determined in homogenates ($n = 8$, males) prepared from control rats (Cont) and from rats acclimated for 5 wk to cold (CA) and subsequently recovered for 2 wk at 24°C (CAR). *D*: images of representative Western blots of total GSK-3β, p-GSK-3β^{Ser9}, and GAPDH as a loading control. *E*, *F*: representative micrographs of longitudinal cryosections of left ventricles stained for p-GSK-3β^{Ser9} (green) and OXPHOS (red; *E*) and quantitative analyses of their colocalization expressed by Mander's M1 correlation coefficient ($n = 5$, males; *F*). *G*, *H*: representative micrographs of longitudinal cryosections of left ventricles stained for total GSK-3β (red) and with phalloidin (green) (*G*, *top*) and quantitative analyses of their colocalization expressed by Mander's M2 correlation coefficient ($n = 5$; *H*). Intensity profile along the test line (yellow) show the translocation of total GSK3β from the I-band region to the H-zone after CA and its normalization after CAR (*G*, *bottom*). *I*, *J*: p-GSK-3β^{Ser9} translocation within the sarcomere ($n = 5$). Scale bar = 10 μm. Data presented in graphs were analyzed by one-way ANOVA with Dunnett's multiple comparisons test. Values are means ± SD. $^{*}P < 0.05$ and $^{**}P < 0.01$ vs. Cont.

protein C (MyBP-C), a key regulator of cardiac contractility that is located in the C-zone of sarcomere, which is positioned laterally within the H-band (44). MyBP-C was shown to be located adjacent to the actin-positive I-band, which is similar as we document for GSK-3β colocalized with the phalloidin-positive staining after CA in the present study. Importantly, GSK-3β-mediated phosphorylation of MyBP-C on Ser^{133} increased the contractility of permeabilized human cardiomyocytes (45). Generally, the MyBP-C phosphorylation maintains thick filament spacing and structure, which was approved as cardioprotective (46). In summary, changes of GSK-3β location elicited by CA may affect calcium sensitivity and contractility of sarcomeres, whereby contributing to the cardioprotective effect. These plausible hypotheses require experimental verification, which is a subject of our future studies.

Our results raise the following question: What is the reason for the difference between CA and CAR in establishing cardioprotection? CA animals feature high level of insulation that prevents heat loss and enlarged BAT that increases heat production, both contributing to improved thermal homeostasis (47). Specific signaling pathways elicited by CA that are activated at the cellular level are still not fully understood (1). At the early stages of CAR, the shift back to room temperature presents a sudden temperature rise by 16°C that leads to a transient overheating episode of the acclimated animals. This event is reminiscent of the well-known "heat stress" phenomenon associated with heat acclimation-mediated cytoprotective memory. Under these conditions, additional cardioprotective signaling pathways are activated (48). Importantly, increased Akt phosphorylation has been reported as a fundamental player in the heat acclimation-elicited protection (49–51).

We conclude that the mechanism of cardioprotection observed after CAR is mediated via the β_2-AR-G_i pathway and Akt activation. This could be related to the additional transient heat episode occurring when the cold acclimated-subjects return to the room temperature. Further studies are needed to unravel downstream targets of the central regulators of the CA process and the downstream targets of the Akt protein after CAR.

ACKNOWLEDGMENT

We thank Prof. Jiri Neuzil, Institute of Molecular Genetics of the Czech Academy of Sciences, Czech Republic, and Dr. Peter van der Ven, Institute for Cell Biology, University of Bonn, Germany for constructive criticism of the manuscript.

GRANTS

This work has been supported by the Charles University Grant Agency (GAUK 641216), Czech Science Foundation (17-07748S), and the Ministry of Education, Youth and Sport of the Czech Republic (SVV-260571/2020). Microscopy was performed in the Laboratory of Confocal and Fluorescence Microscopy cofinanced by the European Regional Development Fund and the state budget of the Czech Republic, Project No. CZ.1.05/4.1.00/16.0347 and CZ.2.16/3.1.00/21515.

DISCLOSURES

No conflicts of interest, financial or otherwise, are declared by the authors.

AUTHOR CONTRIBUTIONS

V.T., A.M., and J.Z. conceived and designed research; V.T., A.M., B.E., L.H., P.V., and J.Z. performed experiments; V.T., A.M., B.E., L.H., and J.Z. analyzed data; V.T., A.M., B.E., O.N., and J.Z. interpreted results of experiments; V.T. and B.E. prepared figures; V.T., O.N., and J.Z. drafted manuscript; J.N., F.K., O.N., and J.Z. edited and revised manuscript; V.T., A.M., B.E., L.H., P.V., J.N., F.K., O.N., and J.Z. approved final version of manuscript.

REFERENCES

1. **Tibenska V, Benesova A, Vebr P, Liptakova A, Hejnova L, Elsnicova B, Drahota Z, Hornikova D, Galatik F, Kolar D, Vybiral S, Alanova P, Novotny J, Kolar F, Novakova O, Zurmanova JM.** Gradual cold acclimation induces cardioprotection without affecting beta-adrenergic receptor-mediated adenylyl cyclase signaling. *J Appl Physiol* 128: 1023–1032, 2020. doi:10.1152/japplphysiol.00511.2019.
2. **Tsibulnikov SY, Maslov LN, Naryzhnaya NV, Ivanov VV, Bushov YV, Voronkov NS, Jaggi AS, Zhang Y, Oeltgen PR.** Impact of cold adaptation on cardiac tolerance to ischemia/reperfusion and glucocorticoid, thyroid hormone levels. *Gen Phys Biophys* 38: 245–251, 2019. doi:10.4149/gpb_2019002.
3. **Brodde OE, Michel M-C.** Adrenergic and muscarinic receptors in the human heart. *Pharmacol Rev* 41: 651–689, 1999.
4. **Barki-Harrington L, Perrino C, Rockman HA.** Network integration of the adrenergic system in cardiac hypertrophy. *Cardiovasc Res* 63: 391–402, 2004. doi:10.1016/j.cardiores.2004.03.011.
5. **Kilts JD, Gerhardt MA, Richardson MD, Sreeram G, Mackensen GB, Grocott HP, White WD, Davis RD, Newman MF, Reves JG, Schwinn DA, Kwatra MM.** β2-Adrenergic and several other g protein-coupled receptors in human atrial membranes activate both G(s) and G(i). *Circ Res* 87: 705–709, 2000. doi:10.1161/01.RES.87.8.705.
6. **Jo SH, Leblais V, Wang PH, Crow MT, Xiao RP.** Phosphatidylinositol 3-kinase functionally compartmentalizes the concurrent G_s signaling during β2-adrenergic stimulation. *Circ Res* 91: 46–53, 2002. doi:10.1161/01.RES.0000024115.67561.54.
7. **Ait-Mamar B, Cailleret M, Rucker-Martin C, Bouabdallah A, Candiani G, Adamy C, Duvaldestin P, Pecker F, Defer N, Pavoine C.** The cytosolic phospholipase A2 pathway, a safeguard of β2-adrenergic cardiac effects in rat. *J Biol Chem* 280: 18881–18890, 2005. doi:10.1074/jbc.M410305200.
8. **Chen-Izu Y, Xiao RP, Izu LT, Cheng H, Kuschel M, Spurgeon H, Lakatta EG.** G(i)-dependent localization of beta(2)-adrenergic receptor signaling to L-type Ca(2+) channels. *Biophys J* 79: 2547–2556, 2000. doi:10.1016/S0006-3495(00)76495-2.
9. **Salie R, Moolman JA, Lochner A.** The role of β-adrenergic receptors in the cardioprotective effects of beta-preconditioning (βPC). *Cardiovasc drugs Ther* 25: 31–46, 2011. doi:10.1007/s10557-010-6275-3.
10. **Tong H, Bernstein D, Murphy E, Steenbergen C.** The role of beta-adrenergic receptor signaling in cardioprotection. *FASEB J* 19: 983–985, 2005. doi:10.1096/fj.04-3067fje.
11. **Hanada M, Feng J, Hemmings BA.** Structure, regulation and function of PKB/AKT—a major therapeutic target. *Biochim Biophys Acta* 1697: 3–16, 2004. doi:10.1016/j.bbapap.2003.11.009.
12. **Chesley A, Lundberg MS, Asai T, Xiao R, Ohtani S, Lakatta EG, Crow MT.** The beta 2-adrenergic receptor delivers an antiapoptotic. *Circ Res* 87: 1172–1179, 2000. doi:10.1161/01.res.87.12.1172.
13. **Kolar D, Gresikova M, Waskova-Arnostova P, Elsnicova B, Kohutova J, Hornikova D, Vebr P, Neckar J, Blahova T, Kasparova D, Novotny J, Kolar F, Novakova O, Zurmanova JM.** Adaptation to chronic continuous hypoxia potentiates Akt/HK2 anti-apoptotic pathway during brief myocardial ischemia/reperfusion insult. *Mol Cell Biochem* 432: 99–108, 2017. doi:10.1007/s11010-017-3001-5.
14. **Su F, Zhao L, Zhang S, Wang J, Chen N, Gong Q, Tang J, Wang H, Yao J, Wang Q, Zhong M, Yan J.** Cardioprotection by PI3K-mediated signaling is required for anti-arrhythmia and myocardial repair in response to ischemic preconditioning in infarcted pig hearts. *Lab Investig* 95: 860–871, 2015. doi:10.1038/labinvest.2015.64.

15. **Yao H, Han X, Han X.** The cardioprotection of the insulin-mediated PI3K/Akt/mTOR signaling pathway. *Am J Cardiovasc Drugs* 14: 433–442, 2014. doi:10.1007/s40256-014-0089-9.
16. **Bopassa J-C, Ferrera R, Gateau-Roesch O, Couture-Lepetit E, Ovize M.** PI 3-kinase regulates the mitochondrial transition pore in controlled reperfusion and postconditioning. *Cardiovasc Res* 69: 178–185, 2006. doi:10.1016/j.cardiores.2005.07.014.
17. **Juhaszova M, Zorov DB, Kim S-H, Pepe S, Fu Q, Fishbein KW, Ziman BD, Wang S, Ytrehus K, Antos CL, Olson EN, Sollott SJ.** Glycogen synthase kinase-3beta mediates convergence of protection signaling to inhibit the mitochondrial permeability transition pore. *J Clin Invest* 113: 1535–1549, 2004. doi:10.1172/JCI19906.
18. **Neckar J, Svatonova A, Weissova R, Drahota Z, Zajickova P, Brabcova I, Kolar D, Alanova P, Vasinova J, Silhavy J, Hlavackova M, Tauchmannova K, Milerova M, Ostadal B, Cervenka L, Zurmanova J, Kalous M, Novakova O, Novotny J, Pravenec M, Kolar F.** Selective replacement of mitochondrial DNA increases the cardioprotective effect of chronic continuous hypoxia in spontaneously hypertensive rats. *Clin Sci (Lond)* 131: 865–881, 2017. doi:10.1042/CS20170083.
19. **Parulek J, Srámek M, Cerveansky˘ M, Novotová M, Zahradník I.** A cell architecture modeling system based on quantitative ultrastructural characteristics. *Methods Mol Biol* 500: 289–312, 2009. doi:10.1007/978-1-59745-525-1_10.
20. **Hahnova K, Kasparova D, Zurmanova J, Neckar J, Kolar F, Novotny J.** Beta-adrenergic signaling in rat heart is similarly affected by continuous and intermittent normobaric hypoxia. *Gen Phys Biophys* 35: 165–173, 2016. doi:10.4149/gpb_2015053.
21. **Klevstig M, Manakov D, Kasparova D, Brabcova I, Papousek F, Zurmanova J, Zidek V, Silhavy J, Neckar J, Pravenec M, Kolar F, Novakova O, Novotny J.** Transgenic rescue of defective Cd36 enhances myocardial adenylyl cyclase signaling in spontaneously hypertensive rats. *Pflugers Arch* 465: 1477–1486, 2013. doi:10.1007/s00424-013-1281-5.
22. **Kasparova D, Neckar J, Dabrowska L, Novotny J, Mraz J, Kolar F, Zurmanova J.** Cardioprotective and nonprotective regimens of chronic hypoxia diversely affect the myocardial antioxidant systems. *Physiol Genomics* 47: 612–620, 2015. doi:10.1152/physiolgenomics.00058.2015.
23. **Ihnatovych I, Hejnova L, Kostrnova A, Mares P, Svoboda P, Novotny J.** Maturation of rat brain is accompanied by differential expression of the long and short splice variants of G(s)alpha protein: identification of cytosolic forms of G(s)alpha. *J Neurochem* 79: 88–97, 2008. doi:10.1046/j.1471-4159.2001.00544.x.
24. **Kohutova J, Elsnicova B, Holzerova K, Neckar J, Sebesta O, Jezkova J, Vecka M, Vebr P, Hornikova D, Szeiffova Bacova B, Egan Benova T, Hlavackova M, Tribulova N, Kolar F, Novakova O, Zurmanova JM.** Anti-arrhythmic cardiac phenotype elicited by chronic intermittent hypoxia is associated with alterations in connexin-43 expression, phosphorylation, and distribution. *Front Endocrinol (Lausanne)* 9: 789, 2019. doi:10.3389/fendo.2018.00789.
25. **Waskova-Arnostova P, Elsnicova B, Kasparova D, Hornikova D, Kolar F, Novotny J, Zurmanova J.** Cardioprotective adaptation of rats to intermittent hypobaric hypoxia is accompanied by the increased association of hexokinase with mitochondria. *J Appl Physiol* 119: 1487–1493, 2015. doi:10.1152/japplphysiol.01035.2014.
26. **Schindelin J, Arganda-Carreras I, Frise E, Kaynig V, Longair M, Pietzsch T, Preibisch S, Rueden C, Saalfeld S, Schmid B, Tinevez J-Y, White DJ, Hartenstein V, Eliceiri K, Tomancak P, Cardona A, Liceiri K, Tomancak PAC.** Fiji: an open source platform for biological image analysis. *Nat Methods* 9: 676–682, 2012. doi:10.1038/nmeth.2019.Fiji.
27. **Micova P, Hahnova K, Hlavackova M, Elsnicova B, Chytilova A, Holzerova K, Zurmanova J, Neckar J, Kolar F, Novakova O, Novotny J.** Chronic intermittent hypoxia affects the cytosolic phospholipase A(2)α/cyclooxygenase 2 pathway via β(2)-adrenoceptor-mediated ERK/p38 stimulation. *Mol Cell Biochem* 423: 151–163, 2016. doi:10.1007/s11010-016-2833-8.
28. **Spadari-Bratfisch RC, dos Santos IN.** Adrenoceptors and adaptive mechanisms in the heart during stress. *Ann NY Acad Sci* 1148: 377–383, 2008. doi:10.1196/annals.1410.075.
29. **Zhu WZ, Zheng M, Koch WJ, Lefkowitz RJ, Kobilka BK, Xiao RP.** Dual modulation of cell survival and cell death by beta(2)-adrenergic signaling in adult mouse cardiac myocytes. *Proc Natl Acad Sci USA* 98: 1607–1612, 2001. doi:10.1073/pnas.98.4.1607.
30. **Waskova-Arnostova P, Elsnicova B, Kasparova D, Sebesta O, Novotny J, Neckar J, Kolar F, Zurmanova J.** Right-to-left ventricular differences in the expression of mitochondrial hexokinase and phosphorylation of Akt. *Cell Physiol Biochem* 31: 66–79, 2013. doi:10.1159/000343350.
31. **Manning BD, Toker A.** AKT/PKB signaling: navigating the network. *Cell* 169: 381–405, 2017. doi:10.1016/j.cell.2017.04.001.
32. **Cardone MH, Roy N, Stennicke HR, Salvesen GS, Franke TF, Stanbridge E, Frisch S, Reed JC.** Regulation of cell death protease caspase-9 by phosphorylation. *Science* 282: 1318–1321, 1998. doi:10.1126/science.282.5392.1318.
33. **Yamaguchi H, Wang HG.** The protein kinase PKB/Akt regulates cell survival and apoptosis by inhibiting Bax conformational change. *Oncogene* 20: 7779–7786, 2001. doi:10.1038/sj.onc.1204984.
34. **Neary CL, Pastorino JG.** Akt inhibition promotes hexokinase 2 redistribution and glucose uptake in cancer cells. *J Cell Physiol* 228: 1943–1948, 2013. doi:10.1002/jcp.24361.
35. **Zhou H, Li XM, Meinkoth J, Pittman RN.** Akt regulates cell survival and apoptosis at a postmitochondrial level. *J Cell Biol* 151: 483–494, 2000. doi:10.1083/jcb.151.3.483.
36. **Davidson SM, Hausenloy D, Duchen MR, Yellon DM.** Signalling via the reperfusion injury signalling kinase (RISK) pathway links closure of the mitochondrial permeability transition pore to cardioprotection. *Int J Biochem Cell Biol* 38: 414–419, 2006. doi:10.1016/j.biocel.2005.09.017.
37. **Pastorino JG, Hoek JB, Shulga N.** Activation of glycogen synthase kinase 3beta disrupts the binding of hexokinase II to mitochondria by phosphorylating voltage-dependent anion channel and potentiates chemotherapy-induced cytotoxicity. *Cancer Res* 65: 10545–10554, 2005. doi:10.1158/0008-5472.CAN-05-1925.
38. **Juhaszova M, Zorov DB, Yaniv Y, Nuss HB, Wang S, Sollott SJ.** Role of glycogen synthase kinase-3beta in cardioprotection. *Circ Res* 104: 1240–1252, 2009. doi:10.1161/CIRCRESAHA.109.197996.
39. **Nishihara M, Miura T, Miki T, Tanno M, Yano T, Naitoh K, Ohori K, Hotta H, Terashima Y, Shimamoto K.** Modulation of the mitochondrial permeability transition pore complex in GSK-3beta-mediated myocardial protection. *J Mol Cell Cardiol* 43: 564–570, 2007. doi:10.1016/j.yjmcc.2007.08.010.
40. **Shah SR, Fatima K, Ansari M.** Recovery of myofilament function through reactivation of glycogen synthase kinase 3β (GSK-3β): mechanism for cardiac resynchronization therapy. *J Interv Card Electrophysiol* 41: 193–194, 2014. doi:10.1007/s10840-014-9939-2.
41. **Sharma AK, Kumar A, Sahu M, Sharma G, Datusalia AK, Rajput SK.** Exercise preconditioning and low dose copper nanoparticles exhibits cardioprotection through targeting GSK-3β phosphorylation in ischemia/reperfusion induced myocardial infarction. *Microvasc Res* 120: 59–66, 2018. doi:10.1016/j.mvr.2018.06.003.
42. **Kirk JA, Holewinski RJ, Kooij V, Agnetti G, Tunin RS, Witayavanitkul N, de Tombe PP, Gao WD, Van Eyk J, Kass DA.** Cardiac resynchronization sensitizes the sarcomere to calcium by reactivating GSK-3β. *J Clin Invest* 124: 129–138, 2014. doi:10.1172/JCI69253.
43. **Neubauer S, Redwood C.** New mechanisms and concepts for cardiac-resynchronization therapy. *N Engl J Med* 370: 1164–1166, 2014. doi:10.1056/NEJMcibr1315508.
44. **Sadayappan S, de Tombe PP.** Cardiac myosin binding protein-C as a central target of cardiac sarcomere signaling: a special mini review series. *Pflugers Arch* 466: 195–200, 2014. doi:10.1007/s00424-013-1396-8.
45. **Kuster DWD, Sequeira V, Najafi A, Boontje NM, Wijnker PJM, Witjas-Paalberends ER, Marston SB, Dos Remedios CG, Carrier L, Demmers JAA, Redwood C, Sadayappan S, van der Velden J.** GSK3β phosphorylates newly identified site in the proline-alanine-rich region of cardiac myosin-binding protein C and alters cross-bridge cycling kinetics in human: short communication. *Circ Res* 112: 633–639, 2013. doi:10.1161/CIRCRESAHA.112.275602.
46. **Sadayappan S, Osinska H, Klevitsky R, Lorenz JN, Sargent M, Molkentin JD, Seidman CE, Seidman JG, Robbins J.** Cardiac myosin binding protein C phosphorylation is cardioprotective. *Proc Natl Acad Sci USA* 103: 16918–16923, 2006. doi:10.1073/pnas.0607069103.
47. **Tansey EA, Johnson CD.** Recent advances in thermoregulation. *Adv Physiol Educ* 39: 139–148, 2015. doi:10.1152/advan.00126.2014.
48. **Horowitz M.** Epigenetics and cytoprotection with heat acclimation. *J Appl Physiol* 120: 702–710, 2016. doi:10.1152/japplphysiol.00552.2015.
49. **Maloyan A, Eli-Berchoer L, Semenza GL, Gerstenblith G, Stern MD, Horowitz M.** HIF-1alpha-targeted pathways are activated by

heat acclimation and contribute to acclimation-ischemic cross-tolerance in the heart. *Physiol Genomics* 23: 79–88, 2005. doi:10.1152/physiolgenomics.00279.2004.

50. **Wei H**, **Vander Heide RS.** Ischemic preconditioning and heat shock activate Akt via a focal adhesion kinase-mediated pathway in Langendorff-perfused adult rat hearts. *Am J Physiol Heart Circ Physiol* 298: H152–H157, 2010. doi:10.1152/ajpheart.00613.2009.

51. **Zhou J**, **Schmid T**, **Frank R**, **Brüne B.** PI3K/Akt is required for heat shock proteins to protect hypoxia-inducible factor 1alpha from pVHL-independent degradation. *J Biol Chem* 279: 13506–13513, 2004. doi:10.1074/jbc.M310164200.

J Appl Physiol 128: 1023–1032, 2020.
First published March 26, 2020; doi:10.1152/japplphysiol.00511.2019.

RESEARCH ARTICLE | *Physiology of Thermal Therapy*

Gradual cold acclimation induces cardioprotection without affecting β-adrenergic receptor-mediated adenylyl cyclase signaling

V. Tibenska,[1]* A. Benesova,[1]* P. Vebr,[1] A. Liptakova,[1] L. Hejnová,[1] B. Elsnicová,[1] Z. Drahota,[2] D. Hornikova,[1] F. Galatík,[1] D. Kolar,[1] S. Vybiral,[1] P. Alánová,[2] J. Novotný,[1] F. Kolar,[2] O. Novakova,[1,2] and J. M. Zurmanova[1]

[1]*Department of Physiology, Faculty of Science, Charles University, Prague, Czech Republic; and* [2]*Institute of Physiology of the Czech Academy of Sciences, Prague, Czech Republic*

Submitted 22 July 2019; accepted in fina form 5 March 2020

Tibenska V, Benesova A, Vebr P, Liptakova A, Hejnová L, Elsnicová B, Drahota Z, Hornikova D, Galatík F, Kolar D, Vybiral S, Alánová P, Novotný J, Kolar F, Novakova O, Zurmanova JM. Gradual cold acclimation induces cardioprotection without affecting β-adrenergic receptor-mediated adenylyl cyclase signaling. *J Appl Physiol* 128: 1023–1032, 2020. First published March 26, 2020; doi:10.1152/japplphysiol.00511.2019.—Novel strategies are needed that can stimulate endogenous signaling pathways to protect the heart from myocardial infarction. The present study tested the hypothesis that appropriate regimen of cold acclimation (CA) may provide a promising approach for improving myocardial resistance to ischemia/reperfusion (I/R) injury without negative side effects. We evaluated myocardial I/R injury, mitochondrial swelling, and β-adrenergic receptor (β-AR)-adenylyl cyclase-mediated signaling. Male Wistar rats were exposed to CA (8°C, 8 h/day for a week, followed by 4 wk at 8°C for 24 h/day), while the recovery group (CAR) was kept at 24°C for an additional 2 wk. The myocardial infarction induced by coronary occlusion for 20 min followed by 3-h reperfusion was reduced from 56% in controls to 30% and 23% after CA and CAR, respectively. In line, the rate of mitochondrial swelling at 200 μM Ca^{2+} was decreased in both groups. Acute administration of metoprolol decreased infarction in control group and did not affect the CA-elicited cardiprotection. Accordingly, neither β1-AR-G_sα-adenylyl cyclase signaling, stimulated with specifi ligands, nor p-PKA/PKA ratios were affected after CA or CAR. Importantly, Western blot and immunofluorescenc analyses revealed β2- and β3-AR protein enrichment in membranes in both experimental groups. We conclude that gradual cold acclimation results in a persisting increase of myocardial resistance to I/R injury without hypertension and hypertrophy. The cardioprotective phenotype is associated with unaltered adenylyl cyclase signaling and increased mitochondrial resistance to Ca^{2+}-overload. The potential role of upregulated β2/β3-AR pathways remains to be elucidated.

NEW & NOTEWORTHY We present a new model of mild gradual cold acclimation increasing tolerance to myocardial ischemia/reperfusion injury without hypertension and hypertrophy. Cardioprotective phenotype is accompanied by unaltered adenylyl cyclase signaling and increased mitochondrial resistance to Ca^{2+}-overload. The potential role of upregulated β2/β3-adrenoreceptor activation is considered. These finding may stimulate the development of novel preventive and therapeutic strategies against myocardial ischemia/reperfusion injury.

adenylyl cyclase; β-adrenergic receptors; cardioprotection; cold acclimation; mitochondria

INTRODUCTION

Acute myocardial infarction followed by heart failure is a frequent cause of disability and death worldwide. To preserve cardiac function, new treatment strategies are needed to protect the heart against acute ischemia/reperfusion (I/R) injury (2, 59).

Acute cold is considered as a cardiovascular risk factor, and a tight correlation between acute cold exposure and winter mortality caused by heart disease was repeatedly reported (50). By contrast, an adequate regimen of cold acclimation (CA) is well known to have beneficia effects such as improved immune response, thermoregulation and vascular reactivity, and increased aerobic metabolism. In addition, CA was studied extensively as a possible protective intervention in the context of metabolic syndrome (32, 46). In animals as well as in humans, CA is characterized by the activation of brown adipose tissue (BAT) and by increased expression of uncoupling proteins predominantly in BAT but also in other tissues, including the heart. Moreover, several signaling molecules possessing potent humoral properties are released from BAT, especially under conditions of thermogenic activation (54). We have previously demonstrated that CA in humans may have a great potential for the prevention of cardiovascular diseases by increasing levels of antioxidants and anti-inflammator cytokines in blood serum (29). Recently, it has been reported that CA increases tolerance to I/R in rats. However, the rather severe conditions of the applied acclimation protocol (4 wk 24 h/day at 4°C) also induced increased blood pressure and left ventricular hypertrophy (52).

Adrenergic stimulation has been shown to be important for the CA-elicited shift from shivering to nonshivering thermogenesis (53). Importantly, we previously documented a desensitization of adrenergic responsiveness of the cardiovascular system in winter swimmers (27, 55). It is known that heart function is predominantly under the control of β-adrenergic signaling. There are three subtypes of β-adrenergic receptors (β-ARs) in the ventricular myocardium: β1-ARs (~70%), β2-ARs (~27%), and β3-ARs (~3%) (9). The β1-ARs coupled to the stimulatory G protein (G_s) are required for hormone-stimulated cAMP generation by adenylyl cyclase. This subse-

* V. Tibenska and A. Benesova contributed equally to this work.

Address for correspondence: J. M. Zurmanova, Charles University, Faculty of Science, Department of Physiology, Vinicna 7, 128 00, Prague 2, Czech Republic (e-mail: jitka.zurmanova@natur.cuni.cz).

Table 1. *Basic parameters*

	Control	Cold Acclimation	Recovery
BW, g	359 ± 22	357 ± 30	371 ± 39
BAT, mg	230 ± 33	594 ± 54***	543 ± 98***
BAT/BW	0.64 ± 0.10	1.67 ± 0.16***	1.47 ± 0.25***
$RT_{firs\ week}$, °C	37.4 ± 0.1	37.1 ± 0.1	—
RT_{CA}, °C	37.0 ± 0.3	37.1 ± 0.4	36.9 ± 0.3
HW, mg	975 ± 29.1	1007 ± 22.0	961 ± 24.5
LV/BW	1.65 ± 0.52	1.77 ± 0.04	1.62 ± 0.1
RV/BW	0.53 ± 0.24	0.55 ± 0.02	0.48 ± 0.02
HW/BW	2.72 ± 0.81	2.82 ± 0.06	2.58 ± 0.05

Values are means ± SE; $n = 12$. BW, body weight; BAT, brown adipose tissue; RT, rectal temperature; CA, cold acclimation; HW, heart weight; LV, left ventricle; RV, right ventricle. ***$P < 0.001$ vs. control.

quently leads to activation of cAMP-dependent protein kinase A (PKA), which phosphorylates proteins essential for cardiac function (56). It has been shown that chronic activation of β1-AR signaling in mice caused progressive hypertrophy and heart failure (16). Moreover, overexpression of $G_s\alpha$ resulted in the development of cardiomyopathy with age (4). At the cellular level, prolonged stimulation of the Gs protein-regulated signaling pathway resulted in Ca^{2+} overload leading to opening of the mitochondrial permeability transition pore (mPTP), stimulation of apoptotic pathways, and myocardial hypertrophy (17, 20, 35), whereas chronic overexpression of β2-ARs was well tolerated in mice (34). Interestingly, PKA may phosphorylate and desensitize the β2-ARs that switch their coupling from the stimulatory (G_s) to the inhibitory (G_i) G proteins, which may initiate the signaling pathways involved in preventing the detrimental effects of β1-AR overstimulation (15, 30). The β3-ARs represent a minor subtype in the heart that is primarily coupled with G_i proteins. Recent studies have shown that cardiac-specifi overexpression of β3-ARs prevented myocardial fibrosi (23) and hypertrophic response (5).

The present study was designed to examine whether mild, gradual CA reduces the extent of myocardial infarction without any negative consequences, and to investigate the potential involvement of β-AR signaling.

METHODS

Acclimation and ischemia/reperfusion injury. Male Wistar rats (7-wk-old; 200 g body wt) obtained from Velaz, Ltd. (http://www.velaz.cz/en) were housed in pairs in cages with sufficien bedding to minimize environmental and social stress. All experiments were performed in the "winter" season (from November till March). The animals were handled in accordance with the *Guide for the Care and Use of Laboratory Animals* published by the U.S. National Institutes of Health (NIH Publication, 8th ed., revised 2011). The experimental protocol was approved by the Animal Care and Use Committee of the Faculty of Science, Charles University, Prague, Czech Republic. Two experimental groups were adapted to 8 ± 1°C for 8 h/day during the firs week and then for 24 h/day during the following 4 wk, either without (CA; $n = 50$ or with 2 wk of recovery at 24 ± 1°C (CAR; $n = 50$). The temperature of acclimation was set-up just above the threshold of shivering and nonshivering thermogenesis in rats (36). The control group (Cont; $n = 50$) was kept at 24 ± 1°C. Rectal temperature was monitored once a day at the same time (between 10 and 11 AM) during the whole experiments. As for infarction analysis, 24 animals per each group were anesthetized (Thiopental at 60 mg/kg) at the end of the acclimation at the respective acclimation temperature to prevent an acute thermoregulatory response. Metoprolol tartrate (Apotex Europe, B.V., Leiden, The Netherlands) was dissolved in a saline and administered intraperitoneally to 12 rats from each group in a dose of 50 mg/kg as a single bolus (1 ml/kg) 20 min before the coronary occlusion. Appropriate controls were given saline in the same volume. Animals were intubated and connected to a rodent ventilator (Ugo Basile, Italy) and ventilated at 60–70 strokes/min (tidal volume of 1.2 ml per 100 g of body weight). The systemic blood pressure was monitored in the cannulated carotid artery and a single lead electrocardiogram was recorded using PowerLab and LabChart Pro software (ADInstruments). Then, the rats were subjected to left thoracotomy and 10-min stabilization, left coronary artery occlusion for 20 min, and subsequent 3-h reperfusion. Subsequently, the heart was excised and the area at risk and the infarct area were delineated by 5% potassium permanganate and frozen. Frozen hearts were cut in 1-mm-thick slices and stained by 1% 2.3.5-triphenyltetrazolium chloride (Sigma-Aldrich) as described previously (39). Infarct size and area at risk were quantifie by Graphic Cell Analyzer software (42).

Crude membrane fractions. In separate groups of animals ($n = 8$ in each group), hearts were rapidly excised from deeply anesthetized rats (Thiopental, 60 mg/kg) and briefl washed in ice-cold saline. Left and right ventricles and septa were separated. The left ventricle (LV) free wall was snap frozen in liquid nitrogen, weighed, and stored in liquid nitrogen until use as described previously (21). Briefly each frozen LV sample was placed in the fivefol volume of ice-cold TMES buffer 10^{-3} M (20 Tris, 3 $MgCl_2$, 1 EDTA, and 250 sucrose, pH 7.4) containing protease and phosphatase inhibitors (cOMPLETE and PhosSTOP, Sigma-Aldrich), cut into small pieces, and homogenized in a glass homogenizer with a motor-driven Teflo pestle at 1,200 rpm for 2 min on ice. The homogenate was centrifuged (2,100 rpm, 10 min, 4°C, Hettich Universal 320 R), the supernatant was collected, and the pellet was rehomogenized in TMES and centrifuged again. The supernatant was mixed with the previous one and centrifuged (23,500 rpm, 30 min, 4°C, Beckman Optima L.90K). The supernatant (cytosolic fraction) was stored at −80°C and used for PKA analyses. The crude membrane fraction in the pellet was rehomogenized in TME buffer, aliquoted, and stored at −80°C until determination of β-ARs, $G_s\alpha$ protein, and adenylyl cyclase activity. Protein concen-

Table 2. *Heart rate and mean arterial blood pressure*

	Baseline $n = 12$	Ischemia $n = 12$	Reperfusion $n = 12$
	Heart rate, beats/min		
Control			
Untreated	386 ± 11	379 ± 10	380 ± 9
Metoprolol	338 ± 8#	321 ± 8#	320 ± 8#
Cold acclimation			
Untreated	375 ± 15	365 ± 14	360 ± 15
Metoprolol	327 ± 10#	307 ± 10#	311 ± 11#
Recovery			
Untreated	387 ± 9	389 ± 12	383 ± 10
Metoprolol	305 ± 6#	296 ± 7#	295 ± 7#
	Blood pressure, mmHg		
Control			
Untreated	82 ± 6	77 ± 3	73 ± 4
Metoprolol	69 ± 4	60 ± 3#	64 ± 4
Cold acclimation			
Untreated	81 ± 8	70 ± 4	62 ± 4†
Metoprolol	60 ± 5#	55 ± 2	58 ± 3
Recovery			
Untreated	93 ± 7	95 ± 7*	89 ± 6*
Metoprolol	61 ± 3#	65 ± 2#	61 ± 3#

Values are means ± SE. *$P < 0.05$ vs. corresponding control group, two-way ANOVA, Dunnett's posttest; #$P < 0.05$ vs. corresponding untreated group, two-way ANOVA, Sidak's posttest; †$P < 0.05$ vs. corresponding baseline, two-way ANOVA, Dunnett's posttest.

tration was measured using the Bradford protein assay (Sigma-Aldrich) (8).

Western blot analysis. Individual samples from each group (20 μg protein per lane, $n = 8$) were resolved by SDS-PAGE electrophoresis using 12% polyacrylamide gels at a constant voltage (200 V) using a Mini-Protean Tetra Cell (Bio-Rad) and subsequently electrotransferred onto nitrocellulose membranes (0.2-μm pore size, Bio-Rad) at a constant voltage of 100 V for 90 min using Wet Blot Module (Bio-Rad) as previously described (28). After blocking with 5% nonfat dry milk in Tris-buffered saline in 10^{-3} M (20 Tris, 500 NaCl, 0.05% Tween 20) for 1 h, the membranes were incubated overnight at 4°C with polyclonal antibodies against β1-ARs (Bioss, bs-0498R), β2-ARs (Bioss, bs-0947R), β3-ARs (Bioss, bs-1063R), $G_s\alpha$ (RCS antibody (26), PKA (Santa Cruz Biotechnology, sc-365615), and PKA phosphorylated at Thr198 (p-PKA, Santa Cruz Biotechnology, sc-32968). The next day, the membranes were washed and incubated with horseradish peroxidase (HRP)-conjugated anti-rabbit antibody (Sigma-Aldrich, A9169) or HRP-conjugated anti-mouse antibody (Invitrogen, no. 31432). Protein bands were visualized by enhanced chemiluminescence (ECL) substrate SuperSignal West Dura Extended Duration Substrate (Thermo Fisher Scientific using the LAS-4000 imaging system (Genetica, Fujifilm) The relative protein levels were quantifie densitometrically using Quantity One Software (Bio-Rad). At least four samples from each group were always run on the same gel, quantifie on the same membrane and normalized to the total protein content per lane determined by Ponceau S staining. Brown adipose tissue was used as a positive control for β3-ARs. The accuracy and reproducibility of the chemiluminescence signal was validated by loading samples in ascending concentrations of 10 to 40 μg of protein per lane and each determination was performed at least three times All figure show representative images of individual Western blots.

Quantitative fluorescence microscopy. In separate groups ($n = 5$ in each group), hearts were rapidly excised from deeply anesthetized rats. They were immediately transferred to the Langendorff apparatus and perfused with relaxing Tyrode solution in 10^{-3} M (140 NaCl, 5.4 KCl, 1 Na_2HPO_4, 1 $MgCl_2 \cdot 6H_2O$, 10 glucose, and 5 HEPES, pH 7.4) and subsequently with freshly prepared 4% formaldehyde in phosphate saline buffer (Sigma-Aldrich) for 2 min and then fixe for 2 h and incubated in 20% sucrose solution overnight. Separated LV tissue samples were frozen in liquid nitrogen and stored at −80°C. Sections (5–7 μm) were cut using a cryostat (Leica CM3050, Leica Microsystems, Wetzlar, Germany), rehydrated in PBS, permeabilized in ice-cold methanol, and shortly incubated in 1% SDS for antigen retrieval. Sections were incubated for 80 min with blocking solution at room temperature (10% donkey serum, 10% goat serum, 0.3% Triton X-100, and 0.3 M glycine in PBS) and stained with rabbit polyclonal anti-β-ARs (see *Western blot analysis*) and subsequently with AlexaFluor 488 conjugated anti-rabbit secondary antibody (LifeTechnologies, A21206). AlexaFluor 647-conjugated wheat germ agglutinin (WGA; Thermo Fisher Scientific W7024) was applied to stain the sarcolemma. Sections were mounted in ProLong Gold Antifade Reagent (Invitrogen, Molecular Probes).

To analyze the subcellular localization of β-ARs and their colocalization with WGA at the sarcolemma, images were taken from at least fiv randomly selected positions from three sections. Images were sequentially scanned using a wide-fiel inverted fluorescenc microscope (Olympus IX2-UCB) equipped with MT20 mercury arc illumination unit (Olympus), a fully motorized stage (Corvus) and a CCD camera (Hamamatsu-Orca C4742-80-12AG). Samples were

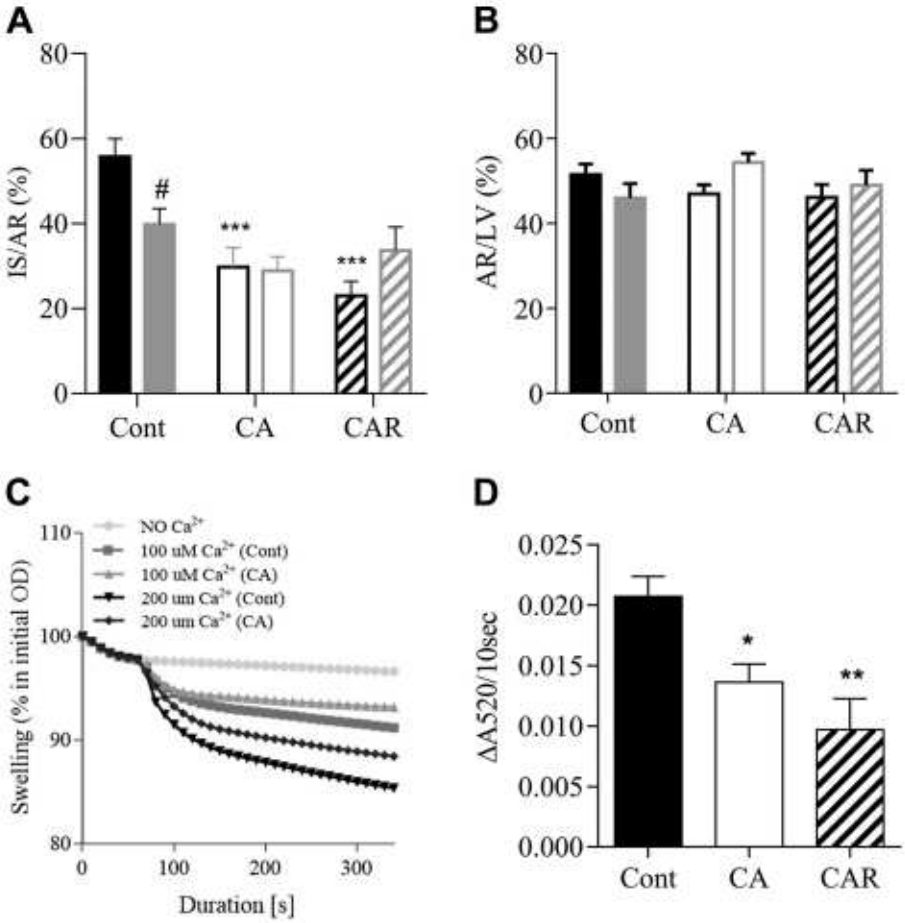

Fig. 1. Myocardial infarct size and mitochondrial swelling rate. The infarct size (IS) expressed as a percentage of area at risk (AR) (*A*) and AR normalized to the left ventricle (LV) (*B*) in control rats (Cont) and those acclimated for 5 wk to cold (CA) and subsequently recovered for 2 wk at 24°C (CAR). Respective gray columns show the effects of metoprolol treatment ($n = 12$ in each group). Representative recordings of Ca^{2+}-induced mitochondrial maximal swelling rate (*C*) and maximal swelling rate at 200 μM Ca^{2+} expressed as a change of the absorbance (ΔA) per 10 s (*D*) ($n = 7$ in each group). OD, optical density. Values are means ± SE. $*P < 0.05$, $**P < 0.01$, $***P < 0.001$ vs. Cont; $\#P < 0.05$ vs. untreated.

observed with a 60 × 1.35NA Plan-Apochromat objective lens with zero gain and 1 × 1 binning. Filter combinations for individual channels were set up as follows: β3-AR (green): U-MWIBA3 (Olympus), excitation: 477.5 nm (bandwidth 17.5 nm), emission: 530 nm (bandwidth 20 nm); and WGA (red): U-N41008 (Chroma Technology Corp.), excitation: 620 nm (bandwidth: 60 nm), emission: 700 nm (bandwidth 7 nm). Each position was optically sectioned at 0.5-μm steps resulting in ~8–12 layers in a Z-stack, depending on specimen thickness.

Colocalization analyses were performed using ImageJ software, a macro for automated image analysis as follows: *1*) each image was calibrated according to magnificatio and image size; *2*) background subtraction using sliding paraboloid option with rolling ball radius fiv pixels was processed to correct uneven illumination; *3*) subcellular colocalization of β3-ARs with sarcolemma and t-tubules was calculated using the *Colocalization Threshold* plug-in of ImageJ (33, 45).

Measurement of mitochondrial swelling. The mitochondrial fraction was isolated from fresh LVs ($n = 7$ in each group) as described previously (39). Mitochondrial swelling was detected as a decrease of absorbance at 520 nm in the Perkin Elmer Lambda spectrophotometer at 30°C in a swelling medium in 10^{-3} M (10 HEPES, 65 KCl, 125 sucrose, 5 succinate, and 1 KPi, pH 7.2) (13). Mitochondria (~0.4 mg of protein) were added to 1 ml of the medium to provide an absorbance of ~1. After 1 min of preincubation of the mitochondrial suspension, $CaCl_2$ solution was added and absorbance changes were detected every 10 s for a further 5 min. The extent of swelling expressed as absorbance change per 5 min ($\Delta A520$/5 min) and the maximum swelling rate after $CaCl_2$ addition obtained after derivation of the swelling curve expressed as absorbance change during 10 s ($\Delta A520$/10 s) were evaluated as parameters of the swelling process (39).

Determination of adenylyl cyclase activity. Adenylyl cyclase activity in crude membrane fractions ($n = 6$ in each group) was determined by measuring the conversion of [α-^{32}P]ATP to [^{32}P]cAMP as previously described (47). Membrane fractions (20 μg of protein) were incubated in a total volume 100 μl of reaction mixture in 10^{-3} M (48 Tris·HCl at pH 8.0, 100 NaCl, 2 $MgCl_2$, 20 GTP, 5 phosphoenolpyruvate, 40 3-isobutyl-1-methylxanthine, 0.1 cAMP, ~15 000 counts/min [^{3}H]cAMP as a tracer, 3.2 U of pyruvate kinase, and 0.8 mg/ml

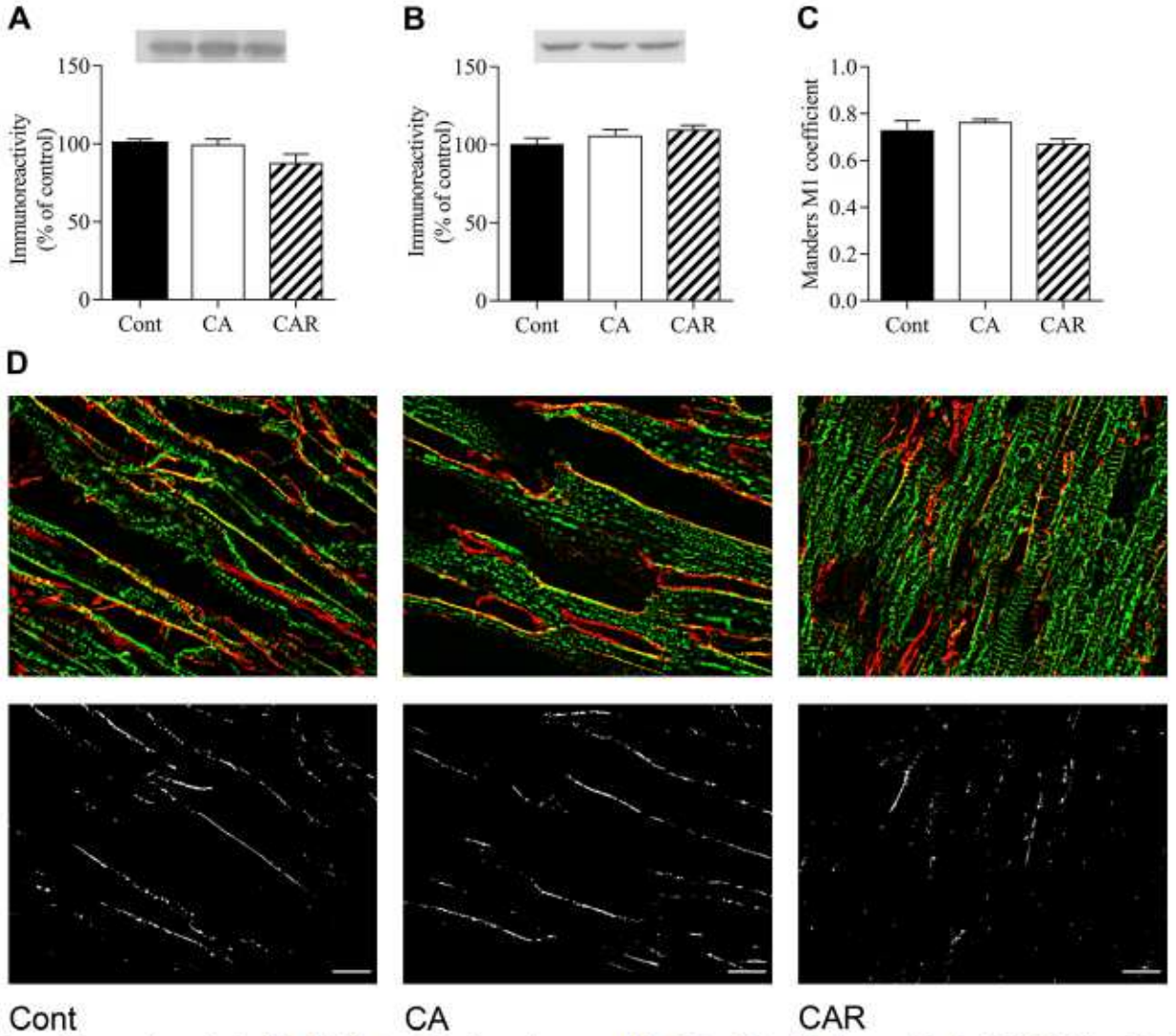

Fig. 2. Myocardial expression and subcellular distribution of β1-adrenergic receptors (β1-ARs) and $G_s\alpha$. Relative protein levels of β1-ARs (*A*) and $G_s\alpha$ (*B*) were determined in myocardial crude membrane fractions ($n = 8$) and β1-ARs colocalization with sarcolemma quantifie by Mander's M1 correlation coefficien ($n = 5$) (*C*) in samples from control rats (Cont) and those acclimated for 5 wk to cold (CA) and subsequently recovered for 2 wk at 24°C (CAR). Representative micrographs of longitudinal cryosections of the left ventricles stained with antibodies against β1-ARs (green) and the sarcolemma counterstained with wheat germ agglutinin (WGA; red); black and white images represent appropriate colocalization pixel map; scale bar = 10 μm (*D*). Values are means ± SE.

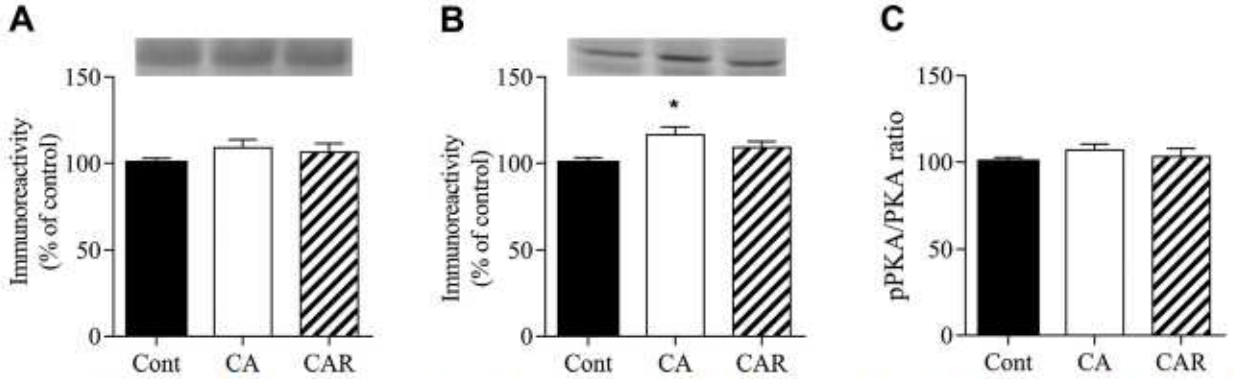

Fig. 3. Myocardial protein kinase A (PKA) expression and phosphorylation (p-PKAThr198). Relative protein levels of PKA (*A*), pPKA (*B*), and the pPKA/PKA ratio (*C*) were determined in the cytosolic fraction ($n = 8$) from control rats (Cont) and those acclimated for 5 wk to cold (CA) and subsequently recovered for 2 wk at 24°C (CAR). Values are means ± SE. $*P < 0.05$ vs. Cont.

BSA). Stimulated adenylyl cyclase activity was measured in the presence of specifi agonists in 10^{-6} M (10 dobutamine, 10 salbutamol, 10 BLR 37344, 10 isoprenaline, and 10 NaF or 10 forskolin). After 1 min of preincubation, 0.4×10^{-3} M ATP was added together with 2,000,000 counts/min [α-^{32}P]ATP and the incubation proceeded for 20 min at 30°C. The reaction was stopped by addition of 200 μl 0.5 M HCl and heated at 100°C for 5 min. Samples were neutralized with 200 μl 1.5 M imidazole. Separation of newly formed [^{32}P]cAMP was performed by using dry alumina column chromatography, and the detected amount of [^{32}P]cAMP was corrected for recovery with [^{3}H]cAMP. Column recovery was 70–75%.

Statistical analysis. For analyses of infarct size, 12 rats were used in each group. Mitochondrial fractions from seven LV samples were used for swelling, crude membrane fractions from eight LVs were used for WB analyses, and six were used for adenylyl cyclase activity in each group. For quantitative immunofluorescenc analysis, samples from fiv hearts per group were used. Data are expressed as means ± SE. Statistical analyses were performed using the GraphPad Prism 8 software (GraphPad, San Diego, CA). The distribution of data was analyzed by Shapiro-Wilk and Komogorov-Smirnov normality tests. For parametric data one-way ANOVA with Tukey multiple comparison test was used to identify significan differences between individual group's means. Two-way ANOVA with Dunnett's multiple comparison test (the effect of cold) and Sidak's multiple comparison test (the effect of metoprolol) was used for the data from metoprolol experiment. $P < 0.05$ was considered statistically significant

RESULTS

First, we validated our model of gradual cold acclimation (CA) by determining the weight of BAT and heart parameters. Subsequently, cardiac ischemic tolerance, blood pressure and heart rate were assessed. Samples of LV myocardium were used for the determination of mitochondrial resistance to calcium overload. Next, we investigated expression of β-ARs and their association with the sarcolemma and downstream activation of PKA. Finally, adenylyl cyclase activities by measurement of cAMP production after different specifi ligand stimulation were assessed.

The efficienc of cold acclimation process was monitored by measuring BAT. The weight of BAT significantl increased by 158% after CA and remained increased by 136% after recovery when compared with the control group. Since the rectal temperature did not differ among the groups, a possible hypothermic state of the animals during the CA period can be excluded. CA affected neither body and heart weight nor the heart-to-body weight ratio (Table 1).

The baseline heart rate and mean arterial blood pressure did not differ among the groups. Acute administration of metoprolol significantl decreased heart rate in all groups at baseline as well as after ischemia and reperfusion and tended to decrease blood pressure, though the later effect usually did not reach significanc (Table 2).

The infarct size was reduced to 30% of area at risk (AR) after CA and to 23% after CAR compared with 56% in controls. Acute administration of metoprolol decreased infarct size in controls to 40% and had no effect in CA and CAR groups (Fig. 1*A*). The average area at risk normalized to the LV (AR/LV) was 46–55% and did not differ among the groups (Fig. 1*B*). In line with the infarct size limiting effect of CA, the maximal mitochondrial swelling rate at 200 μM Ca^{2+} declined

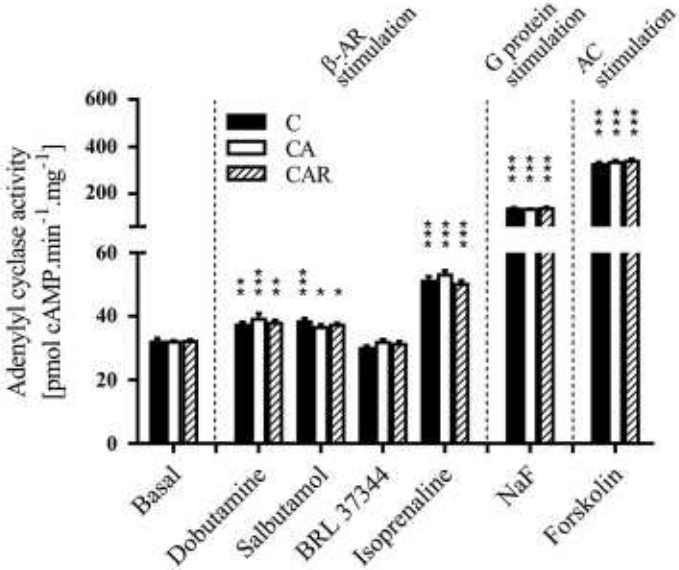

Fig. 4. Myocardial adenylyl cyclase. Activity of adenylyl cyclase (AC) in myocardial crude membrane fraction from control rats (C) and those acclimated for 5 wk to cold (CA) and subsequently recovered for 2 wk at 24°C (CAR) was determined under basal conditions and after stimulation by specifi β-adrenergic (β-AR) agonists (dobutamine for β1-AR, salbutamol for β2-AR, and BLR37344 for β3-AR) and isoprenaline nonspecifi β-AR agonist. NaF was used as activator of G proteins and forskolin as activator of AC ($n = 6$). Values are means ± SE. $*P < 0.05$, $**P < 0.01$, $***P < 0.001$ vs. corresponding basal AC activity.

in both experimental groups by 34% and 54%, respectively, suggesting delayed opening of the mPTP (Fig. 1, *C* and *D*).

Neither Western blot analysis nor quantitative immunofluorescence of β1-ARs showed any significan differences between control and CA or CAR samples. In line, the level of $G_s\alpha$ was not affected (Fig. 2, *A–D*). After CA, the total PKA protein amount was not changed and only pPKA (Thr198) was increased by 17%; however, the ratio of pPKA/PKA was not significantl affected (Fig. 3, *A–C*).

Activity of adenylyl cyclase was measured under basal conditions and in the presence of selected β-adrenergic agonists in all experimental groups. Basal activity of adenylyl cyclase did not differ among the groups. Whereas dobutamine (selective β1-AR agonist) and salbutamol (selective β2-AR agonist) slightly but significantl increased the adenylyl cyclase activity by 16–19%, BLR 37344 (selective β3-AR agonist) did not have any effect. Isoprenaline (nonselective β-adrenergic agonist) markedly increased the adenylyl cyclase activity by 61% without any significan differences among the groups. The ability of G_s protein to activate adenylyl cyclase was tested using fluorid ions (NaF). The NaF increased adenylyl cyclase activity about fourfold without any difference among the groups. Forskolin, a direct activator of adenylyl cyclase, increased its activity 10-fold in all experimental groups and neither CA nor CAR affected its ability to activate the enzyme (Fig. 4).

CA increased the amount of β2-ARs in the membrane fraction by 46% and the fraction that localized at the sarcolemma by 16%. Similarly, CAR was accompanied by a 30% increase in the total amount of β2-ARs, while their colocalization with the sarcolemma did not change compared with controls (Fig. 5, *A–C*). The protein level of β3-ARs increased after CA by 34% and remained increased after CAR by 52%. Analysis of the subcellular distribution of β3-ARs revealed their increased co-localization with the sarcolemma in CA and CAR groups by 18% and 12%, respectively (Fig. 6, *A–C*).

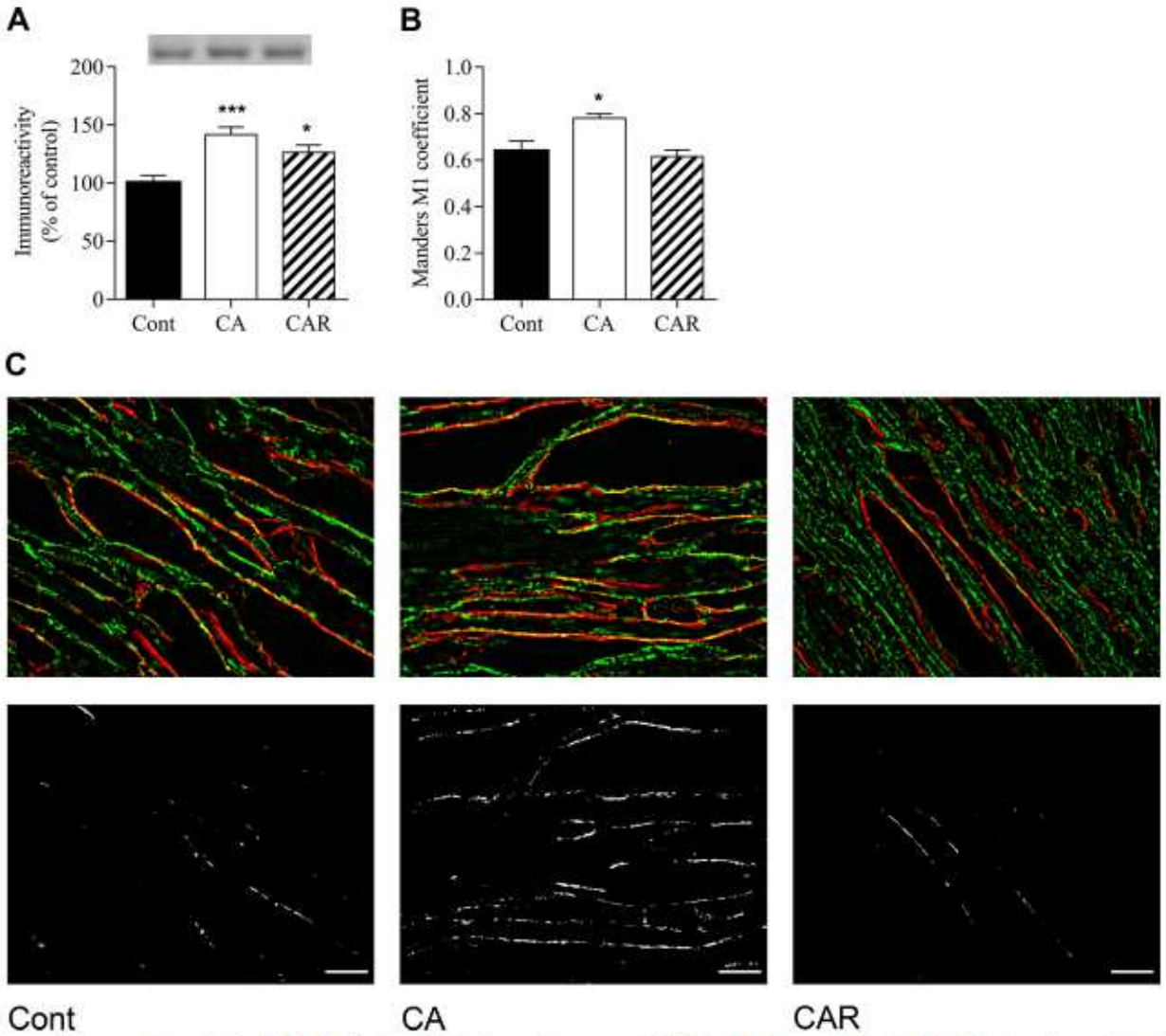

Fig. 5. Myocardial expression and subcellular distribution of β2-adrenergic receptors (β2-ARs). Relative protein level of β2-ARs in crude membrane fractions ($n = 8$) (*A*) and β2-ARs colocalization with sarcolemma quantifie by Mander's M1 correlation coefficien ($n = 5$) (*B*) in control rats (Cont) and those acclimated for 5 wk to cold (CA) and subsequently recovered for 2 wk at 24°C (CAR). Representative micrographs of longitudinal cryosections of the left ventricles stained with antibodies against β2-ARs (green) and the sarcolemma counterstained with WGA (red); black and white images represent appropriate colocalization pixel map; scale bar = 10 μm (*C*). Values are means ± SE. $*P < 0.05$, $***P < 0.001$ vs. Cont.

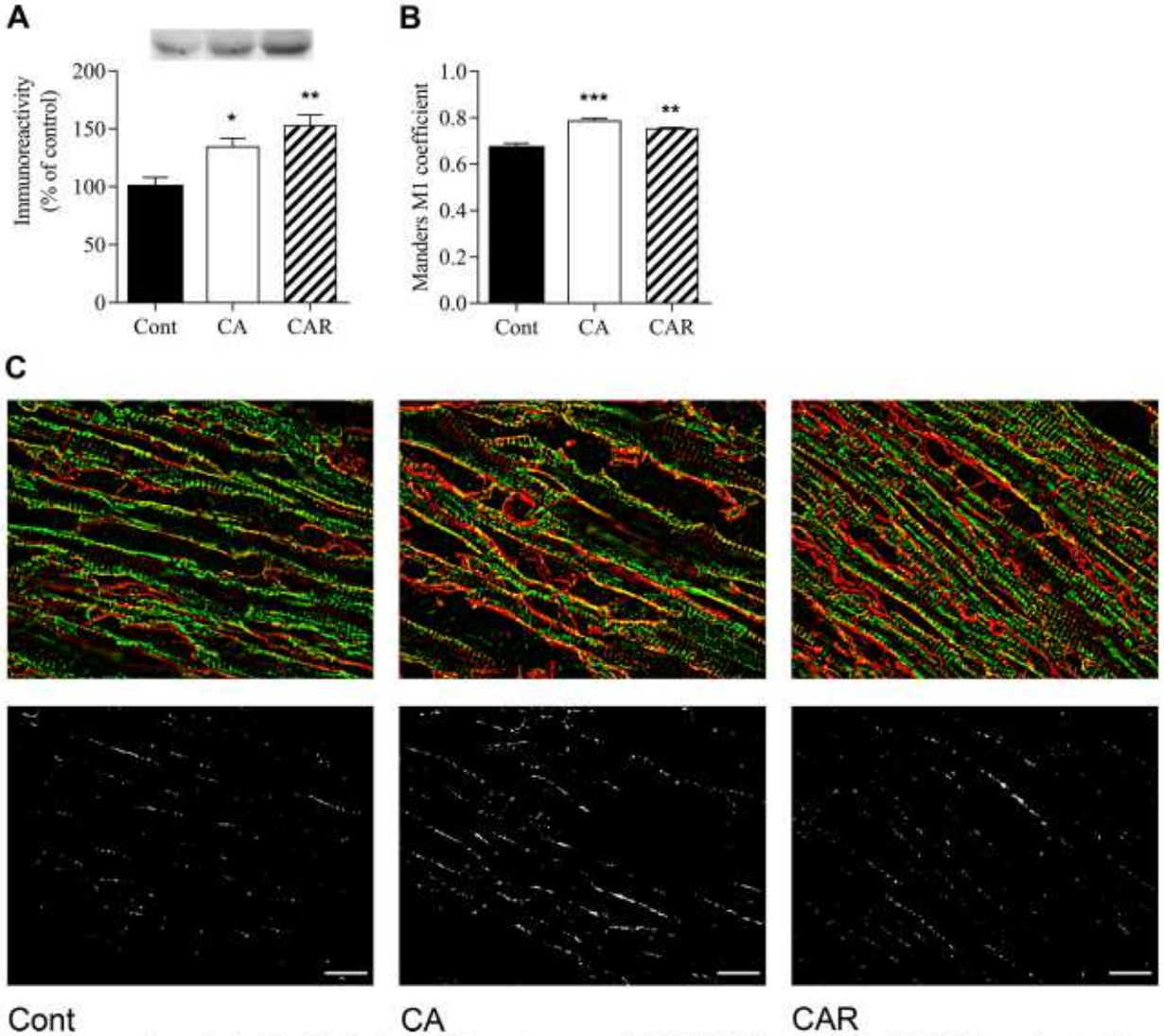

Fig. 6. Myocardial expression and subcellular distribution of β3-adrenergic receptors (β3-ARs). Relative protein level of β3-ARs was determined in myocardial crude membrane fraction (n = 8) (A) and of β3-ARs colocalization with sarcolemma quantifie by Mander's M1 correlation coefficien (n = 5) (*B*) in samples from control rats (Cont) and those acclimated for 5 wk to cold (CA) and subsequently recovered for 2 wk at 24°C (CAR). Representative micrographs of longitudinal cryosections of the left ventricles stained with antibodies against β3-ARs (green) and the sarcolemma counterstained with WGA (red); black and white images represent appropriate colocalization pixel map; scale bar = 10 μm (*C*). Values are means ± SE. *$P < 0.05$, **$P < 0.01$, ***$P < 0.001$ vs. Cont.

DISCUSSION

In the present study we demonstrate infarct size-limiting effect of CA that persisted over the next 2 wk, that was accompanied by decreased sensitivity of mPTP to Ca^{2+}-induced opening. Importantly, we observed neither hypertension nor LV hypertrophy. In view of the essential role of the sympathetic system in CA, we focused on examining whether the development of a cardioprotective phenotype is associated with altered β-AR signaling. Using the specifi agonists on crude membrane fractions, we observed that neither CA nor CAR affected functioning of the myocardial β1/β2/β3-AR-mediated adenylyl cyclase signaling system. Acute administration of metoprolol 20 min before coronary occlusion did not affect CA-elicited cardioprotection. Furthermore, the enhanced myocardial protection was accompanied by increased translocation of β2- and β3-ARs but not of β1-ARs to the sarcolemma.

Prolonged activation of β1-ARs is generally understood as detrimental and β2-AR stimulation as protective. However, it became clear that the protective and detrimental effects depend on the duration and intensity of stimulation of both receptor subtypes (reviewed by (6)). The effect of cold exposure on the heart has been rarely studied at the molecular level, and there are only two reports dealing with AR-mediated signaling. Xing et al. (58) revealed increased adenylyl cyclase activity in skeletal muscle and liver during the firs 3 wk of intermittent daily cold exposure (swimming in 4°C cold water, 30 min per day) that returned to the control value within the fourth week. Tillinger et al. (51) reported that the mRNA level of β1-ARs in the rat heart after 28 days of cold exposure at 4°C did not differ from control level.

In this study, metoprolol administration decreased infarct size in control rats, which is in agreement with previous studies. Metoprolol, a specifi β1-AR antagonist, blocks the

cardiac responses of released catecholamines protecting the myocardium when given before the onset of ischemia (10, 31). The metoprolol effect, seen as a drop of heart rate, may prevent hyperactivation of the PKA pathway and thus attenuate the rate of oxygen and energy substrate depletion within affected cardiomyocytes during ischemia. Importantly, metoprolol administration did not affect the cardioprotection elicited by CA. This observation may suggest that β1-ARs are not a major player in the CA-elicited cardioprotection despite the fact that they play an important role in the development of nonshivering thermogenesis (12).

Abnormalities in G proteins, adenylyl cyclase activity, and cAMP levels may be responsible for the altered cardiac performance and vascular function observed in hypertension and hypertrophy (7). It was repeatedly demonstrated that chronic cold exposure induces both systemic hypertension and hypertrophy (18, 52). Blockade of β-ARs by propranolol confirme the importance of these receptors in the development of hypertension (43, 57). Interestingly, pulmonary hypertension and right ventricular hypertrophy caused by chronic hypoxia was found to be associated with depressed responsiveness to β-adrenergic stimulation and deranged adenylyl cyclase signaling (21, 24). The unaltered function of myocardial β-AR-mediated adenylyl cyclase signaling after mild CA may explain the absence of hypertension in our cardioprotective model. Moreover, we suppose that animal housing in pairs and in well-bedded cages can forestall additive side-effects of cold and social stress that could otherwise result in hypertension (48). Individual housing in a cold environment can have an adverse effect on cardiovascular system and develop hypertension accompanied with irreversible ventricular hypertrophy in rats (49).

The mild increase of phosphorylated PKA after CA observed in the present study may be related to the dual function of the enzyme in adrenergic signaling. Besides the stimulation of adenylyl cyclase, the second important function of PKA-mediated phosphorylation of the β2-ARs is the attenuation of the affinit of the receptor to Gαs and thus the promotion of receptor coupling to $G_i\alpha$ (14, 59). The observed increase in an association of β2-ARs with the sarcolemma after CA may suggest an activation of the β2-AR-G_i-related pathways associated with cell survival and antiapoptotic effects in cardiac myocytes (14, 60). Furthermore, β2-ARs influenc vascular reactivity and may participate in the regulation of blood pressure (37).

Interestingly, the amount of β3-ARs that lack phosphorylation sites and thus are resistant to PKA-mediated phosphorylation (44) was increased in both experimental groups. β3-ARs, predominantly coupled to $G_i\alpha$ and functionally different from other β-AR subtypes, may prevent catecholamine overstimulation (40). Moreover, the β2/β3-AR signaling via $G_i\alpha$ plays an important role in attenuation of hypertrophic remodeling through the inhibition of Ca^{2+} overload (22). This is in line with the absence of myocardial hypertrophy in CA rats in the present study. Interestingly, stimulation of the β3-ARs during I/R improved cardiac function through inhibition of mPTP opening in cardiomyocytes (19). The probability of mPTP opening plays an essential role in cardiac I/R injury and its attenuation is cytoprotective (1, 25, 41). The inhibitory effect of CA on mPTP opening in our study is in line with this view. Importantly, administration of β3-AR agonist was shown to have a limiting effect on infarct size, and clinical application of β3-AR agonists during ischemia and/or early reperfusion was recommended (3, 44). Based on these data, we speculate that the CA-elicited cardioprotection may be at least partially based on noncanonical β2/β3-AR signaling. Nevertheless, the control of β3-ARs activity in the heart is complex (11) and regulation of these receptors in the context of gradual CA needs further thorough investigation.

In conclusion, our study demonstrates for the firs time that mild gradual cold acclimation leads to a persisting infarct size reduction without hypertension and myocardial hypertrophy. The cardioprotective mechanism is independent of cAMP signaling and may involve delayed mPTP opening. The role of upregulated β2/β3-ARs remains to be elucidated. Our experiments identifie gradual cold acclimation as a novel potential preventive and therapeutic strategy against myocardial I/R injury.

ACKNOWLEDGMENTS

We are grateful to Dr Elisabeth Ehler, King's College London, United Kingdom for critical reading of the manuscript and Dr. Peter van der Ven, Institute for Cell Biology, University of Bonn, Germany, for constructive criticism of the manuscript. We sincerely thank Dr. Ivan Zahradnik, Biomedical Research Center SAS, Slovak Academy of Sciences, Bratislava, Slovakia for providing us with Graphic Cell Analyzer software.

GRANTS

This work has been supported by the Charles University Grant Agency (GAUK 188015; 641216), Czech Science Foundation (17-07748S), and the Ministry of Education, Youth and Sport of the Czech Republic (SVV-260434/2019). Microscopy was performed in the Laboratory of Confocal and Fluorescence Microscopy co-finance by the European Regional Development Fund and the state budget of the Czech Republic Project No. CZ.1.05/4.1.00/16.0347 and CZ.2.16/3.1.00/21515.

DISCLOSURES

No conflict of interest, financia or otherwise, are declared by the authors.

AUTHOR CONTRIBUTIONS

V.T., A.B., P.A., J.N., F.K., O.N., and J.M.Z. conceived and designed research; V.T., A.B., P.V., A.L., L.H., B.E., Z.D., D.H., F.G., D.K., S.V., P.A., F.K., O.N., and J.M.Z. performed experiments; V.T., A.B., P.V., A.L., L.H., B.E., Z.D., D.H., F.G., D.K., S.V., P.A., J.N., F.K., O.N., and J.M.Z. analyzed data; V.T., A.B., P.V., A.L., L.H., B.E., Z.D., D.K., S.V., P.A., J.N., F.K., O.N., and J.M.Z. interpreted results of experiments; V.T., A.B., P.V., A.L., L.H., B.E., and D.H. prepared figures V.T., A.B., J.N., F.K., O.N., and J.M.Z. drafted manuscript; V.T., A.B., P.V., S.V., P.A., J.N., F.K., O.N., and J.M.Z. edited and revised manuscript; V.T., A.B., P.V., A.L., L.H., B.E., Z.D., D.H., F.G., D.K., S.V., P.A., J.N., F.K., O.N., and J.M.Z. approved fina version of manuscript.

REFERENCES

1. **Abdallah Y, Kasseckert SA, Iraqi W, Said M, Shahzad T, Erdogan A, Neuhof C, Gündüz D, Schlüter K-D, Tillmanns H, Piper HM, Reusch HP, Ladilov Y.** Interplay between Ca^{2+} cycling and mitochondrial permeability transition pores promotes reperfusion-induced injury of cardiac myocytes. *J Cell Mol Med* 15: 2478–2485, 2011. doi:10.1111/j.1582-4934.2010.01249.x.
2. **Andreadou I, Adamovski P, Bartekova M, Beauloye C, Bertrand L, Biedermann D, Borutaite V, Bøtker HE, Chlopicki S, Dambrova M, Davidson S, Devaux Y, Di Lisa F, Djuric D, Erlinge D, Falcao-Pires I, Galatou E, García-Dorado D, Garcia-Sosa AT, Girão H, Giricz Z, Gyöngyösi M, Healy D, Heusch G, Jakovljevic V, Jovanic J, Kolar F, Kwak BR, Leszek P, Liepinsh E, Longnus S, Marinovic J, Muntean DM, Nezic L, Ovize M, Pagliaro P, Gomes CP C, Pernow J, Persidis A, Phiscke SE, Podesser BK, Prunier F, Ravingerova T, Ruiz-Meana M, Schulz R, Scridon A, Slagsvold KH, Lønborg JT, Turan B, van Royen N, Vendelin M, Walsh S, Yellon D, Zidar N, Zuurbier CJ,**

Ferdinandy P, Hausenloy JD, van Royen N, Vendelin M, Walsh S, Yellon D, Zidar N, Zuurbier CJ, Ferdinandy P, Hausenloy JD. Realizing the therapeutic potential of novel cardioprotective therapies: The EU-CARDIOPROTECTION COST Action–CA16225. *Cond Med* 1: 116–123, 2018.

3. **Aragón JP, Condit ME, Bhushan S, Predmore BL, Patel SS, Grinsfelder DB, Gundewar S, Jha S, Calvert JW, Barouch LA, Lavu M, Wright HM, Lefer DJ.** Beta3-adrenoreceptor stimulation ameliorates myocardial ischemia-reperfusion injury via endothelial nitric oxide synthase and neuronal nitric oxide synthase activation. *J Am Coll Cardiol* 58: 2683–2691, 2011. doi:10.1016/j.jacc.2011.09.033.
4. **Asai K, Yang GP, Geng YJ, Takagi G, Bishop S, Ishikawa Y, Shannon RP, Wagner TE, Vatner DE, Homcy CJ, Vatner SF.** Beta-adrenergic receptor blockade arrests myocyte damage and preserves cardiac function in the transgenic G(salpha) mouse. *J Clin Invest* 104: 551–558, 1999. doi:10.1172/JCI7418.
5. **Belge C, Hammond J, Dubois-Deruy E, Manoury B, Hamelet J, Beauloye C, Markl A, Pouleur AC, Bertrand L, Esfahani H, Jnaoui K, Götz KR, Nikolaev VO, Vanderper A, Herijgers P, Lobysheva I, Iaccarino G, Hilfiker-Kleiner D, Tavernier G, Langin D, Dessy C, Balligand J-L.** Enhanced expression of β3-adrenoceptors in cardiac myocytes attenuates neurohormone-induced hypertrophic remodeling through nitric oxide synthase. *Circulation* 129: 451–462, 2014. doi:10.1161/CIRCULATIONAHA.113.004940.
6. **Bernstein D, Fajardo G, Zhao M.** The role of β-adrenergic receptors in heart failure: differential regulation of cardiotoxicity and cardioprotection. *Prog Pediatr Cardiol* 31: 35–38, 2011. doi:10.1016/j.ppedcard.2010.11.007.
7. **Böhm M, Flesch M, Schnabel P.** β-adrenergic signal transduction in the failing and hypertrophied myocardium. *J Mol Med (Berl)* 75: 842–848, 1997. doi:10.1007/s001090050175.
8. **Bradford MM.** A rapid and sensitive method for the quantitation of microgram quantities of protein utilizing the principle of protein-dye binding. *Anal Biochem* 72: 248–254, 1976. doi:10.1016/0003-2697(76)90527-3.
9. **Brodde OE, Michel MC.** Adrenergic and muscarinic receptors in the human heart. *Pharmacol Rev* 51: 651–690, 1999.
10. **Bullock GR, Leprán I, Parratt JR, Szekeres L, Wainwright CL.** Effects of a combination of metoprolol and dazmegrel on myocardial infarct size in rats. *Br J Pharmacol* 86: 235–240, 1985. doi:10.1111/j.1476-5381.1985.tb09454.x.
11. **Cannavo A, Koch WJ.** Targeting β3-adrenergic receptors in the heart: selective agonism and β-blockade. *J Cardiovasc Pharmacol* 69: 71–78, 2017. doi:10.1097/FJC.0000000000000444.
12. **Cannon B, Nedergaard J.** Brown adipose tissue: function and physiological significance *Physiol Rev* 84: 277–359, 2004. doi:10.1152/physrev.00015.2003.
13. **Castilho RF, Kowaltowski AJ, Vercesi AE.** 3,5,3′-triiodothyronine induces mitochondrial permeability transition mediated by reactive oxygen species and membrane protein thiol oxidation. *Arch Biochem Biophys* 354: 151–157, 1998. doi:10.1006/abbi.1998.0657.
14. **Chesley A, Lundberg MS, Asai T, Xiao RP, Ohtani S, Lakatta EG, Crow MT.** The beta(2)-adrenergic receptor delivers an antiapoptotic signal to cardiac myocytes through G(i)-dependent coupling to phosphatidylinositol 3′-kinase. *Circ Res* 87: 1172–1179, 2000. doi:10.1161/01.RES.87.12.1172.
15. **Daaka Y, Luttrell LM, Lefkowitz RJ.** Switching of the coupling of the beta2-adrenergic receptor to different G proteins by protein kinase A. *Nature* 390: 88–91, 1997. doi:10.1038/36362.
16. **Engelhardt S, Hein L, Wiesmann F, Lohse MJ.** Progressive hypertrophy and heart failure in β1-adrenergic receptor transgenic mice. *Proc Natl Acad Sci USA* 96: 7059–7064, 1999. doi:10.1073/pnas.96.12.7059.
17. **Feng N, Anderson ME.** CaMKII is a nodal signal for multiple programmed cell death pathways in heart. *J Mol Cell Cardiol* 103: 102–109, 2017. doi:10.1016/j.yjmcc.2016.12.007.
18. **Fregly MJ, Kikta DC, Threatte RM, Torres JL, Barney CC.** Development of hypertension in rats during chronic exposure to cold. *J Appl Physiol (1985)* 66: 741–749, 1989. doi:10.1152/jappl.1989.66.2.741.
19. **García-Prieto J, García-Ruiz JM, Sanz-Rosa D, Pun A, García-Alvarez A, Davidson SM, Fernández-Friera L, Nuno-Ayala M, Fernández-Jiménez R, Bernal JA, Izquierdo-Garcia JL, Jimenez-Borreguero J, Pizarro G, Ruiz-Cabello J, Macaya C, Fuster V, Yellon DM, Ibanez B.** β3 adrenergic receptor selective stimulation during ischemia/reperfusion improves cardiac function in translational models through inhibition of mPTP opening in cardiomyocytes. *Basic Res Cardiol* 109: 422, 2014. doi:10.1007/s00395-014-0422-0.
20. **Gaussin V, Tomlinson JE, Depre C, Engelhardt S, Antos CL, Takagi G, Hein L, Topper JN, Liggett SB, Olson EN, Lohse MJ, Vatner SF, Vatner DE.** Common genomic response in different mouse models of beta-adrenergic-induced cardiomyopathy. *Circulation* 108: 2926–2933, 2003. doi:10.1161/01.CIR.0000101922.18151.7B.
21. **Hahnova K, Kasparova D, Zurmanova J, Neckar J, Kolar F, Novotny J.** β-Adrenergic signaling in rat heart is similarly affected by continuous and intermittent normobaric hypoxia. *Gen Physiol Biophys* 35: 165–173, 2016. doi:10.4149/gpb_2015053.
22. **Hammond J, Balligand JL.** Nitric oxide synthase and cyclic GMP signaling in cardiac myocytes: from contractility to remodeling. *J Mol Cell Cardiol* 52: 330–340, 2012. doi:10.1016/j.yjmcc.2011.07.029.
23. **Hermida N, Michel L, Esfahani H, Dubois-Deruy E, Hammond J, Bouzin C, Markl A, Colin H, Steenbergen AV, De Meester C, Beauloye C, Horman S, Yin X, Mayr M, Balligand JL.** Cardiac myocyte β3-adrenergic receptors prevent myocardial fibrosi by modulating oxidant stress-dependent paracrine signaling. *Eur Heart J* 39: 888–898, 2018. doi:10.1093/eurheartj/ehx366.
24. **Hrbasová M, Novotny J, Hejnová L, Kolár F, Neckár J, Svoboda P.** Altered myocardial G_s protein and adenylyl cyclase signaling in rats exposed to chronic hypoxia and normoxic recovery. *J Appl Physiol (1985)* 94: 2423–2432, 2003. doi:10.1152/japplphysiol.00958.2002.
25. **Hurst S, Hoek J, Sheu SS.** Mitochondrial Ca^{2+} and regulation of the permeability transition pore. *J Bioenerg Biomembr* 49: 27–47, 2017. doi:10.1007/s10863-016-9672-x.
26. **Ihnatovych I, Hejnová L, Kostrnová A, Mares P, Svoboda P, Novotný J.** Maturation of rat brain is accompanied by differential expression of the long and short splice variants of G(s)alpha protein: identificatio of cytosolic forms of G(s)alpha. *J Neurochem* 79: 88–97, 2001. doi:10.1046/j.1471-4159.2001.00544.x.
27. **Janský L, Vybíral S, Trubacová M, Okrouhlík J.** Modulation of adrenergic receptors and adrenergic functions in cold adapted humans. *Eur J Appl Physiol* 104: 131–135, 2008. doi:10.1007/s00421-007-0627-0.
28. **Kasparova D, Neckar J, Dabrowska L, Novotny J, Mraz J, Kolar F, Zurmanova J.** Cardioprotective and nonprotective regimens of chronic hypoxia diversely affect the myocardial antioxidant systems. *Physiol Genomics* 47: 612–620, 2015. doi:10.1152/physiolgenomics.00058.2015.
29. **Kralova Lesna I, Rychlikova J, Vavrova L, Vybiral S.** Could human cold adaptation decrease the risk of cardiovascular disease? *J Therm Biol* 52: 192–198, 2015. doi:10.1016/j.jtherbio.2015.07.007.
30. **Kuschel M, Zhou YY, Cheng H, Zhang SJ, Chen Y, Lakatta EG, Xiao RP.** G(i) protein-mediated functional compartmentalization of cardiac β(2)-adrenergic signaling. *J Biol Chem* 274: 22048–22052, 1999. doi:10.1074/jbc.274.31.22048.
31. **Lai Q, Yuan G, Wang H, Liu Z, Kou J, Yu B, Li F.** Metabolomic profilin of metoprolol-induced cardioprotection in a murine model of acute myocardial ischemia. *Biomed Pharmacother* 124: 109820, 2020. doi:10.1016/j.biopha.2020.109820.
32. **Laurberg P, Andersen S, Karmisholt J.** Cold adaptation and thyroid hormone metabolism. *Horm Metab Res* 37: 545–549, 2005. doi:10.1055/s-2005-870420.
33. **Li Z, Xiang T, Yin Y, Niu Y, Yang J, Xie Z.** [Separating independent components in heart period signal]. *Sheng Wu Yi Xue Gong Cheng Xue Za Zhi* 21: 401–405, 2004.
34. **Liggett SB, Tepe NM, Lorenz JN, Canning AM, Jantz TD, Mitarai S, Yatani A, Dorn GW 2nd.** Early and delayed consequences of beta(2)-adrenergic receptor overexpression in mouse hearts: critical role for expression level. *Circulation* 101: 1707–1714, 2000. doi:10.1161/01.CIR.101.14.1707.
35. **Lohse MJ, Engelhardt S, Eschenhagen T.** What is the role of beta-adrenergic signaling in heart failure? *Circ Res* 93: 896–906, 2003. doi:10.1161/01.RES.0000102042.83024.CA.
36. **Løvmo T, Eken T, Bekkestad Rein E, Njå A.** Body temperature control in rats by muscle tone during rest or sleep. *Acta Physiol (Oxf)* 228: e13348, 2020. doi:10.1111/apha.13348.
37. **Masuo K.** Roles of beta2- and beta3-adrenoceptor polymorphisms in hypertension and metabolic syndrome. *Int J Hypertens* 2010: 832821, 2010. doi:10.4061/2010/832821.
39. **Neckář J, Svatoňová A, Weissová R, Drahota Z, Zajíčková P, Brabcová I, Kolář D, Alánová P, Vašinová J, Šilhavý J, Hlaváčková M, Tauchmannová K, Milerová M, Ošťádal B, Červenka L, Žurmanová J, Kalous M, Nováková O, Novotný J, Pravenec M, Kolář F.** Selective

replacement of mitochondrial DNA increases the cardioprotective effect of chronic continuous hypoxia in spontaneously hypertensive rats. *Clin Sci (Lond)* 131: 865–881, 2017. doi:10.1042/CS20170083.

40. **Niu X, Watts VL, Cingolani OH, Sivakumaran V, Leyton-Mange JS, Ellis CL, Miller KL, Vandegaer K, Bedja D, Gabrielson KL, Paolocci N, Kass DA, Barouch LA.** Cardioprotective effect of beta-3 adrenergic receptor agonism: role of neuronal nitric oxide synthase. *J Am Coll Cardiol* 59: 1979–1987, 2012. doi:10.1016/j.jacc.2011.12.046.
41. **Ong SB, Samangouei P, Kalkhoran SB, Hausenloy DJ.** The mitochondrial permeability transition pore and its role in myocardial ischemia reperfusion injury. *J Mol Cell Cardiol* 78: 23–34, 2015. doi:10.1016/j.yjmcc.2014.11.005.
42. **Parulek J, Srámek M, Cerveanský M, Novotová M, Zahradník I.** A cell architecture modeling system based on quantitative ultrastructural characteristics. *Methods Mol Biol* 500: 289–312, 2009. doi:10.1007/978-1-59745-525-1_10.
43. **Prichard BN, Gillam PM.** Treatment of hypertension with propranolol. *BMJ* 1: 7–16, 1969. doi:10.1136/bmj.1.5635.7.
44. **Salie R, Alsalhin AK, Marais E, Lochner A.** Cardioprotective effects of beta3-adrenergic receptor (β3-AR) pre-, per-, and post-treatment in ischemia-reperfusion. *Cardiovasc Drugs Ther* 33: 163–177, 2019. doi:10.1007/s10557-019-06861-5.
45. **Schindelin J, Arganda-Carreras I, Frise E, Kaynig V, Longair M, Pietzsch T, Preibisch S, Rueden C, Saalfeld S, Schmid B, Tinevez J-Y, White DJ, Hartenstein V, Eliceiri K, Tomancak P, Cardona A.** Fiji: an open-source platform for biological-image analysis. *Nat Methods* 9: 676–682, 2012. doi:10.1038/nmeth.2019.
46. **Schrauwen P, Hesselink M.** UCP2 and UCP3 in muscle controlling body metabolism. *J Exp Biol* 205: 2275–2285, 2002.
47. **Skrabalova J, Neckar J, Hejnova L, Bartonova I, Kolar F, Novotny J.** Antiarrhythmic effect of prolonged morphine exposure is accompanied by altered myocardial adenylyl cyclase signaling in rats. *Pharmacol Rep* 64: 351–359, 2012. doi:10.1016/S1734-1140(12)70775-2.
48. **Spruill TM.** Chronic psychosocial stress and hypertension. *Curr Hypertens Rep* 12: 10–16, 2010. doi:10.1007/s11906-009-0084-8.
49. **Sun Z, Cade JR, Fregly MJ, Rowland NE.** Effect of chronic treatment with propranolol on the cardiovascular responses to chronic cold exposure. *Physiol Behav* 62: 379–384, 1997. doi:10.1016/S0031-9384(97)00033-4.
50. **The Eurowinter Group.** Cold exposure and winter mortality from ischaemic heart disease, cerebrovascular disease, respiratory disease, and all causes in warm and cold regions of Europe. *Lancet* 349: 1341–1346, 1997. doi:10.1016/S0140-6736(96)12338-2.
51. **Tillinger A, Myslivecek J, Nováková M, Krizanova O, Kvetnanský R.** Gene expression of adrenoceptors in the hearts of cold-acclimated rats exposed to a novel stressor. *Ann N Y Acad Sci* 1148: 393–399, 2008. doi:10.1196/annals.1410.024.
52. **Tsibulnikov SY, Maslov LN, Naryzhnaya NV, Ivanov VV, Bushov YV, Voronkov NS, Jaggi AS, Zhang Y, Oeltgen PR.** Impact of cold adaptation on cardiac tolerance to ischemia/reperfusion. Role of glucocorticoid and thyroid hormones. *Gen Physiol Biophys* 38: 245–251, 2019. doi:10.4149/gpb_2019002.
53. **van der Lans AA, Hoeks J, Brans B, Vijgen GH, Visser MG, Vosselman MJ, Hansen J, Jörgensen JA, Wu J, Mottaghy FM, Schrauwen P, van Marken Lichtenbelt WD.** Cold acclimation recruits human brown fat and increases nonshivering thermogenesis. *J Clin Invest* 123: 3395–3403, 2013. doi:10.1172/JCI68993.
54. **Villarroya F, Cereijo R, Villarroya J, Giralt M.** Brown adipose tissue as a secretory organ. *Nat Rev Endocrinol* 13: 26–35, 2017. doi:10.1038/nrendo.2016.136.
55. **Vybíral S, Lesná I, Janský L, Zeman V.** Thermoregulation in winter swimmers and physiological significanc of human catecholamine thermogenesis. *Exp Physiol* 85: 321–326, 2000. doi:10.1111/j.1469-445X.2000.01909.x.
56. **Wang J, Gareri C, Rockman HA.** G-protein-coupled receptors in heart disease. *Circ Res* 123: 716–735, 2018. doi:10.1161/CIRCRESAHA.118.311403.
57. **Weissinger J.** Propranolol can inhibit the development of hypertension in SHR. *Clin Exp Hypertens A* 6: 1169–1177, 1984. doi:10.3109/10641968409039589.
58. **Xing JQ, Zhou Y, Chen JF, Li SB, Fang W, Yang J.** Effect of cold adaptation on activities of relevant enzymes and antioxidant system in rats. *Int J Clin Exp Med* 7: 4232–4237, 2014.
59. **Yellon DM, Hausenloy DJ.** Realizing the clinical potential of ischemic preconditioning and postconditioning. *Nat Clin Pract Cardiovasc Med* 2: 568–575, 2005. doi:10.1038/ncpcardio0346.
60. **Zhu WZ, Zheng M, Koch WJ, Lefkowitz RJ, Kobilka BK, Xiao RP.** Dual modulation of cell survival and cell death by β(2)-adrenergic signaling in adult mouse cardiac myocytes. *Proc Natl Acad Sci USA* 98: 1607–1612, 2001. doi:10.1073/pnas.98.4.1607.